

Bodo's Power Systems®

Electronics in Motion and Conversion

May 2021

GETTING TO A CLEANER FUTURE

Design Challenges
and Solutions for
Solar Inverters



Vincotech

WELCOME TO THE HOUSE OF COMPETENCE

ENGINEERING

PRODUCTION

GvA SOLUTIONS

DISTRIBUTION



ENGINEERING **POWER** IS IN OUR NATURE!

Whether small or large development tasks: speed is no witchcraft but the result of perfectly fine-tuned processes in interplay with highest competence - our engineering power for your success.

- Quick design-to-product
- Time and cost savings through synergy effects
- Extensive experience gives you an edge
- State-of-the-art technology
- Simulation and in-house tests ensure reliability

GvA Leistungselektronik GmbH

Boehringer Straße 10 - 12

D-68307 Mannheim

Phone +49 (0) 621/7 89 92-0

info@gva-leistungselektronik.de

www.gva-leistungselektronik.de



GvA
Power Electronics

5MPA Series



High Current Carrying AC Application

- ✓ Low loss, dry film construction
- ✓ Operating temperature range: -55°C to +85°C
- ✓ Available off the shelf

Contact ECI Today! sales@ecicaps.com | sales@ecicaps.ie

www.ecicaps.com

CONTENT

Viewpoint	4	Measurement	42-44
A Successful Premiere		Voltage and Current Measurement Technology for PV Energy Management System on Enhanced DC1500V Solar DC Side	
Events	4	By <i>J&D Electronics</i>	
News	6-14	Power Supply	46-50
Product of the Month	16	Overvoltage Categories in Power Supply Systems	
DC/DC Controllers with an Integrated Active EMI Filter		By <i>Steve Roberts, Innovation Manager, RECOM Power</i>	
Guest Editorial	18	Measurement	52-57
3D Power Electronics Integration and Manufacturing Symposium		Understanding Bandwidth Requirements When Measuring Switching Characteristics in Power Electronic Applications	
By <i>Arnold Alderman, Publicity Chair, 3D-PEIM21, Executive Committee Member, PSMA</i>		By <i>Bernhard Holzinger, Michael Zimmermann, Ryo Takeda, and Mike Hawes, Keysight Technologies</i>	
Cover Story	20-24	Thermal Management	58-61
Getting to a Cleaner Future		2,2W Thermally Conductive Foil with Dielectric Strength up to 6KV used as Thermal Interface Material (TIM) in Power Electronics	
Design Challenges and Solutions for Solar Inverters		By <i>Uwe Lemke, Business Development Manager DACH, Aismalibar S.A., Barcelona</i>	
By <i>Andrew Smith, Product Marketing Manager, and Matthias Tauer, Technical Marketing Manager, Vincotech GmbH</i>		Capacitors	62-63
Power Modules	26-29	Eliminating Voltage Overshoots for High-performance Modules in the Mega-watt Range	
Intelligent Power Modules (IPM) Contributes to Energy Saving and faster Time to Market		By <i>Dipl. Ing. Wolfgang Rambow, Senior Director Sales Technical Support, TDK Electronics AG, Munich, and Dipl. Ing. Marco Honsberg, MBA, Senior Manager Product Management Intelligent Power Modules and Electronics, SEMIKRON GmbH&Co., Nuremberg</i>	
By <i>Massimo Caprioli, Senior FAE at Fuji Electric Europe</i>		Wide Bandgap	64-67
Wide Bandgap	30-31	Evaluate Junction Temperature from Inside	
Extreme GaN – What Happens When eGaN® FETs are Exposed to Voltage and Current Levels Well Above Data Sheet Limits		By <i>Nigel Springett, Ing Büro Springett</i>	
By <i>Robert Strittmatter, Alejandro Pozo, and Alex Lidow Efficient Power Conversion</i>		Power Supply	68-71
Measurement	32-34	Ride Through the MLCC Shortage by Reducing Capacitance Requirements in Your Power Supplies	
LTspice® Emulation Models for the RidleyBox® and AP310 Analyzers		By <i>Atsuhiko Furukawa, Field Applications Engineer, Analog Devices</i>	
By <i>Dr. Ray Ridley, Art Nace and John Beecroft Ridley Engineering, Inc. Camarillo, California USA</i>		Design and Simulation	72-74
Wide Bandgap	36-38	Upscaling Small Real-Time Simulators for Large Power Electronic Systems	
Gallium Nitride (GaN) Power ICs: Turning Academic Dreams into Industry Reality		By <i>Stefan Milovanovic and Drazen Dujic, Power Electronics Laboratory, EPFL, Switzerland</i>	
By <i>Tom Ribarich and Stephen Oliver, Navitas Semiconductor</i>		New Products	76-80
Power Modules	40-41		
High-quality Power Semiconductor Modules now Support Lower Voltages			
By <i>Tomáš Žlnay, Ladislav Radvan, Christian Winter, Roc Blumenthal, Tobias Keller, Hitachi ABB Power Grids</i>			

Sorry, no room for a cartoon this time. *Little Ohm* will be back soon!

The Gallery



Keep it simple!

Sense with MEMS.



© eSmart

WE are here for you!

Join our free webinars on
www.we-online.com/webinars

MEMS Sensor Portfolio & Customer Service

Sensors are an integral part of every future application. Measuring temperature, humidity, pressure or acceleration has never been easier. Take advantage of services like our Software Development Kit and Evaluation Boards available off-the-shelf. Detailed documentations as well as the direct support by trained engineers will leave no questions open.

With excellent measuring accuracy and long-term stability, the sensors provide high precision and accurate output values with intelligent on-chip interrupt functions.

Combine sensors and wireless connectivity – start your IoT application today:

www.we-online.com/sensors

- Support by engineers within 24 h
- Excellent measuring accuracy
- Factory calibrated & ready to use
- On-chip interrupt functions
- Implemented algorithms
- SPI & I²C digital interfaces



#SensewithMEMS

Bodo's Power Systems®**A Media**

Katzbek 17a
D-24235 Laboe, Germany
Phone: +49 4343 42 17 90
Fax: +49 4343 42 17 89
info@bodospower.com
www.bodospower.com

Publisher

Bodo Artl, Dipl.-Ing.
editor@bodospower.com

Editor

Holger Moscheik
Phone + 49 4343 428 5017
holger@bodospower.com

Editor China

Min Xu
Phone: +86 156 18860853
xumin@i2imedia.net

US Support

Bob Dumas
Phone +1 516 978 7230
bob@eetech.com

Creative Direction & Production

Blanka Gehlert
b.gehlert@t-online.de

Free Subscription to qualified readers

Bodo's Power Systems
is available for the following
subscription charges:

Annual charge (12 issues)
is 150 € world wide

Single issue is 18 €
subscription@bodospower.com

**Printing by:**

Brühlsche Universitätsdruckerei GmbH
& Co KG; 35396 Gießen, Germany

A Media and Bodos Power Systems

assume and hereby disclaim any
liability to any person for any loss or
damage by errors or omissions in the
material contained herein regardless
of whether such errors result from
negligence accident or any other cause
whatsoever.



www.bodospower.com

A Successful Premiere

On March 31, the first Wide Bandgap Expert Talk was held very successfully. It started with participants from the field of GaN and soon warmed up to a lively discussion. Like all the virtual roundtables I've seen over the past few months, the conversation has to develop, but once it started, the questions soon poured in via chat. After a full hour we closed the meeting with a good feeling and opened the SiC-session, also with five participants and Bodo as the moderator. Here too, a 60-minute discussion developed, both about the articles and current trends. Bodo and I would like to thank all of the panel experts once again - we are very pleased with the positive feedback that we received from our readers and with the numerous commitments to participate again.

Our initial idea for this format was to hold these regular rounds with the experts changing and I am pleased to have already received enough commitments for our next edition on June 30. To be honest, the interest in the industry is already so great that a quarterly continuation beyond the turn of the year can be considered assured. For the upcoming episode, we will again publish the articles we will be featuring on our website from the beginning of June to give our readers the opportunity to submit questions.

It is not only the big conferences, such as APEC recently announced, that are changing to virtual formats - so is Bodo's Power. Our annual December event will now be held virtual for the second time. The feedback we are receiving is that people still don't want to make travel plans at the moment. Bodo and I totally agree, we too feel that it is still not secure enough with Corona virus and we don't expect it will be for the rest of the year.



So, mark your calendar for "Bodo's Wide Bandgap Event" on December 1-2, 2021. We will once again bring together experts in SiC, GaN and related topics.

Bodo's magazine is delivered by postal service to all places in the world. It is the only magazine that spreads technical information on power electronics globally. We have EETech as a partner serving North America efficiently. If you are using any kind of tablet or smart phone, you will find all our content on the website www.eepower.com. If you speak the language, or just want to have a look, don't miss our Chinese version: www.bodospowerchina.com

My Green Power Tip for the Month:

The days are getting longer again. Let as much natural light as possible into your home and office. It's free, healthy in reasonable doses, and it makes you feel happy!

Kind regards

Events

PCIM Europe digital days 2021

Online May 3-7
<https://pcim.mesago.com>

Sensor + Test 2021

Online May 4-6
www.sensor-test.de

IEMDC 2021

Online May 17-20
<https://iemdc-2021.com>

Battery Show Europe 2021

Online May 18-20
www.thebatteryshow.eu

ECCE Asia 2021

Online May 24-27
<https://ecceasia2021.com>

BEVA Europe 2021

Online May 25-27
www.beva-europe.com

ISPSD 2021

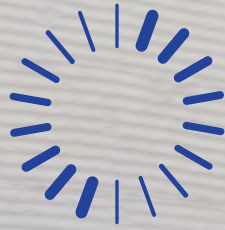
Online May 30 – June 3
www.ispsd2021.com

APEC 2021

Online June 14-17
www.apec-conf.org

3D-PEIM 2021

Osaka, Japan & Online June 21-23
www.3d-peim.org



Optimize the design of EV chargers



CDSR Series

Extremely compact, the LEM CDSR leakage current sensor ensures your next EV charger will have the small size and low cost that customers want, while remaining fully compliant with relevant standards.

In addition, it provides highly flexible connectivity, offering both cable IC-CPD (mode 2) and AC wallbox (mode 3).

The CDSR also uses the latest open-loop fluxgate technology, offering high safety for EV users by measuring AC and DC leakage current below 1mA at frequencies up to 2kHz.

- **Single and three phase configuration**
- **32 Arms nominal current per phase**
- **0.5 mA accuracy at 6mA**
- **Test winding and default output signal**
- **Analog and digital communication (SPI)**
- **Complies with application standards IEC 61851, 62955, 62752, UL 2231**

www.lem.com

LEM

Life Energy Motion

Wolfram Harnack Appointed President



As of April 1st, 2021, ROHM Semiconductor Europe appoints Wolfram Harnack as the company's new President. The former President, Toshimitsu Suzuki, will lead the European Sales Division as General Manager from April 1st from the company's headquarters in Japan. Wolfram Harnack joined ROHM Semiconductor Europe GmbH as Managing Director in October 2020. Toshimitsu Suzuki, the new General Manager of the European Sales Division, justifies the choice of Wolfram Harnack with his long and rich experience

and his comprehensive market knowledge: "With Wolfram Harnack, a strong leader will become the new President of ROHM's European Headquarters. He can build on a solid foundation when it comes

to strategy, business development as well as sales and marketing against an international background."

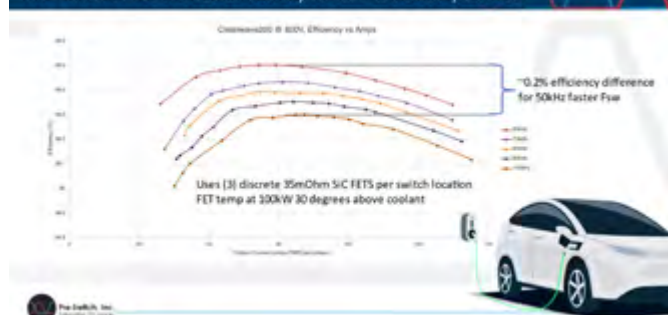
"I am honored to lead a company for which I have already worked with passion and to whose further successes I will now contribute significantly," said Wolfram Harnack on the occasion of his appointment as new President. "ROHM Semiconductor offers a wide range of technologies and is a quality and innovation leader especially in the field of Silicon Carbide and Analog Power devices. The competent team helps customers to achieve their development goals by excellent application support and by providing the necessary insights. In this sense, my key aim is to further extend our customer service and accelerate growth in the automotive and industrial segments, especially in the power and analog area."

www.rohm.com

Technology for EV and Renewables

Pre-Switch has published performance data that shows that its 200kW (space vector modulated) CleanWave200 evaluation inverter exceeds 99.3% at 100kHz using only three discrete, low cost 35 mΩ SiC MOSFETs per switch location. This is expected to revolutionize EV and renewable energy designs. Comments Bruce Renouard, Pre-Switch CEO: "We are shipping the CleanWave200 evaluation systems to initial customers around the world, and the efficiency data we are making public today more than justifies our design goals. Customers could use the Pre-Switch technology with even better MOSFETs and expect to get incremental performance gains, but there is no other

Pre-Switch CleanWave200 system efficiency results



approach that even comes close to 99.3% efficiency at 100kHz with such few, low cost SiC MOSFETs."

The Pre-Switch AI enables users to migrate from lossy, expensive hard-switching implementations to high efficiency, soft-switching designs with a 10X higher switching frequency which produces an almost pure sine wave output. The Pre-Switch controller analyzes multiple inputs on a cycle-by-cycle basis, making adjustments in real time to small, forced-resonant transistors enabling perfect soft-switching in harsh changing environments. Variations in system temperature, device degradation, changing input voltages and abrupt current swings are all accounted for and optimized within the Pre-Switch AI algorithm. The published data plots system efficiency for 50-100 kHz switching speeds, input voltages, power output and current output, enabling system designers to compare the Pre-Switch results to their own requirements. Adds Renouard: "Switching losses using our Pre-Switch technology are effectively zero. If we put that into perspective, an EV with Pre-Switch technology improves inverter efficiencies, producing a pure sine wave output that dramatically improves motor efficiency at low torques where people drive. This will result in an increase its range by up to 12%."

www.pre-switch.com

www.coilcraft.com

The Best Inductor Website Is Better Than Ever!

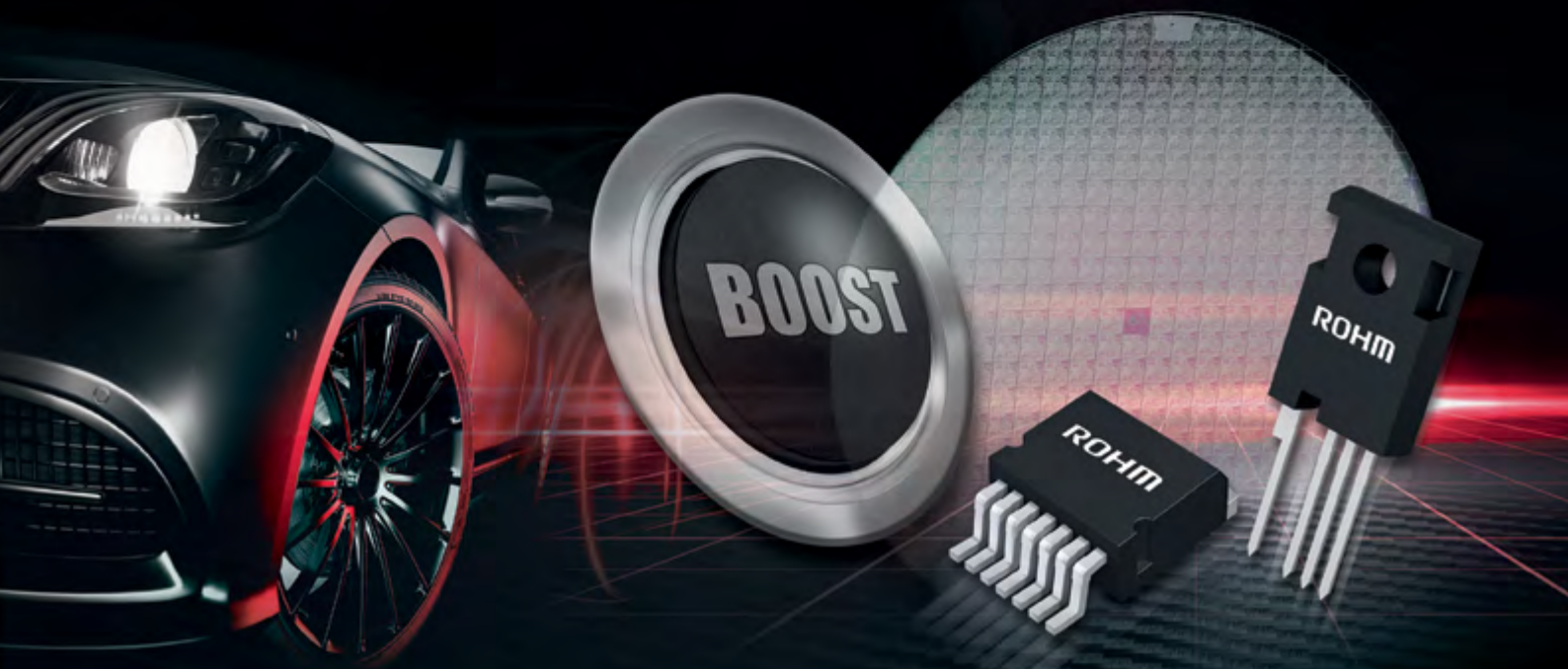
Coilcraft



- Improved Site Navigation
- Easier Ordering/Checkout Process
- The Most Powerful Design Tools
- Expanded Technical & Educational Resources

Come visit and see for yourself!

**SMALLER
STRONGER
FASTER**



BOOST YOUR SYSTEM
EXTRA POWER THANKS TO ROHM SiC TECHNOLOGY

Established, experienced, evolved: As a technology leader ROHM is shaping the power solutions of the future. Our advanced SiC technology boosts the performance of automotive power systems. We produce SiC components in-house in a vertically integrated manufacturing system and thus guarantee the highest quality and constant supply of the market. Take the next development step with our latest SiC solutions.

SMALLER inverter designs
reducing volume and weight

STRONGER performance
by higher power densities

FASTER charging
and efficient power conversion



AUTOMOTIVE



INDUSTRIAL

www.rohm.com/pcim

pcim
EUROPE

APEC 2021 Moves to Virtual Event Format



The safety and well-being of our participants remains our top priority. While we look forward to the moment when everyone who wants to participate at an in-person APEC can do so safely and confidently, we are not there yet. Continued global travel restrictions, unknown guidance on large gatherings, as well as social distancing protocols make it impossible to move forward with an in-person event at this time. APEC 2021 will be presented on the virtual event platform Social27 and will take place Monday, June 14 - Thursday, June 17 with on demand access starting the week of June 9. We understand home life has changed for many of us over the past several months and we have modified the daily schedule slightly to make the conference as accessible as possible during the workweek. As a reminder, all sessions will be recorded so if you are unable to tune-in live, you can view the content on your own schedule.

www.apec-conf.org

Digital Congress on Sensors, Measurement and Metrology

The AMA Association for Sensor and Measurement Technology invites to the international congress: Sensor and Measurement Science International (SMSI) 2021. Due to the COVID19 pandemic, the conference will be held digitally, in parallel with the SENSOR+TEST 2021 trade fair from May 3 to 6, 2021. The official SMSI 2021 program is now available online. SMSI 2021 networks national and international representatives from research, science and industry. Current research results from the fields of sensor technology, measurement technology and metrology will be presented. Topics include: Innovative hydrogen sensors for fuel cell vehicles, novel approaches to modeling thermal-electrical behavior of pyroelectric infrared sensors, the development of non-invasive pressure sensors, and the evaluation of ceramic high-temperature sensor housings. In addition to many technical presentations, SMSI 2021 invites all participants to attend international plenary lectures. Among them, for example, NIST on a Chip: Disseminating the SI through Quantum Sensors. Physikalisch-Technische Bundesanstalt reports on the revised SI for Innovation, Science and the Second Quantum Revolution, and the University of



California on Invariance of Measured Quantities across the Science. The full SMSI 2021 program, registration fees and registration now at: <https://www.smsi-conference.com>

www.ama-sensorik.de

Joint Master's Program in the Field of Power Electronics

Heraeus Electronics and the Fraunhofer Institute for Integrated Systems and Device Technology (IISB) recently launched a joint program for master's theses on power electronics. Both partners agree to jointly supervise two to four master theses per year on current research and development topics. The collaboration, initially planned for two years, is intended to link Fraunhofer IISB's expertise in power



electronics components and systems with current and practically relevant issues and material developments for electronics applications from Heraeus.

"We see the collaboration as a win-win situation in which we can apply our joint strengths to build on each other," says Dr. Sebastian Fritzsche, head of the cooperation program at Heraeus in Hanau. "Heraeus' current development goals include increasing the reliability and efficiency of microelectronic systems, especially systems for power electronics and their use at higher operating temperatures." "Fraunhofer IISB focusses on advanced packaging technologies and new materials for efficient and reliable power modules", adds Dr. Christoph Bayer, group manager for Packaging Technologies at the Fraunhofer institute. The research work for the theses will mainly be carried out in the labs of Fraunhofer IISB in Erlangen, complemented by selective activities at Heraeus in Hanau.

www.heraeus.com

High Voltage IGBT

**PH
PC²**



- High Power Density
- Low Inductance
- Scalable, Easy Paralleling
- Standard and High Isolation Package

25 Years of Success in India

It was the beginning of the 1990s: Hans-Rudolf Schurter took over as Chairman of the Board of Directors from his father Rolf. At the same time, Asia was the emerging continent. China was awakening and beginning to reform. The martial term Tiger Countries was on everyone's lips. SCHURTER, at that time almost exclusively present in Western Europe and the USA, decided to venture east as well in order not to miss this opportunity. But the focus was not on Hong Kong or Singapore. Many Western companies were drawn to China, others to India. The most populous countries on earth promised enormous potential. The choice between the giants China and India was decided in favour of the latter. Hans-Rudolf Schurter assumed

that the Indian mentality would be easier to integrate because of the English legal system and language. However, the first contacts between locals and members of the SCHURTER Group took place on the other side of the planet - in the USA. Bruno Schurter, then managing director of SCHURTER Inc. in Santa Rosa, California, maintained business relations with Asgari Lokhandwala. After his studies, Asgari worked for a company that manufactured power supply units for personal computers. For this purpose, he bought connectors and fuses from SCHURTER Inc. This was the beginning of the association between the Lokhandwala family and SCHURTER.



www.schurter.com

Comprehensive Partnership for Gallium Nitride

Nexperia has announced a comprehensive partnership covering gallium nitride (GaN) power semiconductor devices with United Automotive Electronic Systems Co., Ltd. (UAES). The program will focus on power systems for EVs, with the aim to jointly develop automotive applications using GaN technology. UAES has already started using Nexperia GaN FETs in R&D and collaborative projects including vehicle-mounted chargers and high-voltage DC-to-DC converters for



electric cars. Nexperia's GaN technology has extremely good figures of merit (RDS(on) x QGD) and reverse recovery charge (Qrr) metrics that support high switching frequencies and efficient power conversion. Nexperia produces GaN based on mature and reliable mass production techniques, largely in its own global production facilities, to manufacture products according to automotive AEC-Q101 standards. UAES provides car manufacturers with advanced and comprehensive automotive powertrain and body control system solutions. It specializes in the development, production, and sales of gasoline engine management systems, transmission control systems, vehicle body electronics, and hybrid and electric drive control systems. Its five technology centers in China have world-class laboratories for entire vehicles, engines, automatic transmissions, and electric drive performance development. The advanced equipment effectively provides high-quality engineering services including system development, component development, and calibration for various Chinese car manufacturers.

www.nexperia.com

Solutions for the Production of Compound Semiconductor Devices

Oxford Instruments Plasma Technology and LayTec announce an exclusive collaboration agreement to enable the next generation requirements of advanced semiconductor devices in the high-volume manufacturing (HVM) environment. The partnership aims to develop and integrate LayTec's accuracy and control with Oxford Instruments'



renowned wafer processing expertise.

Together, they will combine plasma process solutions with proven in-situ metrology to achieve next generation device performance and enable a repeatable HVM process to shorten customers' yield ramp. LayTec will develop the in-situ metrology while Oxford Instruments will integrate LayTec's control with its advanced wafer processing solutions to deliver an enhanced solution to the customer.

Driven by market demands for efficient power conversion, the IoT and datacomms compound semiconductor devices based on materials such as GaAs/InP, SiC or GaN, are becoming increasingly used due to their superior performance. However, challenges remain to move the technology from small prototypes to wafer scale, HVM. While device dimensions are relatively large, the often-complex layer structure means that acute accuracy of processing within these layers is required to realise the required process stability and yield to drive down the cost per wafer and accelerate adoption into the target application.

www.oxinst.com

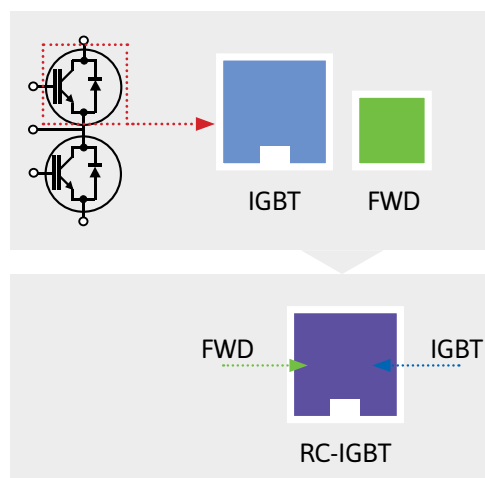


Reverse Conducting IGBT (RC IGBT)

6 in 1 power module with a rating of 1200V and 250A

FEATURES

- ▶ RC technology is combining IGBT and FWD in the same chip
- ▶ Total chip size reduction:
 - Expansion of inverter output current with the same inverter size
- ▶ Chip structure is based on Fuji Electric's actual X series
- ▶ Extended chip area:
 - Chip temperature reduction by lower $R_{th(j-c)}$
- ▶ Improved power cycle lifetime by reduced temperature ripple
- ▶ Solder and press-fit pin type available
- ▶ Significantly reduced power dissipation and T_{vj} during DC lock operation





Mike Morton Announced Chief Executive Officer

TTI announced the appointment of Mike Morton to the position of Chief Executive Officer, effective immediately. Morton has served the company for 40+ years in various leadership positions, most recently providing exceptional leadership as chief operating officer. Through his years with TTI, Morton has played a vital role in building the company to its current level of suc-

cess. His knowledge of the company and vast experience is expected to serve him well as he takes on this new key position.

The announcement follows the passing of TTI's founder, Paul Andrews. Andrews' leadership and guidance propelled the Fort Worth based company to become the fifth largest electronics distributor in North America.

www.ttieurope.com

Dr. Tobias Geyer Honored with Innovation Award

This year the jury has decided to give the SEMIKRON Innovation Award to Dr. Tobias Geyer from ABB Medium-Voltage Drives, Switzerland to acknowledge his pioneering work in the field of Model Predictive Control awarding his innovation regarding 'Model Predictive Pulse Pattern Control'.

Optimized pulse patterns (OPPs) minimize the current distortions per switching frequency during steady-state operation, but achieving high dynamic performance is generally considered impossible. Model predictive pulse pattern control (MP3C) solves this problem by formulating and solving a model predictive control problem. The stator flux vector is controlled along its optimal trajectory by modifying the switching instants of the OPP's switching transitions. MP3C combines the benefits of hysteresis control methods, such as direct torque control, with the optimal steady-state performance of OPPs, by resolving the antagonism between the two. MP3C has been successfully demonstrated and proven in an ABB medium-voltage drive. The control innovation increases the drive's power by up to 50% at high fundamental frequencies.

This year's SEMIKRON Young Engineer Award is given to Dr. Jakub Kucka (now EPFL École Polytechnique Fédérale de Lausanne) for his work on 'Quasi-Two-Level PWM Operation for Modular Multilevel Converters' he has conducted at the Institute for Drive Systems and Power Electronics of Leibniz University Hannover, Germany.



The novel quasi-two-level PWM operation mode revolutionizes the way how the modular multilevel converters are operated in low-frequency medium-voltage drive applications. Thanks to the quasi-two-level PWM operation, the amount of installed modules' capacitance in the modular multilevel converters can be reduced by more than one order of magnitude.

www.semikron.com

Funding to Scale Up Ultracapacitors Production

Skeleton Technologies unveiled its plans to develop first-of-its-kind production technology for manufacturing its ultracapacitors, following the official support announced by German authorities in January. To execute these plans, the company will receive an additional €51 million (\$60 million) from Germany's Federal Ministry for Economic Affairs and Energy and the Free State of Saxony. This project will include the development of a fully-automated ultracapacitor production line in its Großröhrsdorf factory – a first in the industry. The economies of scale provided by this new technology, combined with the use of Skeleton's patented "curved graphene" material, will dramatically drive the production costs down, boosting the competitiveness of ultracapacitors as the key enabling technology for the future of transportation and electrification.

Taavi Madiberk, CEO and co-founder of Skeleton Technologies, explains: "We are continuously investing in R&D – whether it is improving the performance of our products or the process in which we make those products. The next stage of our production will see an implementation of fully automated Industry 4.0 manufacturing techniques – a first-of-its-kind in the ultracapacitor industry. Coupled with our curved graphene material, we are able to dramatically decrease the cost of ultracapacitors. The ultracapacitor industry is in the same

situation as lithium-ion batteries were in 1999, but our advancements in core technology and production capabilities will be able to show a cost reduction faster than for any other energy storage technology. We have a clear road map to lower it by almost 90% after completion of our 5 years project."



www.skeletontech.com



Vincotech

ENHANCE YOUR EV CHARGER

with Vincotech's **SiC MOSFET-based *flow E* half- and H-bridge power modules**

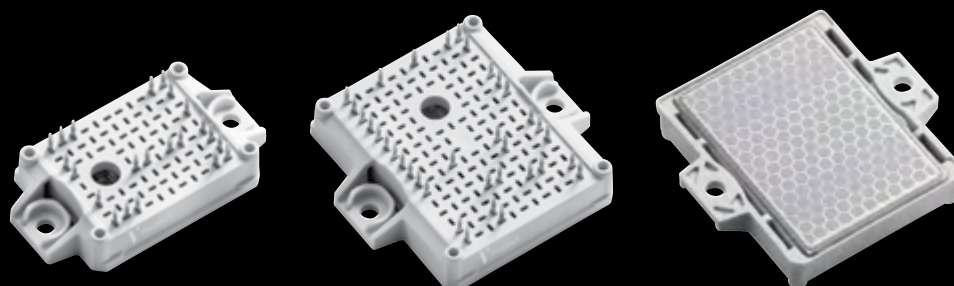
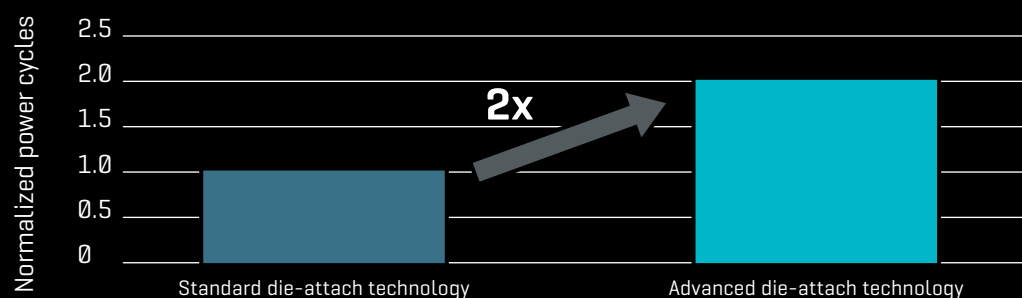
The new *flowDUAL* SiC E1 and *fastPACK* SiC E1/E2 have been developed with the aim to make the EV offboard charger designs faster, smaller and more efficient. The modules are based on latest 650V and 1200V SiC MOSFET chip generations with an on-resistance as low as 5mOhm.

In addition to optimizing performance, Vincotech attaches great importance to reliability. With the new advanced die-attach technology, the new *flow E* SiC MOSFET-based modules can extend the power cycling lifetime by a factor of 2.

Main benefits

- / Factor 2 improved power cycling capability for longer lifetime
- / Multi-sourced SiC-components for more freedom of choice and less supply chain risk
- / Optional integrated capacitors for improved EMC performance
- / Press-fit pins and pre-applied TIM to help reduce production cost

Average PC lifetimes for *flow E* SiC MOSFET-based power modules ($\Delta T=100K$)



Innovation Challenge 2021

This year's Keysight Innovation Challenge focuses on undergraduate engineering and pre-engineering students enrolled in a historically black college or university (HBCU) to innovate new business opportunities and create videos that demonstrate electronics measurement techniques. HBCUs are institutions of higher education in the United States that were established before the Civil Rights Act of 1964 with the intention of primarily serving the African American community. There are currently 101 HBCUs in the United States, including both public and private institutions. This year's Keysight competition is an opportunity for these students attending an HBCU



to share innovative ideas with the world and to inspire future generations of Black engineers.

"This is one of the many ways Keysight is inspiring a strong and sustainable pool of global leaders who will continue to push technology to new heights and bring positive change in the world with rich and diverse perspectives. We are proud and committed to enable this new generation of innovators," said Ee Huei Sin, senior vice president, Keysight Technologies and president of Keysight's Electronic Industrial Solutions Group.

www.keysight.com

Sustainable Operation of Trains

Siemens Mobility and Infineon Technologies have jointly developed auxiliary converters to improve the efficiency of on-board power systems using power semiconductors based on silicon carbide (SiC). Siemens uses the converter for various train platforms. As a result, the platforms are maintenance-friendly, reliable, economical and, above all, power efficient. "With SiC, we achieve higher switching speed as well as efficiency to reduce the size of transformers, capaci-

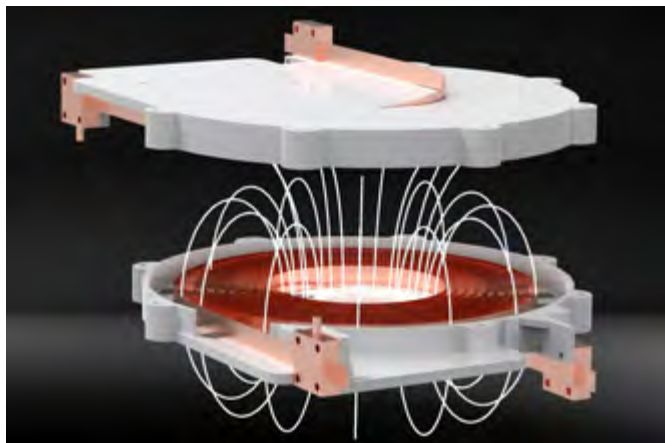


tors, cooling elements and the housing unit. The advantages of this semiconductor material are evident and are now being leveraged in rail-bound vehicles," said Dr. Peter Wawer, President of Infineon's Industrial Power Control Division. In addition to providing the AC voltage (e.g., 3 AC 400 V 50 Hz) required for the vehicle power system, auxiliary converters also deliver the required battery voltage (e.g., 110 V DC). To achieve this, they convert the DC voltage provided at the converter input. They ensure that train passengers can charge laptops and smartphones; the air conditioning and ventilation systems are running; and the on-board restaurant can offer hot and cold drinks and food. Without them, connectivity, information or entertainment services on trains would not be available. As part of the system, SiC reduces the overall costs in the on-board electrical system and the energy consumption of the auxiliary converter. It also enables more compact and lighter converter designs, along with a modular and service-friendly design to ensure lower maintenance costs.

www.infineon.com

Contactless Power Transmission in the Kilowatt Range

A team led by Technical University of Munich (TUM) physicists Christoph Utschick and Prof. Rudolf Gross has succeeded in making a coil with superconducting wires capable of transmitting power in the range of more than five kilowatts contactless and with only small losses. The wide field of conceivable applications include autonomous industrial



robots, medical equipment, vehicles and even aircraft. Contactless power transmission has already established itself as a key technology when it comes to charging small devices such as mobile telephones and electric toothbrushes. Users would also like to see contactless charging made available for larger electric machines such as industrial robots, medical equipment and electric vehicles. Such devices could be placed on a charging station whenever they are not in use. This would make it possible to effectively utilize even short idle times to recharge their batteries. However, the currently available transmission systems for high performance recharging in the kilowatt range and above are large and heavy, since they are based on copper coils.

Working in a research partnership with the companies Würth Elektronik eiSos and superconductor coating specialist Theva Dünnschichttechnik, a team of physicists led by Christoph Utschick and Rudolf Gross have succeeded in creating a coil with superconducting wires capable of contactless power transmission in the order of more than five kilowatts (kW) and without significant loss.

www.tum.de



4-6 May: Infineon's Virtual Power Conference

Flanking PCIM Europe digital days

Energy efficiency in focus

Infineon's Virtual Power Conference will have a special focus on energy efficiency this year. We continue to set the pace for innovation in this area, enabling energy to be generated more efficiently – especially from renewable sources, to be transmitted and distributed with reduced losses and to be used more efficiently across the widest application spectrum from industrial use cases and data centers through electric vehicles to smart buildings.

The key to the next significant step in energy efficiency lies in the use of new technologies such as SiC (silicon carbide) and GaN (gallium nitride). They enable higher power efficiency, a smaller form factor and lower weight. Experience our broad power portfolio and find answers to your system design challenges.



Live expert panels

- › How to translate chip technology and package experience into successful products with CoolSiC™ technology
- › Si or wide-bandgap – which technology is the best fit for SMPS?
- › CoolMOS™ S7(A) SJ MOSFETs – a perfect match for static switching applications
- › iMOTION™ – the family of highly integrated products
- › Easy solutions for bi-directional on-board-chargers
- › Infineon's offering for hydrogen generation and consumption
- › Let's make eMobility work!
- › And many more



Demo highlights

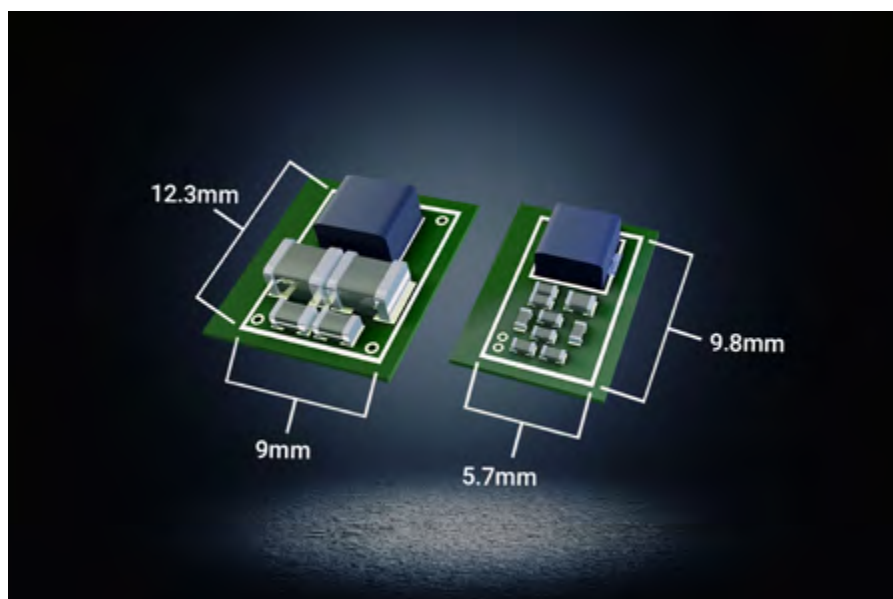
- › New this year at the Virtual Power Conference: a dedicated board corner!
- › The new servo drive without a cooling fan: CoolSiC™ MOSFET 1200 V in D2PAK-7L with .XT interconnection technology enables passive cooling in automation and robotics
- › CoolSiC™ in your journey to electrification with new HybridPACK™ Drive CoolSiC™ MOSFET
- › New Infineon Press Pack IGBT - the ultimate power device for high power drives and wind energy systems
- › XDP™ XDPS2201 – the novel digital hybrid flyback controller providing ultra-high-power density and outstanding efficiency to USB-C chargers
- › And many more



DC/DC Controllers with an Integrated Active EMI Filter

Designers can optimize the size and EMI of the power supply in industrial and automotive electronics with buck controllers

Texas Instruments introduced a family of synchronous DC/DC buck controllers that enable engineers to shrink the size of the power-supply solution and lower its electromagnetic interference (EMI). Featuring an integrated active EMI filter (AEF) and dual-random spread-spectrum (DRSS) technology, the LM25149-Q1 and LM25149 enable engineers to cut the area of the external EMI filter in half, lower the conducted EMI of the power design by as much as 55 dB μ V across multiple frequency bands, or achieve a combination of reduced filter size and low EMI.



Reducing EMI in the power supply is a growing design challenge, especially as electronic content increases in advanced driver assistance systems (ADAS), automotive infotainment and cluster, building automation, and aerospace and defense designs. A traditional way to ensure that a design meets conducted EMI specifications involves increasing the size of the external passive EMI filter, which in turn increases the overall power supply solution size. By integrating the AEF, the buck controllers enable engineers to meet EMI standards while increasing their design's power density. To learn how an integrated AEF works, read the technical article, "How to reduce EMI and shrink power-supply size with an integrated active EMI filter."

Reduce conducted EMI across the entire CISPR 25 Class 5 frequency spectrum

The most stringent industry requirements for low-EMI designs are Comité International Spécial des Perturbations Radioélectriques (CISPR) 25 Class 5 automotive EMI specifications. The devices help engineers meet those requirements by mitigating conducted EMI across multiple frequency bands. The integrated AEF helps detect and reduce conducted EMI in the low-frequency band of 150 kHz to 10 MHz, enabling engineers to attenuate EMI by up to 50 dB μ V at a switching frequency of 440 kHz, relative to a design with the AEF disabled, or as much as 20 dB μ V when compared to a design with a typical passive filter. In both design scenarios, the DRSS technology helps mitigate EMI by an additional 5 dB μ V across low- and high-frequency bands.

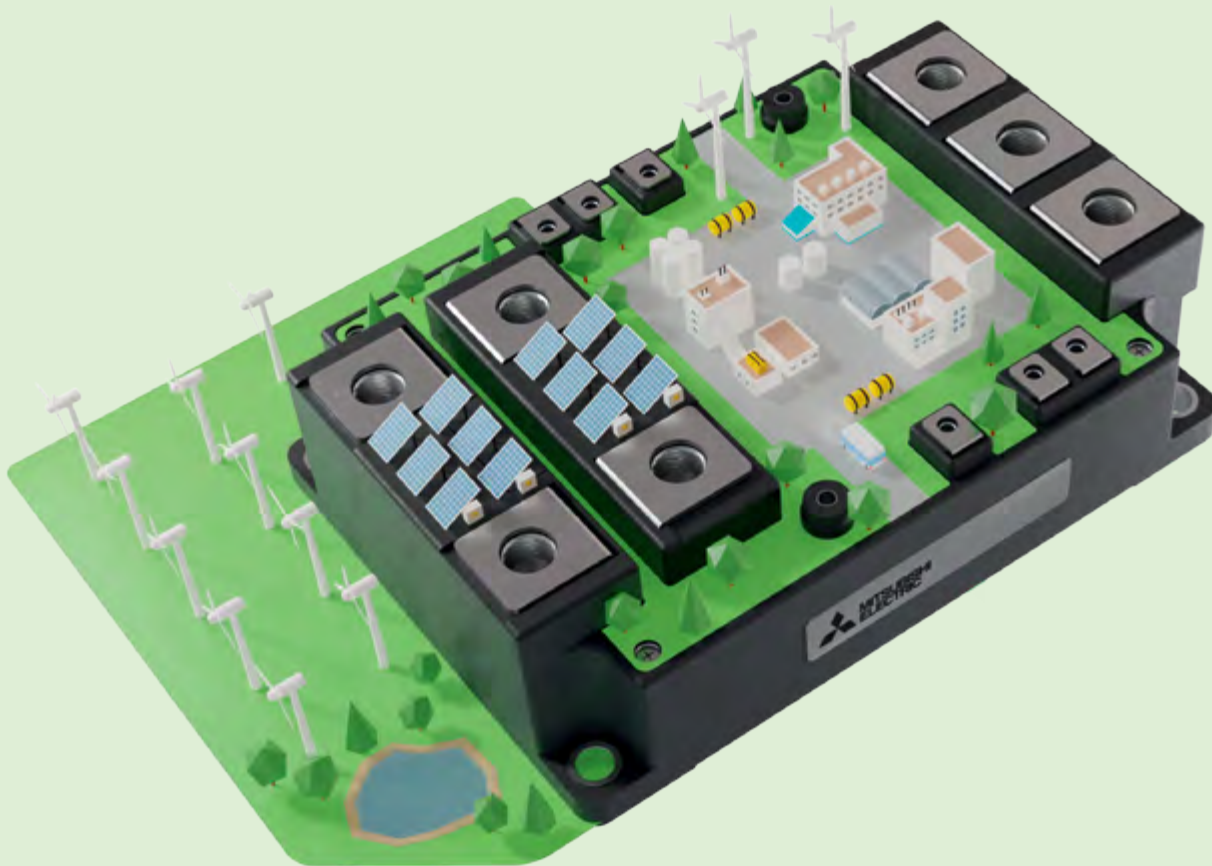
To further reduce EMI, both buck controllers feature frequency synchronization to an external clock, helping engineers mitigate undesired beat frequencies in applications sensitive to EMI. To learn more about EMI mitigation techniques, read the white paper, "Time-Saving and Cost-Effective Innovations for EMI Reduction in Power Supplies."

Shrink the external EMI filter while minimizing solution cost

Maintaining low EMI in the power supply and achieving a small solution size are usually at odds in switching power-supply designs. The buck controllers allow engineers to meet challenging EMI standards and shrink solution size by reducing the area and volume of the passive EMI filter. Compared to competing solutions, engineers can achieve maximum savings of nearly 50% in area and over 75% in volume of the front-end EMI filter at 440 kHz. By lessening the filtering burden on the passive elements, the integrated AEF reduces their size, volume and cost, enabling engineers to achieve the smallest possible low-EMI power design.

The controllers further increase power density by enabling interleaved dual-phase operation and by integrating the bootstrap diode, loop compensation and output-voltage feedback components, which in turn reduces design complexity and cost. Engineers also have an option to use external feedback and loop compensation to further optimize their designs.

www.ti.com



YOU CAN BUILD ON IT.

OUR POWER MODULES – YOUR GREEN DEAL.

7th Generation IGBT Module LV100 Package

- // New standardized package for high power applications
- // Highest power density
- // Latest 7th Gen. IGBT and Diode chips
- // Thermal cycle failure free SLC package technology
- // Easy paralleling providing scalable solutions
- // Advanced layout provides low stray inductance and symmetrical current sharing

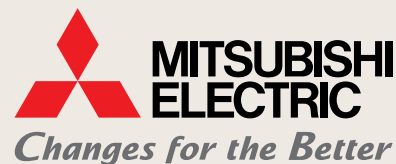
More Information:

semis.info@mee.com / www.mitsubishichips.eu

pcim
EUROPE *digital days*

Discover this and further products during our online sessions.

03 – 07 May 2021



3D Power Electronics Integration and Manufacturing Symposium

The Third Biennial International Symposium on 3D Power Electronics Integration and Manufacturing (3D-PEIM-21) will be held for the first time in Asia on June 21-23, 2021, at the Suita Campus of Osaka University Japan. Because Japan may not be open to foreign travelers, everyone can attend this live event virtually. You can switch between virtual and in-person attendance up to May 21st.

By Arnold Alderman, Publicity Chair, 3D-PEIM21, Executive Committee Member, PSMA

We are building on the continued 2016 and 2018 Symposia's success with the 3D-PEIM-21, again assembling world-class experts representing far-reaching topics on additive, embedded, co-designed, and integrative packaging technologies. By creating the 3D-PEIM Symposium, the PSMA Packaging Committee offers power electronics researchers an excellent opportunity to learn about leading-edge R&D innovations in 3D power packaging. The focus of the Symposium will be on additive, embedded, co-designed, and integrative packaging technologies. Sessions will address mechanical, materials, reliability, and manufacturability issues in deploying smart power-dense components and modules, exploring the path to developing and manufacturing future 3D power electronics systems. Recognizing the importance of the Symposium, all previous speakers signed up for the postponed 2020 3D-PEIM event have committed to participating in our upcoming 2021 3D-PEIM.



This Symposium is one of numerous PSMA sponsored events that is part of its ongoing commitment to educate and inform the power electronics industry.

The Technical Program Co-Chairs are Prof. Katsuaki Suganuma, Osaka University, Japan, Dr. Minoru Ueshima, Senior Manager, Daicel, Japan, and Prof. Guo-Quan Lu, Virginia Tech.



General Chair Professor Tsuyoshi Funaki states, "I am glad we are the first to host the 3D-PEIM Symposium outside the USA. It is very appropriate that 3D-PEIM 2021 is held here because there are many power device and peripheral packaging material manufacturers in Japan. We are planning on providing an amazing on-site or virtual experience for all attendees. I also believe that all attendees will gain significantly advanced packaging knowledge through discussions at this event".



Technical Program

The detailed program with time zone information for virtual attendees is available at www.3d-peim.org/program. The presentations will be live from both in-person and virtual presenters. Due to time zone challenges, all sessions will be recorded and available to paid attendees after the Symposium.

Opportunities Available for Exhibit Partnerships.

The Symposium will feature table-top exhibits during the breaks, lunch periods, and evening networking sessions for in-person attendees.

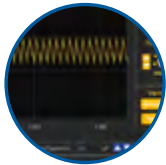
Virtual attendees will be able to interact with speakers and the audience during live question and answer sessions. Lastly, in-person attendees will have a guided tour of the Osaka University Laboratory for Power Electronics and Electrical Energy and the Graduate School of Engineering Gallery. Additional information and registration details are available at:

www.3d-peim.org

RIDLEYBOX®



THE WORLD'S FIRST TALKING TEST CENTER



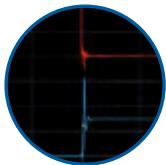
RidleyWorks® Lifetime License

- Power Stage Designer
- Power Stage Waveforms
- Magnetics Designer
- Transfer Function Bode Plots
- Closed Loop Design
- Automated FRA Control
- LTspice® Automated Link
- PSIM® Automated Link



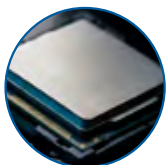
4-Channel Frequency Response Analyzer

- Frequency Range 100 mHz - 20 MHz
- Source Control from 1 mV - 4 V p-p
- Built-In Injection Isolator
- Bandwidth 1 Hz - 1 kHz
- Automated Setup from RidleyWorks®
- Direct Data Flow into RidleyWorks®



4-Channel 200 MHz Oscilloscope

- Picoscope® 5444D 4-Channel Oscilloscope
- 200 MHz Bandwidth
- 1 GS/s at 8-bit res; 62.5 MS/s at 16-bit res
- Signal Generator up to 20 MHz
- Computer Controlled



Embedded Computer

- Intel® Computer with 32 GB RAM, 256 GB SSD
- Intel® HD Graphics 620
- Integrated Dual Band Wireless, Bluetooth 4.2
- Dual HDMI and USB Ports, Ethernet



Differential Probes



Accessories



Line Injector



Output Impedance



Impedance Test Kit



725 W Ventura Blvd, Suite 112 • Camarillo CA 93010 USA • +1 805 504 2212

POWER SUPPLY DESIGN CENTER • WWW.RIDLEYENGINEERING.COM

Getting to a Cleaner Future

Design Challenges and Solutions for Solar Inverters

Renewable Energy is the key to a cleaner future and solar energy is leading the way. Designers of solar inverters face a multidimensional challenge to ensure solar power continues to meet the growing demand for clean energy. This article explores these challenges by comparing the latest solutions in terms of efficiency, weight, cost and reliability, and shows that flying capacitor topologies can offer unique opportunities for system optimization.

*By Andrew Smith, Product Marketing Manager,
and Matthias Tauer, Technical Marketing Manager, Vincotech GmbH*

Climate change is one of the key challenges facing today's society. The global demand to fight rising carbon dioxide levels, pollution, and to reduce our dependency on fossil fuels, is driving governments towards a clean energy future. Research Institutions and Industry are working to identify and deploy new ways to meet the growing demand for clean energy. Renewable power is the key to a clean energy future, already providing almost 25% of the global power demand, and solar power is the fastest growing part of the renewable energy landscape. In recent years, more solar generation capacity has been added than fossil fuel and nuclear power combined, and almost twice as much as wind

Over 700 GW of solar power has been deployed globally, with more than 100 GW being installed during 2020. Both cumulative and annual power installation are forecast to double in the next 5 years. The majority has been in utility-scale systems (>100 kW) but, increasingly in recent years, the consumer market has seen significant growth, especially when coupled with storage systems. Utility-scale systems are split between central-inverter and string-inverter systems. Historically, central-inverter systems have received the majority of investment. However, string-inverter systems are expected to become the dominant type in the next 5 years due to falling costs, increased flexibility

maintenance typically involves simple replacement of the failing inverter module. Local storage of replacement modules means problems can be quickly resolved. This helps ensure security of power supply, thereby minimizing brown- or blackouts.

High efficiency, maximum power capability, low weight and high reliability are some of the critical requirements designers need to consider to support these key string-inverter system features. High efficiency is needed to maximize the power generated from the PV panels and minimize power loss. This helps reduce heatsink requirements and system weight. Maximizing the power generation per inverter reduces the number of modular sub-systems required for a given power output. This reduces the footprint of an overall sub-system. Low system weight ensures that inverters can be easily installed and replaced, without the need for special lifting equipment. This enables quick system installation and a rapid response to system failures, especially in difficult-to-reach locations. High system reliability helps reduce maintenance requirements, even when systems are working in harsh environments, further improving longevity of supply. Vincotech's latest generation of power modules for the solar market introduces new design concepts which specifically target these design requirements – high efficiency, maximum power density, low weight and high reliability. Careful selection of innovative topologies and the latest semiconductors enables significant system level benefits. The following detailed analysis of the power conversion steps in an inverter system shows how and where Vincotech's latest modules are addressing these design requirements and the system benefits provided.

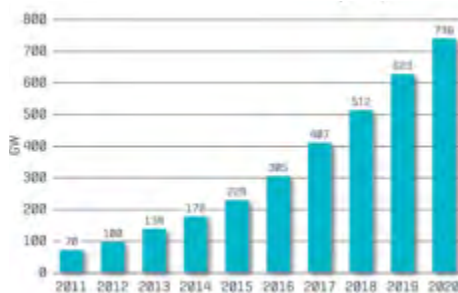


Figure 1: Total installed solar PV capacity [4]

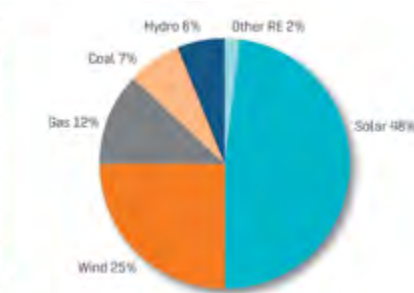


Figure 2: Power capacity installed in 2019 [5]

power. Solar power generating capacity grew to 48% of all new power installations during 2019-2020, and countries such as Germany, Italy, Greece and Chile are already producing almost 10% of their national demand. Huge investments continue to be made in all segments of the solar market, including the consumer, industrial and utility sectors.

and ease of maintenance. Central-inverter systems are based on multiple PV panels feeding into a single large inverter hub. In contrast, string-inverter systems place the inverters together with smaller "strings" of PV panels. These sub-systems are then combined before output. Consequently, as demand grows, additional string-inverter sub-systems can easily be added. As string-inverters are usually modular in design,



RT BOX 1:
THE ORIGINAL

RT BOX 2:
MULTI-CORE

RT BOX 3:
HIGH I/O COUNT

THE REAL-TIME FAMILY HAS GROWN

Building blocks for HIL simulation
and rapid control prototyping

Power electronics for 1500V multistring inverter systems

PV Inverter systems require DC/DC boost converters, as part of the Maximum Power Point Tracker (MPPT), to adjust the PV panel output voltage to the required DC-link voltage level. This is then input into DC/AC converters which deliver the solar energy to the public grid.

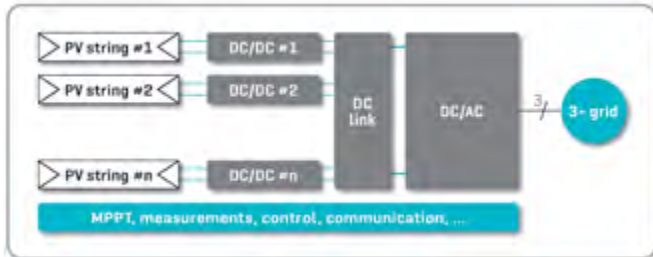


Figure 3: High level block diagram of PV inverter

Various topologies can be used for the booster and inverter stages and in the next two sections these are compared in terms of efficiency, cost and system benefit.

Cost and performance comparison of boost topologies

Two-level and three-level symmetric boosters are commonly used in the input stage of the inverter, and three-level flying capacitor boosters are starting to be used in the latest systems.

2L

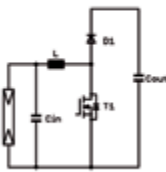


Figure 4: two-level boost circuit

3L-sym

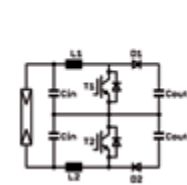


Figure 5: three-level symmetric boost circuit

3L-FC

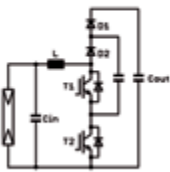


Figure 6: three-level flying capacitor boost circuit

Three-level topologies introduce an additional third voltage level. This reduces the voltage across the boost inductor, boost switch and diode to half the value required for two-level. Consequently, for a given ripple current, the inductor can be reduced to half its value when compared to a two-level topology. The overall inductor volume, weight and cost is therefore reduced. This is an additional system benefit which should be kept in mind as it is not considered in the following power module cost benchmark.

In the symmetric boost topology, the third voltage level is created by splitting the boost circuit into a 'symmetrical' positive and negative part. The additional third voltage level is generated by splitting the input and output capacitors (C_{in} , C_{out}) and connecting them to the neutral point. The pulse-width modulation (PWM) pattern needs to be adjusted to ensure symmetry of the neutral point.

In the flying capacitor boost topology, the third voltage level is generated, as the topology name indicates, by a floating or flying capacitor (C-FC). The flying capacitor is charged to half of the output voltage. A key advantage of flying capacitor topology is the "artificial" increase of inductor current frequency. In case of three-level flying capacitor, the inductor current frequency is doubled compared to the semiconductor switching frequency. This leads to smaller, lighter and cheaper inductors. Also, only one boost inductor is required whereas a three-level symmetrical booster requires two.

The following benchmark compares the two-level, three-level symmetric and three-level flying capacitor topologies in terms of cost and performance for a 40-45 kW boost leg in a 1500 V multistring solar inverter.

Chipset	two-level	three-level symmetric	three-level flying capacitor
Si/SiC hybrid	not examined because efficiency meets not the requirement		950 V fast Si IGBT 1200 V SiC diode
Full SiC	1700 V SiC MOSFET 1700 V SiC diode		1200 V SiC MOSFET 1200 V SiC diode

The efficiency and cost comparisons (figures 7 & 8) show that the full SiC two-level booster has the lowest efficiency and the highest price. The hybrid chipset was not evaluated as it would have had an even lower efficiency in this frequency range. In addition, 1700 V blocking voltage might be too low for 1500 V systems when cosmic radiation requirements are considered and using 2200 V components would further reduce the efficiency and increase the module cost.

The comparisons also show that the three-level flying capacitor (FC) booster has a higher efficiency than the symmetric booster. Since both topologies use the same components, they have the same module price.

The hybrid Si/SiC flying capacitor booster has the highest efficiency up to 50 kHz inductor current frequency. Above 50 kHz, the full SiC flying capacitor booster has the highest efficiency, but also a higher price than the hybrid circuit.

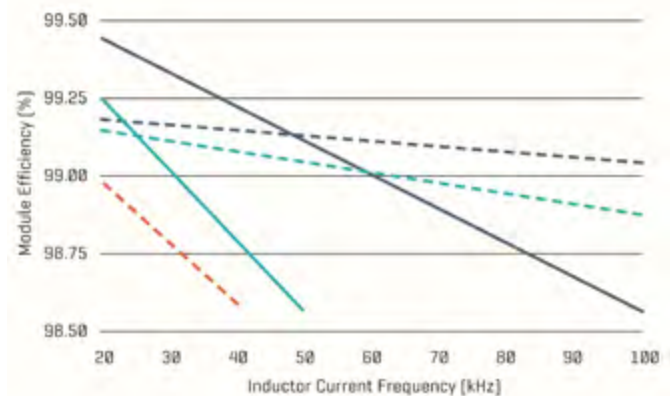


Figure 7: Module efficiency benchmark – conditions:

$$V_{in} = 760 \text{ V}, V_{out} = 1200 \text{ V}, P_{dc} = 42 \text{ kW}$$

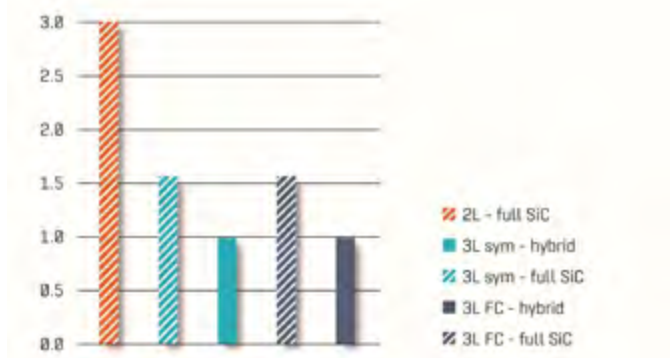


Figure 8: Module cost benchmark

Consequently, it is clear that the flying capacitor topology has best price/performance ratio compared to both the two-level and three-level symmetric topologies. For systems up to 50 kHz inductor current frequency, hybrid three-level flying capacitor topology offers the best price/performance ratio, whereas above 50 kHz, full SiC has the best efficiency.

Cost and performance comparison of inverter topologies

Many different inverter topologies have been proposed in the past. NPC and ANPC are widely used in 1500 V multistring inverters. Mixed voltage NPC (MNPC) is still used in residential and commercial 1000 V systems, but is gradually being replaced by NPC. Three-level and four-level flying capacitor inverters are starting to be used in the latest systems.



Figure 9: MNPC inverter topology

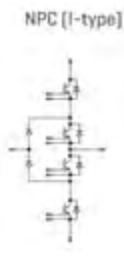


Figure 10: NPC inverter topology

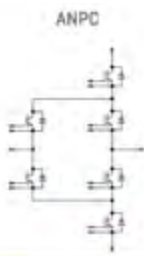


Figure 11: ANPC inverter topology

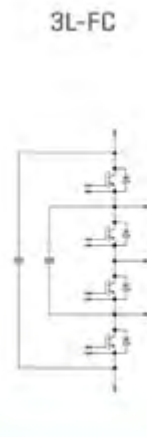


Figure 12: 3-level flying capacitor inverter topology

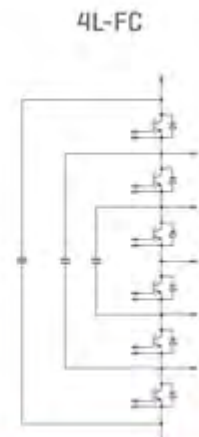


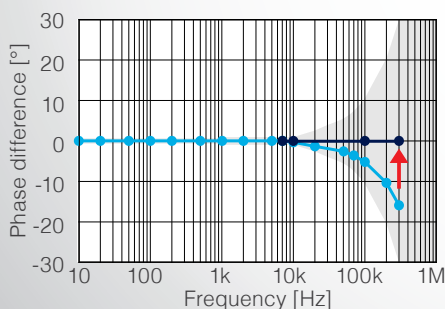
Figure 13: 4-level flying capacitor inverter topology

NPC, ANPC and flying capacitor topologies provide a higher system blocking voltage than the individual components. For example, an NPC using 950 V components will provide 1900 V blocking voltage. If a four-level flying capacitor topology is used in 1500V PV inverter, components with only 650 V blocking voltage are needed. Typically components with lower blocking voltages are faster, have lower switching losses and are usually lower cost.

How do you handle Phase Shift Error in your Power Analysis?

The Flagship Power Analyzer PW6001

- Phase Shift Correction Function
- Harmonics & Motor Analysis
- 5MS/s, 18-bit resolution
- DC to 2MHz
- ± 0.02 accuracy



Compensating Phase Shift to Flat

Learn more:

www.hioki.com/europe
hioki@hioki.eu



HIOKI

NPC and ANPC topologies have similar losses, and therefore efficiency, when used in systems driving predominantly non-reactive loads. However, the ANPC has clear efficiency advantages for $\cos\phi < 1$ and, for the sake of completeness, bidirectional operation. The losses in NPC and ANPC are concentrated in the semiconductors operated with high frequency PWM. These components are subject to conduction and switching losses. In most cases, the temperature of the fast switching semiconductors limit the maximum module output power.

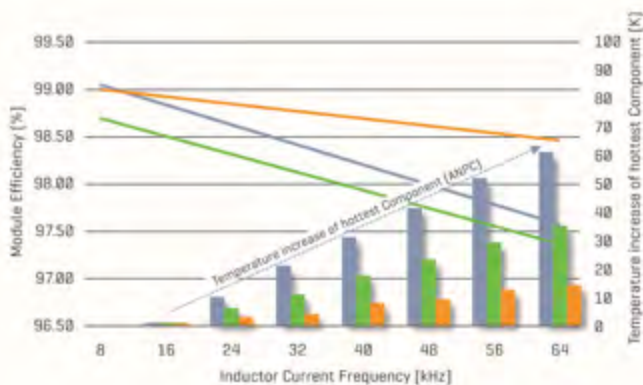


Figure 14: Module efficiency benchmark – conditions:
 $V_{dc} = 1350 \text{ V}$, $V_{ac} = 460 \text{ V}$, $P_{ac} = 117 \text{ kW per phase}$, $\cos\phi = 1$

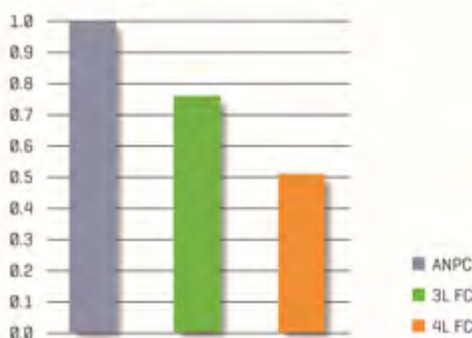


Figure 15: Module cost benchmark

In general, the losses in a flying capacitor inverter are distributed evenly across all components. This means a flying capacitor inverter has a lower junction temperature than NPC or ANPC for the same output power. Alternatively, a flying capacitor inverter enables a higher output power at same junction temperature as NPC & ANPC.

The flying capacitor inverter also supports full reactive power and bidirectional operation. A more detailed description of the operation of flying capacitor inverter topology is provided in reference [2].

A key advantage of flying capacitor inverter, as with the flying capacitor booster, is the “artificial” increase of inductor current frequency. For a three-level flying capacitor topology, the inductor current frequency is double the semiconductor switching frequency and, in the case of four-level, it's triple. The inductor size can be drastically reduced or, by keeping the same inductor current frequency, the semiconductor switching frequency can be reduced by factor of 2 or 3 respectively. This reduces the switching losses and results in a higher efficiency than NPC and ANPC.

The efficiency comparison (figure 14) shows that an ANPC operated at 16 kHz inductor current frequency has same efficiency as four-level flying capacitor inverter at 32 kHz. By moving from ANPC to four-level flying capacitor the inductor current frequency can be doubled. Consequently, the inductor volume and, to a first approximation, the inductor cost can be reduced by 40%. In addition, as shown in the cost comparison (figure 15), the power module cost for a four-level flying capacitor is 50% that of the ANPC, which results in a significant system cost reduction.

High reliability is another key design requirement in PV inverters. The temperature of the hottest component of 4-level flying capacitor operated at 32 kHz inductor current frequency is only 4K higher than the ANPC operated at 16 kHz. Nevertheless, any temperature rise has an effect on module lifetime. Vincotech's recently introduced new advanced die attach technology addresses this and increases the reliability at higher junction temperatures. Accelerated lifetime testing confirms that the new technology increases the module lifetime at 150°C junction temperature by at least 10 times.

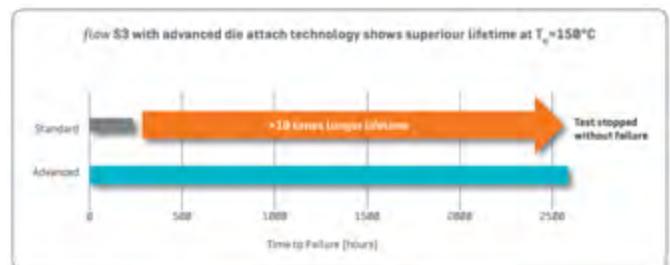


Figure 16: Result of accelerated lifetime test of standard and advanced die attach technology

Summary and solutions for high power multistring inverters

The performance and cost comparisons clearly show that the flying capacitor topology, in both booster and inverter, provide significant efficiency improvements, module and system level cost savings, and weight reduction in the inductor and heat sink requirements. These new topologies provide designers of next generation PV inverter systems with solutions to address the critical design requirements of high efficiency, maximum power density, low weight and extended reliability.

Vincotech offers a broad range of power modules optimized for the solar market. Combining symmetric boosters (LR6x family) or flying capacitor boosters (LS6x family) with ANPC inverters (LQx9 family) or the flying capacitor inverters (LMx9 family), Vincotech provides fully optimized and tailor-made solutions for 1500 V systems. With these innovative technologies, Vincotech is providing solutions to help us get to a cleaner future.

References

- [1] “Symmetrical Boost Concept for Solar Applications up to 1000V”, Temesi, Frisch, 01/2009
- [2] “Flying Capacitor Topology for Ultra Efficient Inverter Applications”, Frisch, Temesi, 01/2021
- [3] “The Advantages and Operation of Flying-Capacitor Boosters”, Antoni, 10/2020
- [4] Figure 1: Statistics from IEA PVPS report “Trends in Photovoltaic Applications 2020” (International Energy Agency, Photovoltaic Power Systems, Technical Collaboration Programme)
- [5] Figure 2: Statistics from SolarPower Europe 2020 report



Electronic
Concepts

Film Capacitor Innovation Without Limits

www.ecicaps.com

LH3 Series



TOLERANCES
(EXCEPT AS NOTED)
0.5 mm

**ESL 7nH
typical**

- ✓ Film Capacitor Designed for Next Generation Inverters
- ✓ Operating temperature to +105°C
- ✓ High RMS current capability- greater than 400Arms
- ✓ Innovative terminal design to reduce inductance

Contact ECI Today! sales@ecicaps.com | sales@ecicaps.ie

Intelligent Power Modules (IPM) Contributes to Energy Saving and faster Time to Market

The past decades has been characterized by an increased request of attention to the environment and to reduce the global warming by increasing the efficiency of the systems. During that period of time, IPMs have been enlarging their presence on many application/ systems because of their high level of integration (Power Stage, Drivers, Protections and, in some cases) that makes easier and faster the designers' development phase, permits to reduce overall dimensions and get more reliable final products.

By Massimo Caprioli, Senior FAE at Fuji Electric Europe

Fuji Electric has developed and is now starting to introduce the 7th Generation IGBT-IPM – as heritage of previous technologies – a family of devices that will permit to reduce losses, improve the performances and save the space of mounting. These IPMs, by embedding the latest 7th Gen – X series chips (able to operate up to 175°C) and a new dedicated control IC, enables the system to operate at 150°C continuously, achieving loss reduction of about 10% and an output current increase of about 31%.

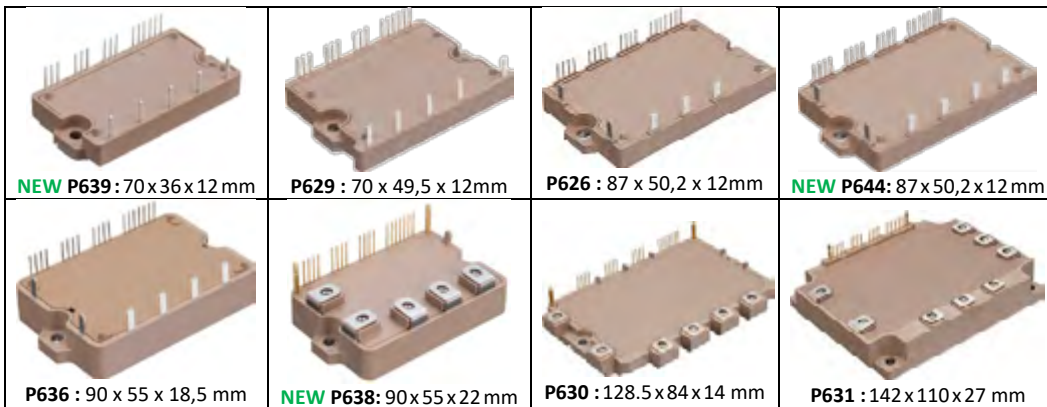
Since the releasing of the first IGBT module in 1988, Fuji Electric has been developing and using several technology innovations to achieve loss reduction, size shrinking, higher power density and improved reliability to satisfy the unceasing demanding request of the market. This permitted the designers to implement smart technical solutions and get high performances on their systems whatever consumer, industrial and automotive they were. IPMs followed this approach issuing a higher level of integration by embedding a driver (control circuit and protections) dedicated to the IGBTs chips used into the module. Within the new 7th Gen IPMs, the first thing that comes up to a first glance is the various lineup of package.

Each manufacturer has followed his own way adapting the design to its best package solution:

Fuji Electric decided to have package compatibility with its previous 6th Gen V-series IPMs to permit existing users to get some performance improvements on those systems already in production. As well, taking advantage from the new 7th Gen dice/chip size and technology, 3 new packages like the P638, P639 and P644 having smaller layout but same current capability and thermal performances of bigger packages are introduced. Depending on package, the 7th Gen X-series IPM is providing full inverter (6 in 1) configuration as well as inverter plus brake (7 in 1) topology for both 650V and 1200V technologies as shown in the table 1:

Product Line-up by Package, Vce and Iout					New		Conventional		Iout enhanced		
Rating	Config.	20A	30A	50A	75A	100A	150A	200A	250A	300A	450A
650V	6 in 1	P639									
				P629							
				P626							
	7 in 1			P638							
				P644							
						P636					
6 in 1						P630					
	7 in 1							P631			
1200V	6 in 1	P639									
				P629							
				P626							
	7 in 1			P638							
				P644							
						P636					
6 in 1						P630					
	7 in 1							P631			

Some of the modules mentioned in the table have high dissipation insulating substrate and Warning/Alarm for temperature control signals to output.



Everytime a new component is designed and produced, we consider all the materials used to get the performance at their top maintaining a high level of reliability.

Therefore, some technical improvements have been introduced to achieve such targets by focusing on chips/ dice, package materials, driving circuit and improved functionalities.

New UJ4C Series

Generation 4, 750V SiC FETs



Say Hello to the Future!

Introducing the industry's first 750V high performance SiC FETs.

- More design headroom; excellent for 400/500V bus
- RDS(on): 18mΩ/60mΩ
- Superior performance and efficiency
Figures of Merit
 - Best-in-class RDS(on) x Area delivers 45-75% lower conduction losses for a given footprint and package type
 - Hard switched: Lowest total losses based on low Eoss / Qoss x RDS(on)
 - Soft switched: Low RDS(on) x Coss(tr) enables higher power density
- Driven with gate voltages compatible with SiC MOSFETs, Si MOSFETs or IGBTs
- TO-247 in 3-lead & 4-lead Kelvin source
- AEC-Q101 qualified

► [Learn more at unitedsic.com/gen4](https://www.unitedsic.com/gen4)



FETJet™ CALCULATOR

Evaluate UnitedSiC devices in a variety of circuit topologies to quickly and confidently make data-driven design decisions.

- Instantly select optimal SiC device
- Delivers loss and thermal estimates

► [DESIGN NOW unitedsic.com/fet-jet](https://www.unitedsic.com/fet-jet)

New 7th Gen Chips/Dice

The 7th Gen IPM is using the latest Fuji Electric chip technology that brought some improvements which can be summarized as:

- Thinner drift layer = reduced $V_{CE(sat)}$ and E_{off}
- More fine pattern of trench pitch = improved of trade-off characteristics
- Optimized Field-Stop layer = improved breakdown voltage and low leakage current at high temperature
- Miniaturization = increased channel density (chip per module) / increased power density

These dices/chip technology are integrating 2 sensors :

- Current that mirrors the flow in the main emitter terminal,
- Temperature placed in the middle of the chip providing its real junction temperature.

these functions are used by the internal protection circuit to warning and alarm/shut-down the power section in case of issues before they can lead to the module disruption.

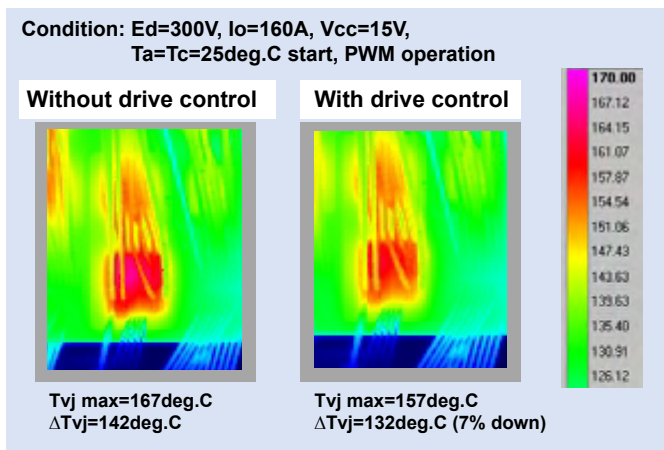
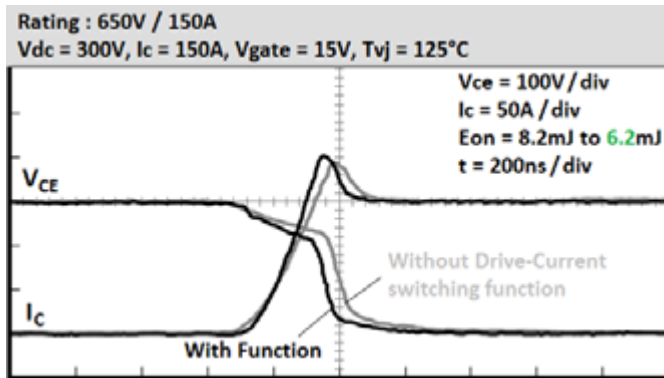
Driving Control Circuit

In order to get the best performance possible (loss, thermal, switching response, EMI/EMC, etc.) a dedicated new driver circuit has been designed and embedded into the 7th Gen IPM.

The 7th Gen IPM comes with a dedicated turn-on drive-current function that maintain the same high performance over the high temperature operating range.

At high temperatures, this function increases the current driving of the IGBT and reduces the turn-on loss; as well, the IGBT temperature is detected on chip to enable the changing of drive-current at optimum timings.

The improved switching performances and the reduced turn-on loss set up by the drive-current function used in the 7th Gen IPMs is shown in the figure below:



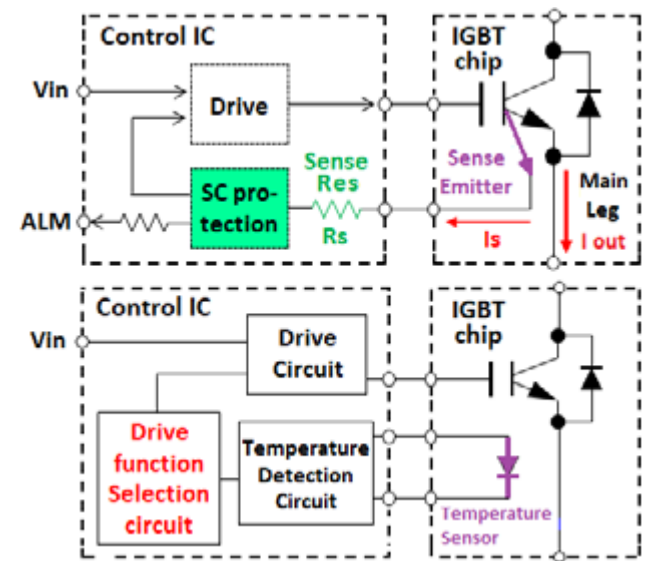
This new function reduced the turn-on loss of about 24% compared to the without the drive-current control.

The drive-current function has also optimized the switching characteristics to get much lower impact on the emission noise.

In addition, the operating behavior of this new circuitry in conjunction improved the thermal response too. It has been measured a reduction of about 7% despite the miniaturization of the chips and the reduced dimensions of some packages as well as the increased power density, as shown in the figure **below** :

Protection Circuit

The reduced on-voltage achieved by increasing channel density enhances current flow and, by consequence, reduces short-circuit withstand capability. So, the 7th Gen IPM is made faster the operation of the short-circuit protection and improved the protection circuit too.



The 7th Gen IPMs are using chips having current and thermal sensors integrated on it to provide fast reaction time and 3 kinds of protections circuits:

- Over Current / Short Circuit (fast intervention : 1µsec)
- Thermal / Over Heating (warning and alarm thresholds)
- Under Voltage Lock Out

which are delivering on the output – to the microcontroller – the related warning and alarm output signals that identify the fault occurred.

Warning and alarm signals are brought out on 2 output terminals where the alarm output permits to discriminate the fault occurred by means of 3 different length pulses over just one wire to properly manage the event and build-up a maintenance log report.

The warning signal is not influencing the operation of the IPM, besides the alarm signal stops the input signals – coming from the microcontroller – and shut-down the power section to preserve the module integrity from destruction.

Therefore, when the additional temperature-warning signal is set to the output, the IPM continues to operate as per the PWM signals sent by the microcontroller.

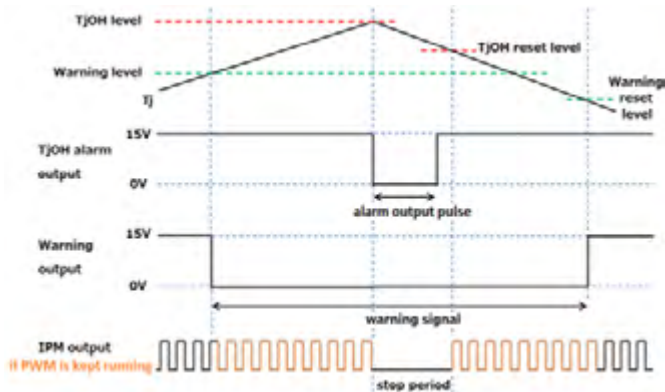
In particular, if an equipment has a cooling failure (such as fin clogging, fan failure, compound depletion, etc.), a temperature warning signal will be sent to the microcontroller when the IGBT chip reach a certain temperature threshold.

The microcontroller having received the warning can decide to modify the PWM control to reduce the load current or stop it depending on system requirements.

By consequence, the designer can apply a smart way to follow the temperature variations and wisely manage the warning / alarm signals:

- by managing the PWM signals sent to IPM's inputs,
- and/or wait the automatic stop released by internal protection circuit.

as shown in the figure below.



Another improvement has been added in the "7 in 1" configuration where the 7th Gen IPMs are including an independent brake circuit that is not affected by the protection circuits during the issuing of alarms; this allows, in motor control application, to operate in regenerative mode.

In conventional IPMs, when after a failure detection an alarm of lower arm is set, the protection circuit deactivates the whole lower arm to stop all the operations.

Therefore, the brake IGBT will also be deactivated and the brake circuit would not be able to regenerate the energy created by the rotating motor so that the DC link voltage will tend to increase. The new 7th Gen IPM function will prevent overvoltage breakdown issues unless an abnormality occurs in the brake circuit. All the 7th Gen IPM improvements shown above are thus ensuring a high level of overall reliability.

Conclusion

The past decade has been characterized by an increase of expectation to contribute to power save and conservation by means of an efficient use of energy in order to mitigate the global warming and help to achieve a responsible and sustainable growth.

Having in mind such a request and purpose, Fuji Electric developed and offers the 7th Gen / X series Intelligent Power Modules, a family of "easy to use" devices that facilitate the aim of developing higher efficiency, more reliable, compact circuits and cost saving solutions for industrial application like motor control, air conditioning, elevators, pumps, compressors, fans, etc.

These versatile components - "an almost Plug and Play solution" - can help designers and systems manufacturers to shorten the development time, improving the overall requirements and performance expectations and be quickly ready to sell their systems satisfying the Time to Market challenging requests. All the above makes the Fuji Electric 7th Gen X Series IPM a very attractive device for many applications.

www.fujielectric-europe.com

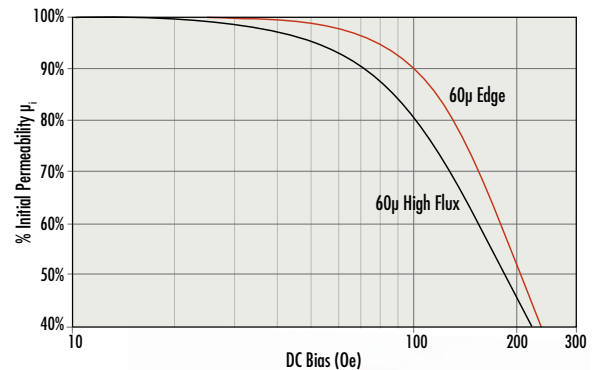
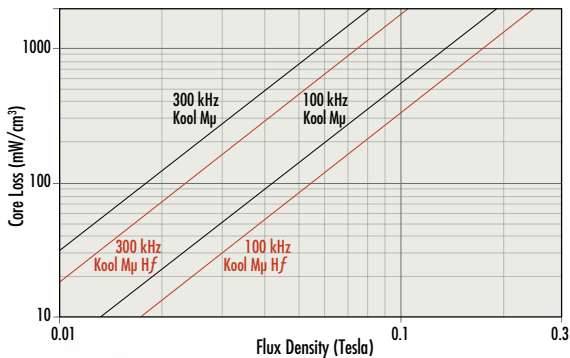
Kool M μ [®] Hf Powder Cores

Lowest Losses for High Frequencies
Optimized for 200-500 kHz

Edge[®] Powder Cores

Best DC Bias for Cutting Edge
Performance and Compact Design

VISIT US AT PCIM DIGITAL DAYS



www.mag-inc.com



Extreme GaN – What Happens When eGaN[®] FETs are Exposed to Voltage and Current Levels Well Above Data Sheet Limits

Recently, Efficient Power Conversion (EPC) did a series of tests to take eGaN FETs beyond their data sheet limits to quantify the effects of large amounts of overstress voltage and current and the results are published here for the first time.

*By Robert Strittmatter, Alejandro Pozo, and Alex Lidow
Efficient Power Conversion*

GaN transistors, and more recently integrated circuits, have been in mass production for over a decade [1] with several manufacturers reporting tens of millions of units shipped with billions of hours in actual end-use applications. The track record has been extraordinarily successful, and one of the key reasons is that GaN devices are far more rugged than their silicon MOSFET ancestors [2].

Beyond Data Sheet Voltage Limits

EPC tested several fifth generation 100 V-rated EPC2045 eGaN FETs with up to 150 V drain-source bias under hard-switching conditions described in [2]. Figure 1 shows the normalized $R_{DS(on)}$ of the EPC2045 devices being hard-switched at voltages ranging from 60 V to 150 V. At lower drain voltages within datasheet limits, the model predicts no or small $R_{DS(on)}$ increase that grows linearly with the $\log(t)$. At extreme voltages, over datasheet limits, the growth begins to deviate from the linear dependence on $\log(t)$. In this figure the $R_{DS(on)}$ is extrapolated using methods described in [2] to project out to 10-year operation. These projections, superimposed on the actual data, are derived using the physics-based models based on hot carrier injection and trapping that were developed in [2].

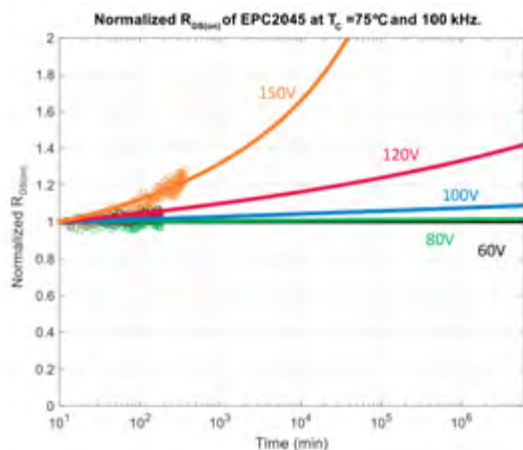


Figure 1: Measured and normalized values for $R_{DS(on)}$ of a 100 V-rated EPC2045 at 75°C under various hard-switched voltages. Solid lines are the predicted results under these conditions using the hot carrier injection trapping model of [2].

Figure 2 shows the impact of temperature on the rate of increase in $R_{DS(on)}$ with the predicted values from the model superimposed on the plot. Model agreement is good and, as previously reported, there is a reduction in trapping with increasing temperature, so it is expected that $R_{DS(on)}$ would shift less at higher temperatures. It is important to note that the devices do not fail abruptly because of this extreme voltage over-stress.

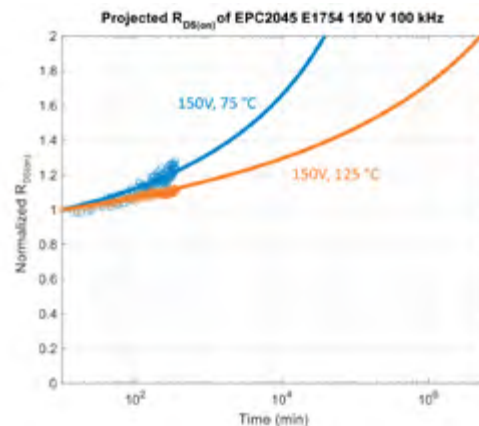


Figure 2: Measured and normalized values for $R_{DS(on)}$ of a 100 V-rated EPC2045 hard-switched at 150 V at two different temperatures. Solid lines are the predicted results under these conditions using the hot carrier injection trapping model of [2].

Beyond Data Sheet Current Limits

EPC tested several parts to over 500,000 cycles under short-circuit conditions that caused device currents that were about four times the maximum rated pulse current listed on their data sheets. In the test setup, gate bias of either 5 or 6 VDC was applied to the device under test (DUT) gate. Drain bias was set at 10 VDC and a 60 mF capacitor was connected across the drain supply. A low $R_{DS(on)}$ high side transistor in series with the DUT controlled the otherwise unlimited flow of current. The control transistor was then pulsed with 5- μ s pulses at 1 Hz to give the channel time to re-equilibrate. Table 1 shows the various types of devices tested, their data sheet rating for maximum pulsed current, and the amount of short-circuit current that pulsed through the device during each cycle at the start of the test.

- Custom Design
- 1 kV to 100 kV
- Up to 150 kJoule per single Element
- Total Safety

Table 2 shows the various key device parameters for a representative device, the EPC2051, a 1.1 mm² device from the fifth-generation family of eGaN FETs. Even under these extreme conditions of 150 A pulses that are four times the data sheet maximum ratings, all electrical characteristics remained within data sheet specifications. There was, however, a small reduction in the amount of short circuit current “consumed” by the DUT over time, consistent with the small increase in V_{TH} .

Device	Type	Datasheet Pulsed (A)	V_{OS}	Mean (A)	Sigma (A)
EPC2203	80V AEC Gen4	17	5	63	4.3
			6	79	4.6
EPC2212	100V AEC Gen4	75	5	226	3.9
			6	292	6.4
EPC2051	100V Gen5	37	5	124	1.8
			6	158	2.4
EPC2052	100V Gen5	74	5	268	2.9
			6	297	4.0
EPC2207	200V Gen5	54	5	180	8.6
			6	241	9.1

Table 1: Devices tested under extreme pulsed short circuit current, typically four times the maximum data sheet limit.

EPC2051	t = 0	100k Pulses	500k Pulses	Post 10 min. 175 °C Anneal
V_{TH} (V)	1.8	2.0	2.1	1.8
I_{GSS} (uA)	11	33	55	23
I_{DSS} (uA)	7	5.5	5.1	5.6
R_{DSON} (mΩ)	22	22.3	22.3	22
$I_{short\ circuit}$	152	141	135	150

Table 2: Key device parameters for EPC2051 at the start of pulse testing, after 100 k pulses, after 500 k pulses, and after a 175°C, 10 minute anneal. Device parameters stayed within data sheet limits at all times.

After this 500k pulse sequence, this part underwent an unbiased 10 minute anneal at 175°C. As can be seen in the right-hand column of Table 2, the electrical parameters and short-circuit current recovered to near their values before being subjected to repetitive pulse stresses. This recovery indicates that no permanent damage occurred from repetitive high-current pulses.

How to Use This New Information

EPC does not recommend using the information in this document instead of the parameters and maximum conditions listed in the product data sheets. EPC is testing under extreme conditions to better understand and characterize intrinsic failure mechanisms that will lead to better performance and reliability in future generations of eGaN transistors and integrated circuits. EPC is continuing these tests on large, statistically significant sample sizes and based upon results may increase the absolute maximum limits on data sheets of existing products in the future.

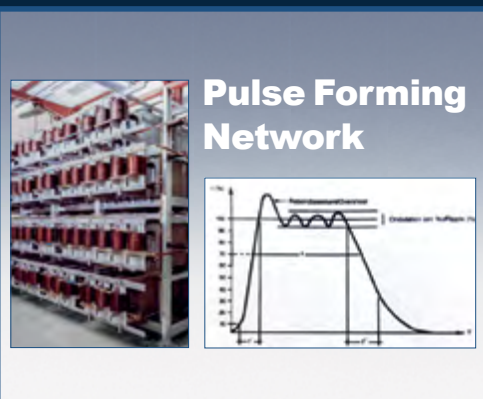
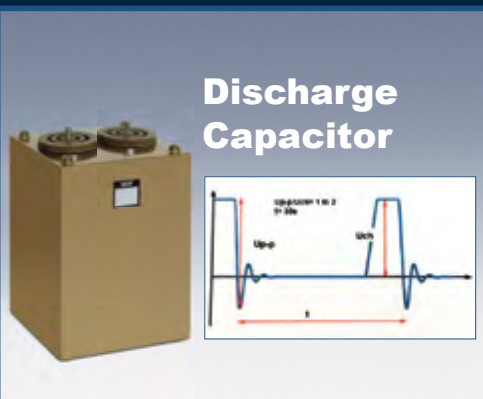
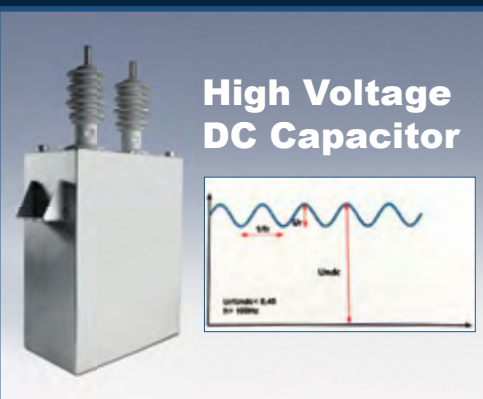
Conclusions

GaN is an amazing new semiconductor material with especially high potential in power conversion applications. In the eleven years since they first went into mass production, eGaN FETs have demonstrated field reliability well in excess of the aging power MOSFET [2] for two key reasons; (1) eGaN devices are designed using a test-to-fail methodology [3] that pinpoints intrinsic

failure mechanisms that can be attenuated or eliminated in subsequent technology generations, and (2) wide bandgap devices, in general, are less susceptible to degradation due to temperature. In fact, the intrinsic failure mechanisms for gate-voltage stress and drain-source voltage stress have a negative temperature coefficient making operation under extreme conditions for long periods of time a practical new tool for power system design engineers.

References

- [1] A. Lidow, M. de Rooij, J. Strydom, D. Reusch, and J. Glaser, GaN Transistors for Efficient Power Conversion. Third Edition, Wiley, ISBN 978-1-119-59414-7.
- [2] Alejandro Pozo, Shengke Zhang, Gordon Stecklein, Ricardo Garcia, John Glaser, Zhikai Tang, and Robert Strittmatter, “EPC eGaN Device Reliability Testing: Phase 12,” Available: <https://epc-co.com/epc/Portals/0/epc/documents/product-training/Reliability%20Report%20Phase%202012.pdf>
- [3] A. Lidow, R. Strittmatter, S. Zhang, and A. Pozo, “Intrinsic Failure Mechanisms in GaN-on-Si Power Transistors,” IEEE Power Electronics Magazine, December 2020.



LTspice® Emulation Models for the RidleyBox® and AP310 Analyzers

Unpredictable and widely varying power stages and controllers demand measurements in the lab to confirm proper and reliable design information. The same techniques can be applied to simulation of your circuits. In this article, we describe a fast and high-performance frequency response analyzer circuit model for LTspice®.

*By Dr. Ray Ridley, Art Nace and John Beecroft
Ridley Engineering, Inc. Camarillo, California USA*

This model uses past foundational work by Mike Engelhardt [2] coupled with our advanced knowledge of the real-world functioning of hardware analyzers.

This gives access to the following:

1. Fast and clean simulation of the Bode plots,
2. Predictions for circuits that have no small-signal model available, and
3. Better results than small-signal models

Hardware Laboratory Instruments

There are more frequency response analyzers available on the market now than when I began in the power electronics business in 1981. Two of the best are the [AP Instruments Model 310](#) analyzer from AP Instruments, and the new [RidleyBox®](#) from Ridley Engineering. These two products span the range of analyzers from a high-end product to a complete and affordable product solution.

The features of the AP310 are crucial for obtaining reliable noise-free measurements. There is much to be learned from this analyzer that we will apply to achieve good results in the LTspice models within this article. We also implemented as many of these features and techniques as possible to the RidleyBox. In this article we will show how to emulate these analyzers in LTspice® models. You can learn more about other analyzers and measurement techniques in reference [1].

Emulating Frequency Response Analyzers in LTspice

The paper in reference [2] describes the fundamental techniques used for measuring transfer functions in LTspice®. For a test example, we set up a 100 kHz buck converter operating with voltage-mode control. The



AP310 and RidleyBox Test Equipment

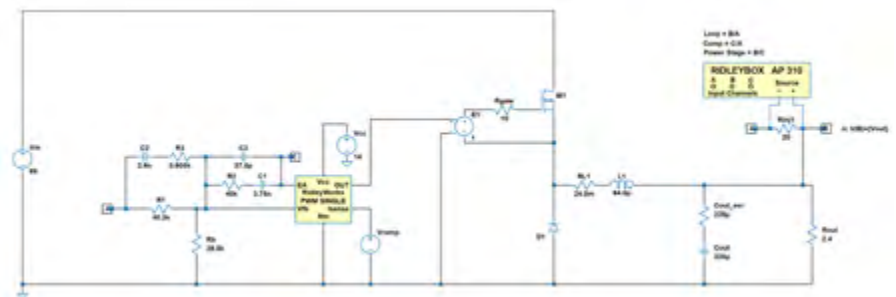


Figure 1: Buck converter test circuit with Frequency Response Analyzer subcircuit in LTspice®.

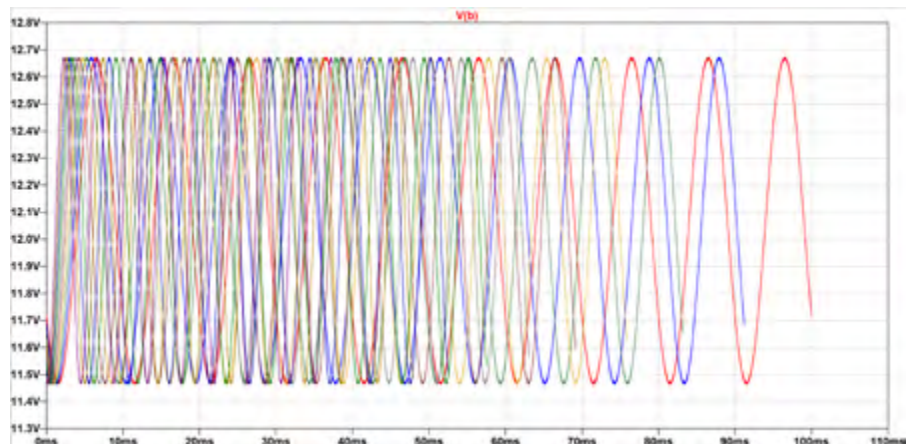


Figure 2: Typical simulation waveforms of original analyzer circuit and commands. Individual sinewaves are injected one at a time.

analyzer was first set up with the original suggestions in [2], not using any of our advanced features. The schematic of the test circuit is shown in Figure 1.

Figure 2 shows the simulated output voltage of the converter as the analyzer sweeps from 100 Hz to 100 kHz. Each frequency is injected one at a time, and simulation waveforms are processed to extract the gain and phase response.

You can clearly see the problems in this plot. While the overall shape of the loop is present, there is a lot of noise at both low and high frequencies. This is not a curve that instills confidence in design credibility. The long processing time discourages further attempts at reducing the noise since this usually entails even longer simulation times.

In the original paper, one schematic suggests using 10 cycles of simulation at each frequency, and the other schematic suggests 25 cycles. The simulation of Figure 3 implemented 10 cycles, so we would anticipate a 37-minute simulation time with 25 cycles.

Anyone who has run a real frequency response analyzer in the lab on their hardware knows that the same kind of results are obtained if you do not have the instrument settings dialed correctly. We frequently see analyzers sitting unused on the shelf in companies and hear the comment that “no one remembers how to use it properly”.

The same is true for the simulation of the swept loop gain in LTspice®. You have to know how to control the emulated instrument properly. We have introduced 7 new control parameters to the analyzer setup to emulate the features of the AP Instruments analyzer and the RidleyBox. These new controls are:

- 1) Start Amplitude
- 2) Finish Amplitude
- 3) Start Break Frequency
- 4) Stop Break Frequency
- 5) Dwell Time
- 6) Bandwidth
- 7) High Frequency Noise Reduction

The profound effect of these combined control settings can be seen in Figure 4. The swept loop gain is now perfectly smooth and can be reliably used for design and for worst-case analysis of a finished design. This is now a serious tool for the power designer.

In addition to the very smooth curves, there is a drastic reduction in the simulation and processing time. It is now under three minutes—six times better than the original

analyzer settings. While smoothing out the curve is the main priority to make this a credible tool, we will see later that even faster sweeps are possible once this is done.

Advanced Analyzer Settings

In the world of analyzer hardware, AP Instruments introduced the first variable and programmable source in 1995. This was implemented at our request since we knew it was crucial to change the source size with frequency as you sweep a loop. That experience was learned after many years working in front of an HP4194A where you had to constantly adjust the source size while the loop was sweeping.

The same feature must be implemented in the software version of a good frequency response analyzer if you expect to see good results. Figure 5 shows how the source varies with frequency as you sweep from low to high values. In this example, the initial injection is 2 V, and the final value is 0.1 V. For the sweep in Figure 3, the initial set point was 0.6 V, and the final value is a very small 3 mV. The system measured does not have a lot of phase margin, and the injection must be kept small to avoid nonlinearities and a distorted curve.

On the LTspice® schematic, the source is set with the following parameter commands, and the RidleyBox/AP310 component uses these values to adjust the source as the frequency is swept from low to high.

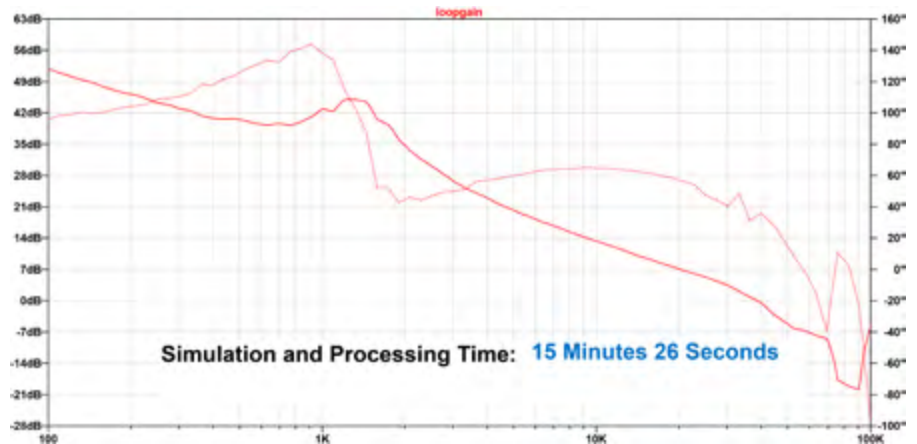


Figure 3: Loop gain using original paper settings (10 mV signal).

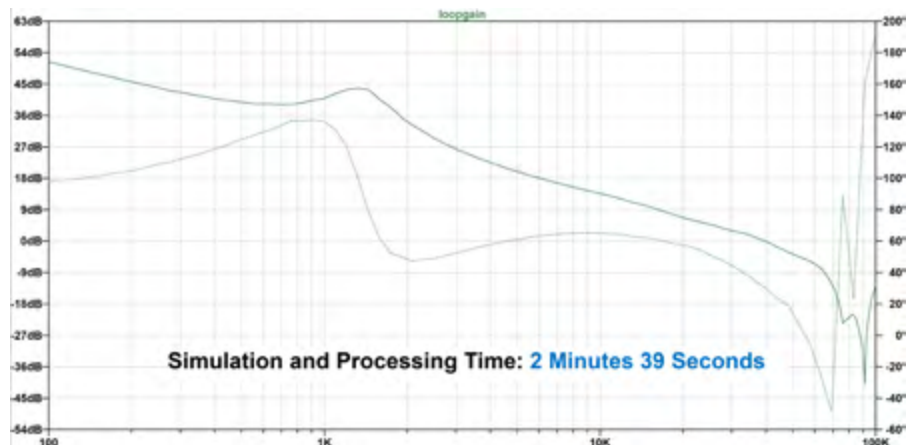


Figure 4: Swept loop gain using advanced analyzer settings and noise reduction.

TIGRIS
Elektronik GmbH

**Individual Solutions
for Your Success**

- Our work begins with listening
- We develop a detailed understanding of your application
- We design and manufacture power electric systems optimally suited to your application
- From several watts up to the 1-MW range
- From a few units up to several thousand units per year
- Certified to ISO 9001 and ISO 13485

Just talk to us.

Visit our virtual expo stand on 3rd to 7th May 2021 at messe.tigris.eu or simply phone us on +49 (0)30-76 88 083-0

TIGRIS Elektronik GmbH
Teltowkanalstraße 2 · 12247 Berlin · Germany
Phone +49 (0)30 - 76 88 083 - 0 · www.tigris.eu

SOURCE AMPLITUDE

```
.param Start_Amp=0.6
.param Finish_Amp=0.3m
.param LFBreak=500
.param HFBreak=20.00K
```

Start_Amp should not be larger than about 5% of the dc output voltage. A high value is needed here to be able to measure the very low input channel reliably.

Finish_Amp is a much smaller number—usually less than 10% of the start amplitude. For sensitive, low phase margin systems such as that in Figure 3, the value must be reduced until no distortion in the curve is observed. This is very much an empirical process, both in the lab with test hardware, or when using LTspice® to emulate the hardware.

LFBreak is the frequency at which the signal starts to reduce from its initial value. Typically, this is 1-10% of the anticipated crossover frequency.

HFBreak is the frequency at which the signal reaches its final value. This is usually just before the anticipated crossover frequency.

The measurement resolution is set with the following commands:

RECEIVER RESOLUTION

```
.param RidleyBoxDwell=1m
.param RidleyBoxBW=1
.param RidleyBoxNR=2000
```

RidleyBoxDwell is the settling time after starting each new frequency. There must be enough time to allow the natural system transients to stabilize.

RidleyBoxBW determines the receiver bandwidth for the measurement channels. A low number indicates the fastest sweep. More difficult and noisy systems may require a higher number than 1 to improve the sweep smoothness.

RidleyBoxNR determines the frequency at which additional noise reduction is introduced. This technique is unique to the emulated analyzer and is not needed for hardware testing.

High-Speed Sweep Settings

When you are involved in design, you want sweeps to be as fast as possible for multiple iterations of a design. In this case, you can start at a frequency below the resonant frequency of the LC filter (to confirm its proper location) and use fewer data points. The curve is not quite as smooth, but you can see that it is more than sufficient for design with a sweep time under 30 seconds. This is truly amazing – LTspice® was never regarded as a practical platform for this kind of work in

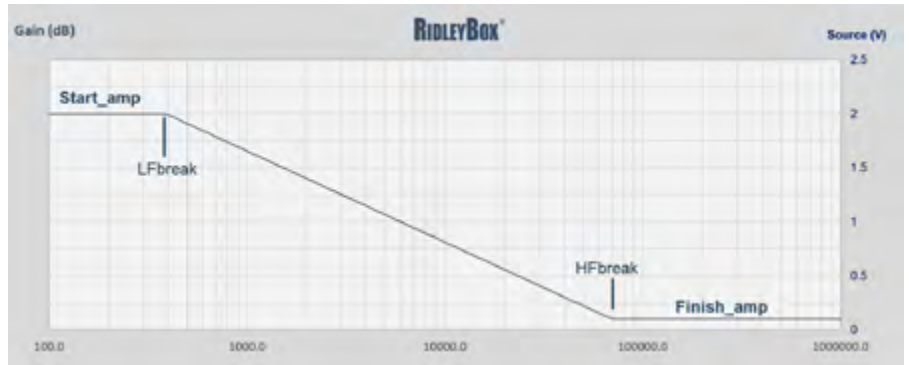


Figure 5: RidleyBox/AP310 LTspice® component variable source profile.

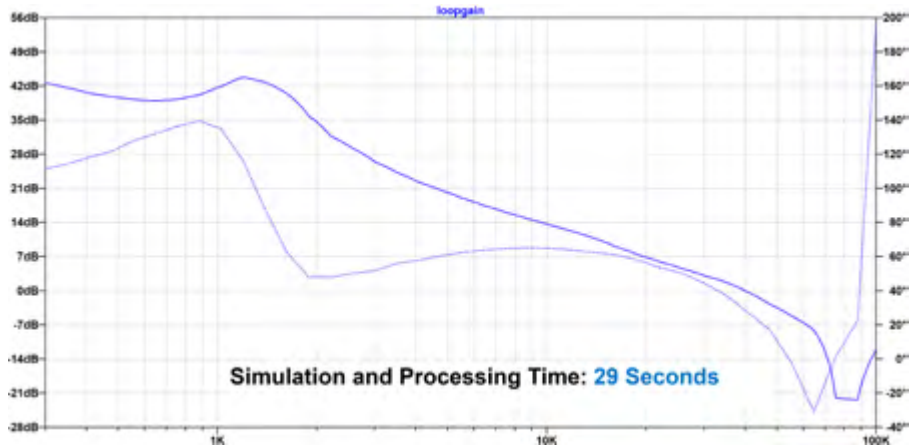


Figure 6: High-speed swept loop gain – start at 300 Hz, 15 points/decade.

the past. When you are involved in design, you want sweeps to be as fast as possible for multiple iterations of a design. In this case, you can start at a frequency below the resonant frequency of the LC filter (to confirm its proper location) and use fewer data points. The curve is not quite as smooth, but you can see that it is more than sufficient for design with a sweep time under 30 seconds. This is truly amazing – LTspice® was never regarded as a practical platform for this kind of work in the past.

Summary

In this article we have shown that you can combine knowledge of frequency response analyzers with the features of LTspice® to obtain fast and dependable Bode plots for design and final system analysis. This is not a feature typically associated with LTspice®, and it opens up a new way to analyze systems without having small-signal models.

In the next article of this series, we will show how this approach will provide better results than small-signal models. We will also show how most small-signal models have fundamental limitations in their application to high-performance systems.

This should be a relief to many engineers. Deriving small-signal models is a very time-consuming process and accurate models simply do not exist for many systems.

References

1. [Frequency Response Measurement Two-Hour Masterclass](#). An extended training session with live measurement examples on switching power supplies.
2. [Building a Frequency Response Analyzer in LTspice®](#) by Mike Engelhardt.
3. [RidleyWorks™](#) design software contains complete analyzer models with automated setups for your power supply application and for LTspice emulation of frequency-response analyzers.
4. Learn power supply design in our [Hands-on Workshops](#) for power supply design.
5. Join over 5,000 engineers on our Facebook group titled [Power Supply Design Center](#). Advanced in-depth discussion group for all topics related to power supply design.
6. [Injection isolators](#) for loop measurement. Learn why the Ridley Isolator outperforms anything else on the market.

If only: designing smaller, faster chargers was easier...



The world's first MasterGaN 600V half-bridge driver with two integrated GaN power transistors



ACCELERATE THE CREATION OF NEXT-GENERATION COMPACT AND EFFICIENT CHARGERS AND POWER ADAPTERS

Advantages of our MasterGaN platform embedding a half-bridge driver based on silicon technology along with a pair of gallium-nitride (GaN) transistor.

- **Higher efficiency:** reduced power losses and power consumption that exceed the most stringent energy requirements
- **Higher power density:** higher switching speed reduces systems size and cost. Four times smaller than a traditional silicon solution
- **Faster time-to-market:** packaged solution simplifies the design and ensures a higher level of performance
- **More robust:** offline driver optimized for GaN HEMT for fast, effective and safe driving and layout simplification

Board area and weight are becoming limiting factors as power demands increase. Reducing size and weight can **cut the total cost of ownership** by making **installation and maintenance both easier and quicker**.

Part number	General description	Supply voltage max (V)	Key features	Output Current max (A)	High side $R_{DS(on)}$ (mΩ)	Low Side $R_{DS(on)}$ (mΩ)
MASTERGAN1	High power density 600V half-bridge high voltage driver with two 650V enhancement mode GaN HEMT	11	Undervoltage lockout, interlocking function, Over-temperature, Bootstrap diode	10	150	150
MASTERGAN2				6.5	225	150
MASTERGAN4				6.5	225	225



EVALMASTERGAN



EVLIMG1-250WLLC



www.st.com/mastergan

Gallium Nitride (GaN) Power ICs: Turning Academic Dreams into Industry Reality

Gallium nitride (GaN) is the key enabler for high-frequency, and simultaneously high-efficiency topologies.

Like Leonardo da Vinci (1452-1519) and his amazing inventions, including the 'helicopter' and 'robotic knight', electronics academics have long been frustrated that their ideas cannot become reality due to the limited materials available at the time.

Leonardo would be amazed at today's lightweight alloys and tiny, high-speed electric stepper motors compared to his rudimentary ironwork and waterpower.

Now, old, slow, lossy silicon chips are consigned to history, as new, fast, efficient gallium nitride (GaN) power ICs turn academic dreams into industrial reality from mobile fast chargers to data center power supplies.

*By Tom Ribarich and Stephen Oliver,
Navitas Semiconductor*

Gallium Nitride¹: High-Speed Enabler

High-speed – or rather – high-frequency power topologies mean smaller and smaller passive components, to the extreme case that in a 40 MHz phi-2 converter at Stanford Universityⁱⁱ, the ferrite material completely disappears in an 'air-core' inductor.

The flyback converter has had several proposed improvements, such as the high-frequency quasi-resonant (HFQR) from Professor Fred Lee at Virginia Polytechnic (VPT) in 1988ⁱⁱⁱ, and R. Watson's active-clamp flyback (ACF), also from VPT in 1996^{iv} which eliminated snubber loss. However, in each case, the output capacitance (C_{OSS}) of the silicon MOSFET created such high switching losses that implementation was not feasible – so no commercial control ICs would be financially viable.

Twenty years later, in 2016, a prototype 25 W^{vi} ACF switching at 1 MHz was designed by Xiucheng Huang at VPT using Navitas GaN-Fast power ICs and a TI DSP controller (C2000). Further MHz work using a GaNFast half-bridge power IC was completed at Zhejiang University in 2019^{vii}. Though tiny designs, the DSP is designed for high-power industrial applications, and has a relatively high leakage current. As a result, the designs couldn't meet US DoE Level VI^{viii} low-power standby requirements – in effect from February 2016 - so were not commercially practical.

GaNFast power ICs were the enabler for high-frequency systems, based on a) GaN's physical advantages over silicon, and b) robust^{ix} performance and ease-of-use resulting from monolithic integration of GaN power (FET) and driver, plus protection and control. Since mass production release, GaNFast power ICs have been rated at 2 MHz which is 20x faster than typical converter switching frequency of 50-60 kHz.

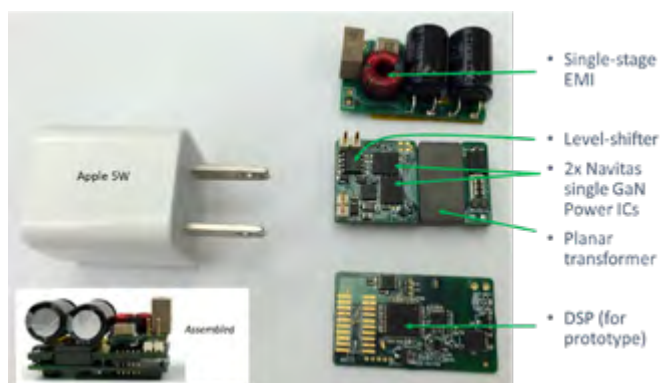


Figure 1: Left: High-performance, high-frequency 1 MHz 25 W active-clamp flyback (ACF) prototype from CPES (Virginia Polytechnic), using Navitas gallium nitride (GaN) power ICs, planar transformer and C2000 DSP. Prototype achieved 17 W/in³ (estimate, cased).

A reliable, high-performance, high-speed GaN powertrain meant that control IC companies could confidently invest time and resources to design and release speed-optimized ASICs which met DoE Level VI requirements and be part of cost-effective system bills of material (BoMs). The first Level VI-compatible high-frequency controller was the TI UCC28780 with a headline peak frequency of 1 MHz for ACF, which was used in the world's first, and thinnest 45W USB-C fast charger – the Mu One^x. This was quickly followed by the HFQR NCP1342 from On Semi, which increased switching frequency 4x from 50 kHz to 200 kHz, ending a frustrating 30-year wait.

A recent upgrade to ACF has been the 'Pulsed-ACF'^{xi}, as used in OPPO's 50W Mini "Cookie" charger, which achieves another 'vanishing act'. The electrolytic 'bulk cap' can occupy 40% of the total charger size but a proprietary innovation creates the world's first charger using 'pulsed' power conversion. This eliminates the electrolytic bulk capacitor, and the rectified 100 Hz pulsating DC feeds directly into the high-frequency ACF circuit which can maintain a smooth output to charge the phone's battery, even when the input voltage range is wide. A follow-on benefit is that OPPO-proprietary 'direct-charge' approach means that during each pulse gap, the polarization effect in the phone battery is eliminated so reducing wear-out mechanisms and extending battery life.



Figure 2: OPPO 50W Mini "Cookie" charger, showing high-frequency planar magnetics and elimination of electrolytic bulk capacitor.

Higher Power, Higher Speeds

As we move to higher powers (>75W), power factor correction (PFC) is required, and we also face the perennial problem of the lossy diode bridge rectifier.

Traditional PFC has been constant current (CCM) or discontinuous conduction mode (DCM) boost with a main switch and diode. GaN's wide band-gap sibling – silicon carbide (SiC) – has helped to

minimize diode drop and reverse-recovery losses. However, silicon's switching losses (specifically C_{OSS}) continued to limit frequency to around 50-60 kHz^{xii}. In a similar story to the ACF, the introduction of GaN power ICs spurred new PWM controllers. One example chip-set was the NCP1631 interleaved CrCM boost, NCP13992 LLC, and NCP4305/43080 SR PWM controllers as used in the world's smallest 300W reference design by Onsemi^{xiii}. This was the inspiration for the Asus / NVIDIA AC-48V 300 W laptop charger using GaN power ICs^{xiv}.

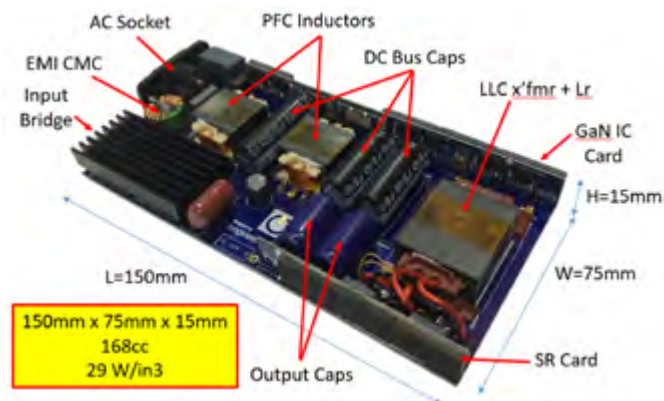


Figure 3: 300 W AC-19 V_{DC} reference design using GaN power ICs: Interleaved CrCM/DCM Boost using NCP1632 (with frequency-fold-back function to reduce power consumption), minimum 200 kHz (90 VAC, peak-of-line) to maximum 450 kHz. LLC using NCP13992 (with adaptive dead-time features, soft-start, comprehensive protection and HV start-up) and NCP4305/NCP43080 (SR), 500 kHz normal operation (with higher frequency during load / start-up burst conditions).

The next architectural advance was the 'bridge-less' boost PFC from Milan Jovanovic^{xv} which combined the AC bridge rectifier plus PFC circuit, and used two switches for AC-rectification and two more switches for the PFC function. This was described in 2008 and was used in high-power server AC-48V and AC-12V power supplies but remained low-frequency due to hard-switching silicon FETs, so had a small increase in efficiency but no change in power density. A later development was the 'totem-pole' variant^{xvi} but still only 50 kHz. With gallium nitride, the frequency-related limits of silicon are overcome, and high-frequency CrCM 'totem-pole' PFC becomes a reality.

Aluminium Electrolytic Capacitors Screw terminal Type

Aluminium Electrolytic Capacitors Snap in Type

Electrolytic Capacitors K1M and K2M

Metallized Polypropylene D.C. link Capacitors

Kendeil™

POWER ELECTRONIC CAPACITORS

For a 300 W laptop adapter, the upgrade from AC-bridge plus 50 kHz boost PFC, to 200-500 kHz CrCM totem-pole using a new Level VI-compliant PWM controller and new GaN power ICs like the NV6128^{xvii} achieves power density over 1.1 W/cc. This is 3x smaller and lighter than current tier-1 OEM designs.

Moving up in power and frequency, a prototype 3.2 kW AC-54 V data center power supply was built at the University of Texas, Austin using a 100% gallium nitride powertrain with an interleaved CrCM totem-pole PFC running from 350 kHz to 1.5 MHz (sweep using CrCM).^{xviii} 650 V GaN power ICs were used on all legs of the totem-pole and primary LLC, with 80 V GaN FETs on the secondary rectification side. Both PFC and DC-DC stages used planar magnetics and the C2000 DSP for control. As a data center SMPS is not classified as an 'external supply', the Level VI standby loss requirement does apply so in this case, the PWM controller was ready, waiting for gallium nitride to fulfill the academic's needs, achieving 4.4 W/cc (73 W/in³).

Gallium Nitride: Living the Dream

Even in the renaissance period, the rate of technological innovation could not keep up with Leonardo's dreams. Today, gallium nitride - in the form of the GaN power IC - delivers efficient, high-speed performance that has ended decades-long frustration; to fulfill academics' dreams and advance them to industry-proven realities.

References

- i "Gallium nitride", <https://www.navitassemi.com/gallium-nitride-the-next-generation-of-power/>
- ii Kinzer. "Breaking Speed Limits with GaN Power ICs", APEC 2016 Keynote, <https://www.navitassemi.com/articles/>
- iii F. C. Lee, "High-frequency quasi-resonant converter technologies," in Proceedings of the IEEE, vol. 76, no. 4, pp. 377-390, April 1988, doi: 10.1109/5.4424. <https://ieeexplore.ieee.org/document/4424>
- iv R. Watson, F. C. Lee and G. C. Hua, "Utilization of an active-clamp circuit to achieve soft switching in flyback converters," in IEEE Transactions on Power Electronics, vol. 11, no. 1, pp. 162-169, Jan. 1996, doi: 10.1109/63.484429.
- v D. Kinzer, Navitas "Welcome to the Post-Silicon World: Wide Bandgap Powers Ahead", keynote PCIM 2016.
- vi S. Oliver, T. Ribarich, "State-of-the-Art Mobile Charging: Topologies, Technologies and Performance", APEC 2017, Industrial Session IS05, <https://www.navitassemi.com/articles/>
- vii D. Gu, J. Xi and L. He, "A Digital PWM Controller of MHz Active Clamp Flyback with GaN Devices for AC-DC Adapter," IECON 2019, doi: 10.1109/IECON.2019.8927336. <https://ieeexplore.ieee.org/document/8927336>
- viii "Efficiency standards for external power supplies" [Level VI]. CUI, <https://www.cui.com/efficiency-standards>
- ix N. Fichtenbaum, "GaN Integrated Circuits for Power Electronics," 2019 Device Research Conference (DRC), doi: 10.1109/DRC46940.2019.9046333. <https://www.navitassemi.com/articles/>
- x "Navitas' GaNFast™ Enables World's Thinnest Travel Adapter", Navitas press release, March 2018, <https://www.navitassemi.com/navitas-ganfast-enables-worlds-thinnest-travel-adapter/>
- xi "GaNFast Power ICs Enable OPPO's 50W Mini 'Cookie' – the World's Smallest, Thinnest Fast Charger", Navitas press release August 2020, <https://www.navitassemi.com/ganfast-power-ics-enable-oppos-50w-mini-cookie-the-worlds-smallest-thinnest-fast-charger/>
- xii Gallium Nitride (GaN) output capacitance (COSS) is 20c lower than silicon at <30 V VDS. D. Kinzer, Navitas "Welcome to the Post-Silicon World: Wide Bandgap Powers Ahead", keynote PCIM 2016.
- xiii T. Ribarich, P. Bredemeier and S. Oliver, "GaN High Density 300W AC-DC Converter," PCIM Europe 2019. Paper at <https://ieeexplore.ieee.org/document/8767722>, poster at <https://www.navitassemi.com/articles/>
- xiv "Navitas Enables World's Smallest Adapter for World's Fastest Laptop", Navitas press release, October 2019, <https://www.navitassemi.com/navitas-enables-worlds-smallest-adapter-for-worlds-fastest-laptop>
- xv L. Huber, Y. Jang, and M. M. Jovanović, "Performance evaluation of bridgeless PFC boost rectifiers," IEEE Trans. Power Electron., vol. 23, no. 3, pp. 1381-1390, May 2008. <https://ieeexplore.ieee.org/document/4483680>
- xvi B. Su and Z. Lu, "An Interleaved Totem-Pole Boost Bridgeless Rectifier, etc." IEEE Trans. on Power Elec., vol. 25, June 2010, doi: 10.1109/TPEL.2010.2040633. <https://ieeexplore.ieee.org/document/5393032>
- xvii NV6128 650/800V gallium nitride (GaNFast) power IC: <https://www.navitassemi.com/download/>
- xviii Yu et al, "Monolithic GaN Power ICs Enable High Density High Frequency 3.2 KW AC-DC Rectifier," PCIM Europe 2018; Nuremberg, Germany, pp. 1-4. <https://ieeexplore.ieee.org/document/8402956>

www.navitassemi.com

POWER ELECTRONICS CAPACITORS



DC link capacitors ■ AC filter capacitors ■ Snubber capacitors ■ Energy storage capacitors



www.zez-silko.com



Extension of CoolSiC™ Easy family

New EasyDUAL™ with AlN ceramic for better thermal performance and improved EasyPACK™ 3-level module in ANPC topology

EasyPACK™ CoolSiC™ MOSFET power module 1200 V in 3-level ANPC topology

- > 3-level ANPC topology
- > CoolSiC™ MOSFET 1200 V
- > TRENCHSTOP™ IGBT7
- > Improved Si diode current rating supports the entire $\cos \phi$ range and is thus a perfect fit for energy storage

Benefits

- > 150 kW power in solar when two modules run in parallel mode
- > 75 kW power per module in energy storage systems

EasyDUAL™ CoolSiC™ MOSFET power module 1200 V in half-bridge configuration with AlN ceramic

- > Half-bridge configuration
- > CoolSiC™ MOSFET 1200 V
- > High-performance Aluminum Nitride (AlN) ceramic

Benefits

- > R_{thJH} improvement by 40%
- > Increased output power or longer lifetime
- > Minimization of cavity between module and heat sink

> Register for Infineon's Virtual Power Conference:
www.infineon.com/pcim



www.infineon.com/new-sic-modules



High-quality Power Semiconductor Modules now Support Lower Voltages

Hitachi ABB Power Grids Semiconductors is well known for its high-reliability power semiconductors that support medium and high voltage applications, including IGBT power semiconductors used in the main traction chain of rail rolling stock, press-pack devices used in HVDC (High Voltage Direct Current distribution) and other T&D (Transmission and Distribution) applications, as well as various power semiconductors used in industrial applications such as medium voltage drives. Building on its experience of high-performance, high-reliability devices for voltages above 3.3 kV, Hitachi ABB Power Grids is now strengthening its product portfolio with support for lower voltages.

By Tomáš Žlnay, Ladislav Radvan, Christian Winter, Roc Blumenthal, Tobias Keller; Hitachi ABB Power Grids

This article examines the use of power semiconductors in a low voltage drive with the general architecture shown below:

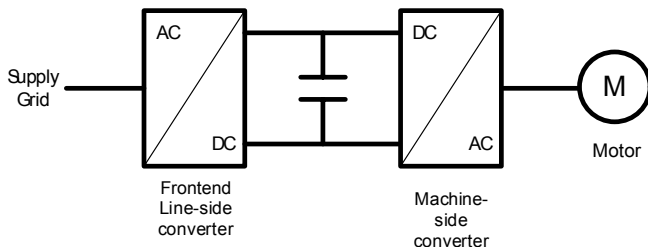


Figure 1: General architecture of a low voltage drive

The Front End, also called a line-side converter, converts an AC voltage to DC and supplies it to the DC-Link. Depending on the operating scheme, diodes, thyristors or even IGBTs might be used for this application. Typically products such as Hitachi ABB Power Grids Semiconductors' 60Pak diode and thyristor modules might be used because they feature industry-standard housings and very low losses together with the highest operating temperatures. This allows these devices to deliver the highest performance under load cycling, high thermal utilization, increased overload capability and many more benefits.



Figure 2: 60Pak BiPolar module

The 60Pak product family has a press-force construction, where the assembly is pressed by the main spring to the base plate (cooler) instead of a soldered connection. This construction produces a better performance, particularly improved reliability over the device's lifetime. The dual spring clamping system helps to achieve impressive IOL (Intermittent Operational Life) performance, longer lifetime and enhanced resistance to temperature changes. The dual spring system consists of the main square spring on the top and a pair of auxiliary springs. This unique setup enables close to ideal efficiency in a well-known hockey puck housing.

In the pictures below you can see the force distribution of the two-spring system compared with ceramic + metal and plastic insulator force spreaders.

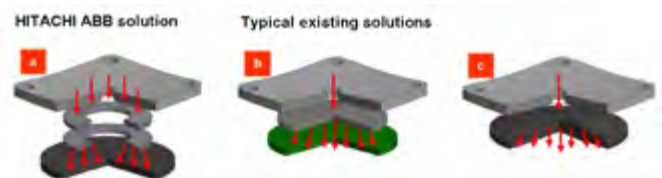


Figure 3: a) Dual spring construction, b) Ceramic + metal force spreader, c) Only plastic force spreader

The modules passed the reliability tests shown below:

Storage at high temperature $t = 1000\text{h}$, $T_c = 125^\circ\text{C}$	✓	High temperature reverse bias $t = 1000\text{h}$, $T_c = 125^\circ\text{C}$, $V_{AC(\text{peak})} = 2/3 V_{\text{RBM}}$	✓
Storage at low temperature $t = 500\text{h}$, $T_c = -40^\circ\text{C}$	✓	High humidity, high temperature reverse bias $t = 1000\text{h}$, 85% RH	✓
Thermal cycling load (intermittent operating life, power cycling) $N \geq 20\,000$ cycles, $\Delta T_j = 80^\circ\text{C}$	✓	Verification of maximum module ratings $T_j = T_{j\text{max}} = 160^\circ\text{C}$	✓
Change of temperature $T_c = -40^\circ\text{C} / 160^\circ\text{C}$	✓	Shock and vibration (mounted modules and in transport box)	✓
		Partial discharge $\text{Qpd} < 10 \text{ pC}$	✓

The results show that this approach to module design brings the performance and reliability associated with Hitachi ABB Power Grids, medium and high-voltage devices to lower voltages.

For the active Front End, or machine-side converter, that connects the DC-link to the motor, LoPak modules are a popular choice. These LoPak modules are now available for 1200 V voltage class systems, and with pre-applied TIM (Thermal Interface Material) that helps to increase reliability over the drive's lifetime.

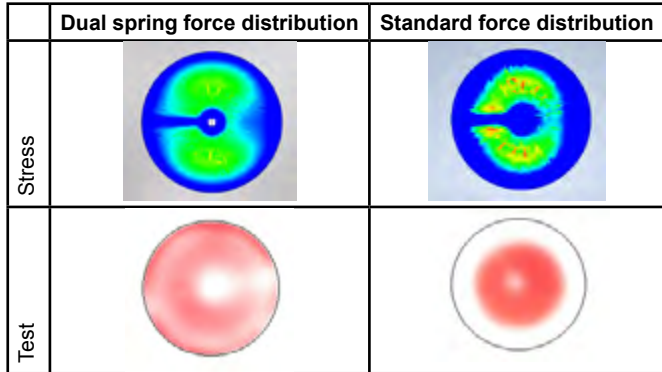


Figure 4: Comparison of standard force distribution with dual spring force distribution

Even at lower voltages, engineers not only want to create new inverter designs, but would also like the ability to upgrade their existing designs to handle higher power using the same module package. This allows a faster time-to-market, less disruption of manufacturing lines, and potentially lower unit costs.

Building on its experience of high-performance, high-reliability devices for voltages above 3.3 kV, Hitachi ABB Power Grids has expanded its product portfolio by introducing a family of 1200 V power modules to complement the existing 1700 V family, starting with a 1200 V, 900 A x 2 module using an upgraded LoPak module package.

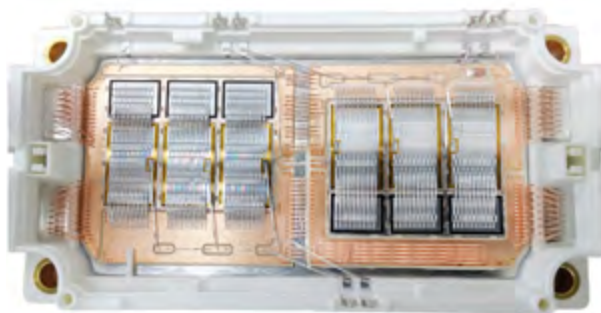


Figure 5: 1200 V, 900 A X 2 LoPak module

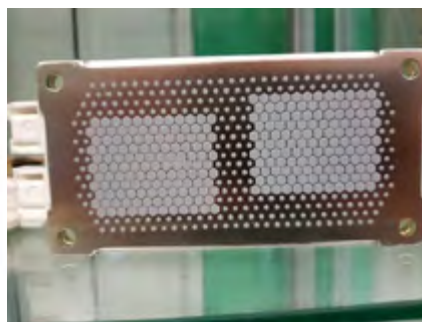


Figure 6: Module base plate with TIM

The "heart" of these new modules is the next generation of ultra-low-loss, rugged Trench IGBT technology used to fabricate the silicon switch and optimized diodes. The IGBT devices have an aggressive fine gate pitch cell with novel termination and a degradation-free technology developed by Hitachi ABB Power Grids. This allows the device to switch higher current densities using an optimized operation point, with ideal characteristics for alternative power (wind and PV) and industrial (motor driver) applications.

Using the existing LoPak module design enables additional transient over-current capability by taking advantage of the IGBT module's maximum operating junction temperature of 175 °C, compared to the typical 150 °C. The new 1200 V product is configured as a 900 A phase-leg (half-bridge) IGBT module, providing outstanding safe operating area (SOA) and over-temperature capability. Within its class, LoPak uniquely benefits from the know-how in robust electrical performance and high reliability.

Careful design and virtual prototyping ensured the LoPak module's current distribution is well-balanced during switching and is well controlled under overload conditions. Additional analysis was undertaken to understand the impact of the higher total current for the 1200 V, 900 A x 2 product housed in the LoPak package with respect to materials and parasitics. The existing LoPak1 housing already included the use of a copper (Cu) base plate, press-fit connectors for the control terminals and the option to have a pre-applied Thermal Interface Material (TIM) on the base plate to improve the thermal conductivity (R_{th}) of the module.

The analysis led to the redesign of the Cu pattern on the DBC substrate to place the chips in the best locations to minimize the temperature interactions, the stray inductance, capacitance and resistance of the package, and optimize the current sharing between the IGBT/diode pairs.

Property	Cu	Al
Electrical resistivity	1.7 $\mu\text{Ohm}\cdot\text{cm}$	2.7 $\mu\text{Ohm}\cdot\text{cm}$
Thermal conductivity	400 W/m ² K	220 W/m ² K
CTE	16.5 ppm	25 ppm
Yield strength	≈140 MPa	≈29 MPa
Elastic modulus	110-140 GPa	~50 GPa
Melting temperature	~1083 °C	~660 °C

Figure 7: Properties of Cu and Al

Other optimizations of the LoPak materials include changing the bond wire material to Cu for the DBC/DBC and DBC/power terminal, to take advantage of the Cu material properties to support the very high current levels. The number of wires has been increased and a coated Cu power terminal is now used to support the increased power rating (Figures 7 and 8). Other than these changes, the LoPak module form and function remain the same as before.

The new 1200 V family of LoPak module products carry the same DNA for high reliability and robustness as the entire family of Hitachi ABB Power Grids's high-power semiconductors.



Figure 8: DBC/DBC, DBC/Power terminal wire bonding

Voltage and Current Measurement Technology for PV Energy Management System on Enhanced DC1500V Solar DC Side

DC voltage sensor using isolation amplifier technology and DC current sensor certified by IEC61010-1 PD2 CAT III to increase the efficiency of solar power

By J&D Electronics

To increase the efficiency of solar power energy, the voltage of the DC power line is upgraded from DC1000V to DC1500V. The increased power generation voltage is certainly attractive, but the insulation rating of the entire PV system should be increased and the equipment involved should also be able to operate at higher voltages. This situation raises the need for high-precision voltage and current sensors for DC1500V power lines.

J&D designed a voltage sensor to provide high insulation technology that can withstand 1500V, enabling high precision using Ultra Precision Zero-Drift Op Amps.

1. DC 1500V high accuracy voltage sensor; IDVT-series. Hybrid design using reinforced isolation amplifier technology and Ultra Precision Zero-Drift Op Amps

The temperature of the Solar power plant usually rises to 40° in the summer day. In addition, the temperature inside the Distribution board can reach 100 degrees in the worst case. Therefore, the voltage sensor must maintain accuracy even at these high temperatures. J&D's voltage sensor was developed with high voltage isolation reinforced amplifier technology. Voltage Sensors – IDVT series begins with an internal High voltage resistor network. This network measures DC Voltage by directly contacting both the Positive High Voltage (+HT) and the Negative High Voltage (-HT). This Voltage signal is transmitted to the secondary side of the sensor through an insulated Reinforced transformer that isolates the Primary High Voltage from the Secondary Low Voltage. The resulting signal is then converted through an auto-zeroing techniques amplifier into either Voltage signal. Therefore, the circuit converts a primary Voltage into a secondary Voltage that is proportional to the input.

The reinforced isolation amplifier technology and the hybrid design using Ultra Precision Zero-Drift Op Amps not only maintain high accuracy at high temperatures, but also achieve accuracy with 5V to 30V free wide range voltage. When you refer to figure 1-1 you can find that the Voltage sensor can provide high precision despite the high temperature.

Features:

- (1) Power consumption : 5W
 - (2) Input voltage : DC1500V
 - (3) Output voltage : $\pm 0.5V$
 - (4) Accuracy : 0.5%
 - (5) Ambient Operating temperature : -40° to +105°
- (Reference Figure 1-1)

2. High-insulation and High-accuracy current sensor JPS-H Series for DC1500V power line monitoring. Temperature Reinforced Amplifier Technology

J&D, the first in the world, has developed a product designed with high insulation so that it can be used stably in the DC 1500V line. JPS-H is a sensor that develops input voltage from 600V to 1500V and is a product that has obtained PD2 certification and CATIII 1500V certification of IEC-61010-1.

JPS-H series begins with an internal Insulation distance design split core technology network.

This network is measured using two hall elements and a permalloy core based on advanced open loop technology and resulting signal is then converted through an auto-zeroing techniques amplifier into either Voltage signal. A split-core sensor that can be easily installed

Temperature characteristic graph

Primary voltage : 1500VDC / Secondary output : 0.5VDC

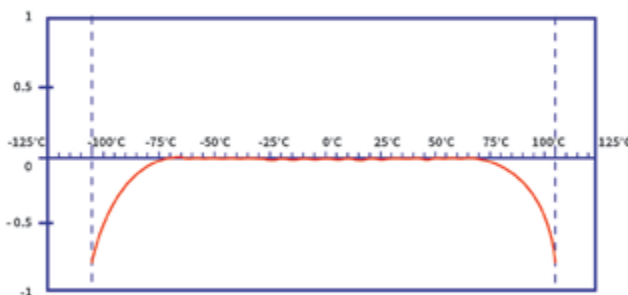


(Figure 1-1. Voltage sensor)

Temperature characteristic graph

Primary current : 400ADC / Secondary output : 0.5VDC

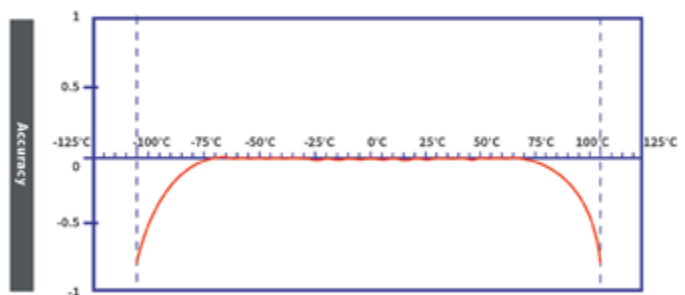
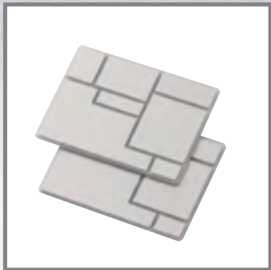


(Figure 1-2. Current sensor)

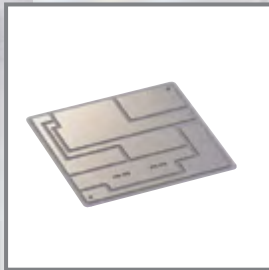
Figure 1: Temperature accuracy data

Solutions for your Power Modules from One Source



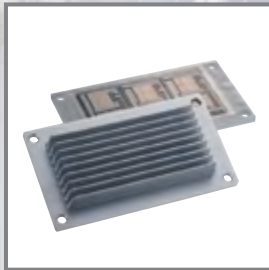
AIN-AMB Substrates

Thin-AIN-AMB substrates with lowest thermal resistance and cost efficiency in comparison to Si₃N₄ AMB substrates.



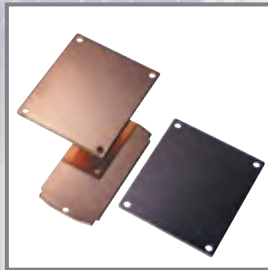
DAB-Substrates

DAB substrates (Almic) with excellent reliability and PD properties in comparison to DBC or AMB substrates.



Integrated Substrates

High innovative substrates, embedded in Al-baseplate or Al-heatsink, enabling >25% improved power capacity increase and >70% reduction in weight on module level.



Cu Baseplates

Balanced material combination for high thermal conductivity and minimized warpage for high reliability in comparison to conventional Cu baseplates (SE-Cu, SF-Cu).



New

Cu-Mo clad Baseplates*

Effective material combination of higher thermal conductivity and lower thermal expandability (CTE-adjusted to Al₂O₃) for excellent reliability, smaller size and lighter weight.

*Co-Development with The Goodsystem Corp.

for generations

DOWA

DOWA HD Europe GmbH

info@dowa-europe.com

www.dowa-europe.com



on a cable and designed by hybridizing Hall element twin technology and Ultra Precision Zero-Drift Op Amps is designed to maintain high precision even at high temperatures.

This can solve problems of high operating temperatures because it is installed where solar power is maximized for the best energy capture performance due to the feature of the PV system.

0.5% accuracy can be achieved even with a low power consumption which is 5V to 30V free wide voltage. Also, figure 1-2 shows High accuracy of current measurement is possible even at high temperature.

Features:

- (1) Power consumption : 5V
- (2) Rated current : DC 400A
- (3) Output voltage: $\pm 0.5V$
- (4) Accuracy : 0.5%
- (5) Ambient Operating temperature : -40° to $+105^{\circ}$
(Reference Figure 1-2)

3. J&D's options. CTid technology and UI.

Increasing demand for green energy is one of the driving forces behind the adoption of PV DC1500V power. In addition, as the amount of energy supplied from renewable energy such as PV power increases, power lines must be measured in high quality efficiency and critical power protection is always important for abnormal situations, from solar panels to PV inverter systems. Solar panels commonly use a PV Inverter that works with the DC-DC converter to connect the generated power to the grid.

However, a common problem of power electronics is the generation and emission of harmonic currents, which dramatically reduce the quality of the injected current. To identify this issue, it is very important to measure the power quality and efficiency by measuring the voltage and current of the DC 1500V line.

In addition, one of the main considerations is to ensure system reliability and safety under all environmental conditions and temperatures when converting primary voltage and current from DC to AC.

J&D Electronics plans to launch J&D's voltage and current sensor and eGauge meters that can be used for DC1500V power lines all over the world. J&D's voltage and current sensors can optionally built-in

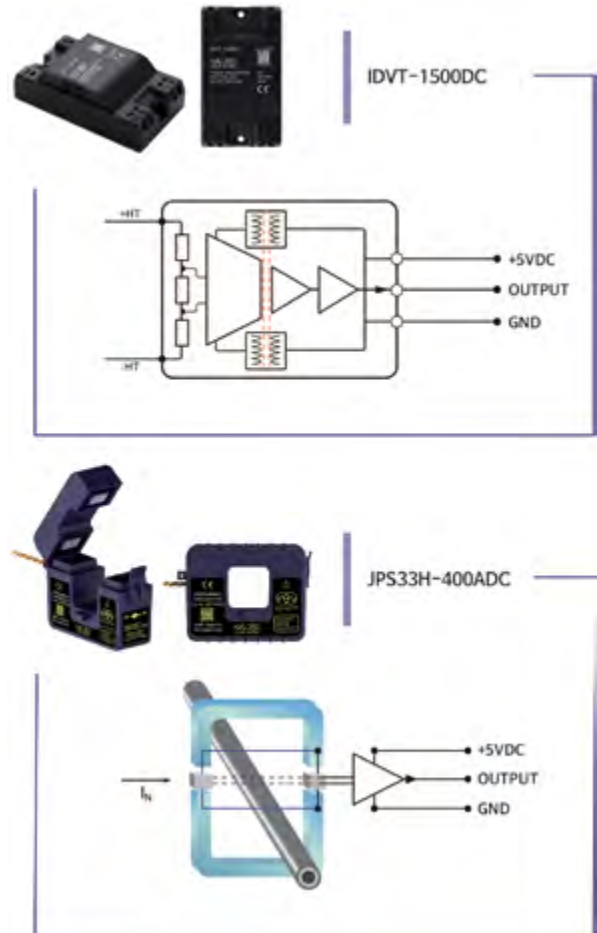


Figure 2: IDVT, JPS product image and schematic diagram

eGauge's CTid technology. If you use the voltage sensor IDVT series and the current sensor JPS-H series which built-in CTid technology together with a gateway AC/DC energy meter using eGauge's CTid technology, you can operate a solar power plant with stable power.

Real time PV energy monitoring system with eGauge

Figure 3: The patent number, SENSWAY Meter with CTid

Danfoss is part of the PCIM Europe conference program



pcim
EUROPE ...digital
days

Full Bridge SiC Module for Charger Applications

Monday, May 3rd – 14:05 CEST

Development of the laser beam based high-current contacting technology and an integrated lead frame stack structure

Monday, May 3rd – 16:40 CEST

Bearing Shield Integrated SiC-Based Traction Inverter for a Dual Three Phase PMSM Drive System

Wednesday, May 5th – 14:10 CEST

Measures to improve efficiency, peak power density and current density in an automotive SiC drive train inverter – Sensitivity analysis of design parameters

Wednesday, May 5th – 14:25 CEST

Accelerated Qualification of Highly Reliable Chip Interconnect Technology by Power Cycling Under Thermal Overload

Thursday, May 6th – 11:05 CEST



www.siliconpower.danfoss.com

ENGINEERING
TOMORROW

Danfoss

Overvoltage Categories in Power Supply Systems

The operating environment for mains-powered electrical equipment is separated into four overvoltage category (OVC) areas according to their level of surge protection. This article describes how these four areas differ and how the AC/DC power supplies rated for the OVC II area might be used in the OVC III area in certain circumstances.

By Steve Roberts, Innovation Manager, RECOM Power

Most users of mains-powered equipment are confident that they can simply plug in their device to a convenient socket, and their device will function correctly, safely, and reliably. Stringent and mandatory international standards for power supplies support this notion. Even a modular product embedded within another equipment is required to meet a minimum level of electrical safety isolation and electromagnetic compatibility including immunity to voltage surges and transients.

The fact is, anywhere in the home, office, or factory where the mains power comes from wall sockets, it is likely to provide an environment where the mains power is relatively 'clean' without undue voltage transients that could damage the end-equipment. However, as you move progressively back through the infrastructure wiring to a distribution board and then further to the AC supply connection for a building, the possibility of seeing overvoltage from external events such as lightning strikes and load dumps from other installations on the utility network, which are obvious risks, goes on increasing.

OVCs in the environment

There are applications where single-phase or multiple-phase AC/DC power supplies are permanently wired to central distribution panels, for example, home chargers for electric vehicles or DIN-rail mounting power supplies. In these locations, the more severe transient amplitudes and energy levels require the power converters to have additional overvoltage protection when compared to that required for a plug-in power supply.

Overvoltage Category	Relevant equipment
OVC I	Equipment for connection to circuits in which measures are taken to limit transient overvoltages to an appropriately low level.
OVC II	Energy-consuming equipment to be supplied from the fixed installation. Examples of such equipment are appliances, portable tools and other similar household loads.
OVC III	Equipment in fixed installations and for cases where the reliability and the availability of the equipment is subject to special requirements. Examples of such equipment are switches in the fixed installation and equipment for industrial use with permanent connection to the fixed installation.
OVC IV	Equipment connected at the origin of the installation. Examples of such equipment are electricity meters and primary overcurrent protection equipment.

Table 1: OVCs according to IEC 60664-1:2020



The international standard IEC 60664-1, i.e., 'Insulation coordination for equipment within low-voltage supply systems', defines four installation categories labeled OVC I to OVC IV as presented in OVC I relates to powered equipment that is connected downstream from a well-protected isolated supply such as a computer fed with DC by a laptop charger, while OVC IV applies to a power utility's equipment connected directly to the incoming supply (Figure 1). This means that a majority of the mains-powered equipment within buildings fall into the OVC II and OVC III categories. As a generalization, OVC II includes all domestic, workshop, and office equipment that is fitted with a mains plug and is individually protected by a fuse or circuit breaker. OVC III refers, primarily, to hard-wired equipment fitted inside a switch cabinet or distribution panel such as relays, circuit breakers, and fixed-installation power supplies.

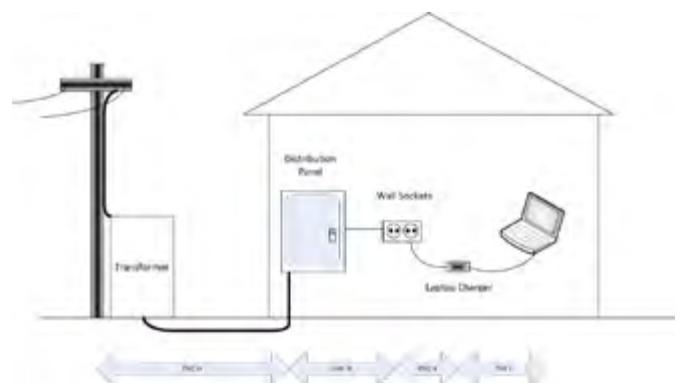


Figure 1: Diagrammatic representation of the OVC IV to OVC I environments

HITACHI **ABB**

HITACHI ABB POWER GRIDS



NEW LOPAK MODULE: NOW FOR 1200 V APPLICATIONS, SAME FAMILIAR PACKAGING

Building on our heritage of developing high-performance, high-reliability devices, Hitachi ABB Power Grids announces a new 1200 V, 900 A rated phase-leg configuration in an improved LoPak1 module. Benefitting from our next generation of ultra-low-loss, rugged Trench IGBT devices, it enables new and existing designs to be upgraded to higher power ratings using the familiar LoPak module package. The new device also boasts a wide short circuit safe operating area capability and minimizes losses.



When specifically discussing protection against lightning, the IEC 62305-1 standard defines 'zones' LPZ 0 to LPZ 3 that correspond to the OVC areas IV to I. The standard IEC 61643-11 for Surge Protective Devices (SPDs) also ties in with these definitions with the protection device classes I, II, and III, corresponding to LPZ 0, 1, and 2 respectively.

The IEC 61643-11 standard also defines the different test waveforms required to prove the effectiveness of the suppression devices, i.e., a 10/350µs transient that would result from a direct lightning strike and a combined 8/20µs + 1.2/50µs characteristic that would result from an indirect (induced) lightning strike or from atmospheric lightning. A multi-stage suppression system is required to protect against all these different surge events (Figure 2).

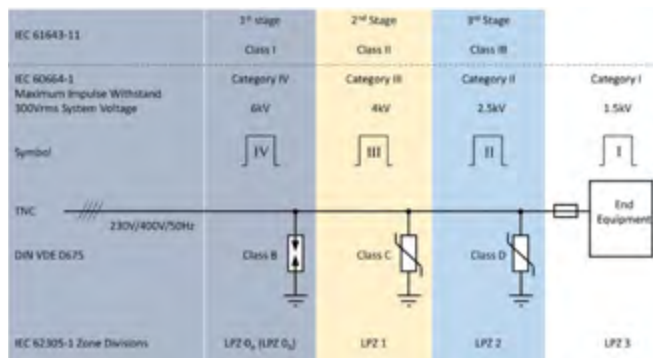


Figure 2: IEC 60664-1 OVC equivalence to IEC 62305-1 zones and IEC 61643-11 protective device classes

An end-of-life indication (acoustic or visual) to inform the user if the SPDs have been compromised by high energy or repeated lightning strikes is also generally required by these installation codes.

OVC differences

Equipment in different OVCs must withstand different impulse voltages that correspond to the expected transients on the low-voltage distribution network.

IEC 60664-1 includes the following information in this regard (Table 2):

Nominal system supply voltage		Voltage line – neutral derived from nominal voltages AC or DC up to and including	Rated impulse voltage			
Three Phase (V)	Single Phase (V)		OVC I	OVC II	OVC III	OVC IV
		50	330	500	800	1500
		100	500	800	1500	2500
	120-240	150	800	1500	2500	4000
230/400	277/480	300	1500	2500	4000	6000
400/690		600	2500	4000	6000	8000
1000		1000	4000	6000	8000	12000

Table 2: Rated impulse voltages for different system voltages and OVCs

It must be noted that the values in Table 2 are the rated 1.2/50µs peak impulse voltages for basic insulation. For double or reinforced insulation, the next higher voltage category is used. For example, for the 300Vrms OVC II, the reinforced isolation requires a rating for a 4000V impulse voltage.

However, when testing for compliance is carried out, the operational altitude must also be factored in. The impulse test voltage values given in Table 2 are for 2000m, but for lower altitudes, the values increase. Thus, 4000V rated increases to 4923V rated at sea level.

Table F.5 of IEC 60664-1 presents the correction factors in this regard.

On the other hand, the required minimum clearance distances increase at higher altitudes. For example, the altitude correction factor for clearances is 1.00 at 2000m, but it increases to 1.48 at 5000m. Table F.1 of IEC 62109-1 presents the correction factors in this regard.

OVC III power supplies require enhanced safety barriers

Power supplies intended for OVC III areas need enhanced specifications for withstand voltages and clearance distances compared to the more common OVC II rated types. These could be met with a preceding isolation transformer to reduce transients to OVC II levels, but this is often an unwieldy and expensive solution. A better solution is to design the power supply such that it can be directly connected to the supply in an OVC III environment.

An implication for AC/DC power supply design is that clearance distances between line and accessible parts have to be increased substantially. An AC/DC product with basic insulation designed for being used in an OVC II environment requires a 3.0mm minimum clearance for isolation barriers rated at 4kV, but for an OVC III environment, the impulse voltage rating increases to 6kV, requiring a 5.5mm minimum clearance (Tables F1 and F2 in the IEC 60664-1 standard). However, most AC/DC converters have reinforced isolation barriers. The standard requires that “the value corresponding to the next highest impulse voltage” be used. This means that a reinforced isolation converter needs clearances of 5.5mm/8.0mm for OVC II/ OVC III installations respectively.

IEC 60664-1 and IEC 61558-1 also specify dielectric strength test voltages at 50/60Hz that can be as high as the impulse test value. For example, IEC 61558-1 requires a dielectric test voltage of 4200Vrms = 5938Vpk for 300Vrms working voltage and OVC III/reinforced insulation, without specifying the altitude (Table 14 in the IEC 61558-1 standard). This is similar to the impulse test value from IEC 60664-1, which is 6kV at 2000m altitude. However, one test is for the dielectric strength for 60 seconds, while the other is a short transient impulse voltage.

The most appropriate safety standard that applies to a power converter depends on the actual application. The products for use in an OVC III environment are often best covered by the IEC 61558-1 standard about ‘Safety of transformers, reactors, power supply units and combinations thereof’. In this standard, Annex R references IEC 60664-1’s levels for the impulse test voltages. Fortunately, the safety clearance requirements in IEC 61558-1 are the same as in IEC 60664-1 Both the standards use the same altitude correction factors above 2000m.

The users may also choose to apply the IEC 62477-1 standard about ‘Safety requirements for power electronic converter systems and equipment’ for their products for OVC III areas. This standard also references the IEC 60664-1 impulse values, creepage/clearances, dielectric test voltages, and altitude correction factors.

The standard IEC 61010-1 about ‘Safety requirements for electrical equipment for measurement, control and laboratory use’ is the most appropriate for the test and measurement equipment used in OVC III areas. This standard specifies a clearance distance of 6mm for 300Vac reinforced isolation (Table K.3 in the IEC 61010-1 standard) compared to 8mm in the IEC 60664-1 standard. The altitude correction factors are the same. However, the other test requirements in the



INCREASING POWER DENSITY FOR MOTOR DRIVES WITH SILICON CARBIDE



COMPACT DUAL INLINE PACKAGE

Footprint 58.7mm x 41.4mm

FEATURES

- Utilizes Silicon Carbon MOSFETs for superior performance
- High continuous output current – 30 A
- High supply voltage– 650 V maximum
- Fast switching frequency – 400 kHz
- Integrated with digitally controlled gate drive
- Under-voltage lock-out and active Miller clamping

TARGET APPLICATIONS

- BLDC Motor Drivers
- Variable Frequency Drives
- DC/AC Converters
- Power Inverters
- Test Equipment

APEX MICROTECHNOLOGY INC.

5980 N Shannon Road
Tucson, Arizona 85741 USA
T: +1.520.690.8600
F: +1.520.888.3329

SALES SUPPORT

Toll Free: +1.800.862.1032
eMail: custserv@apexanalog.com

TECHNICAL SUPPORT

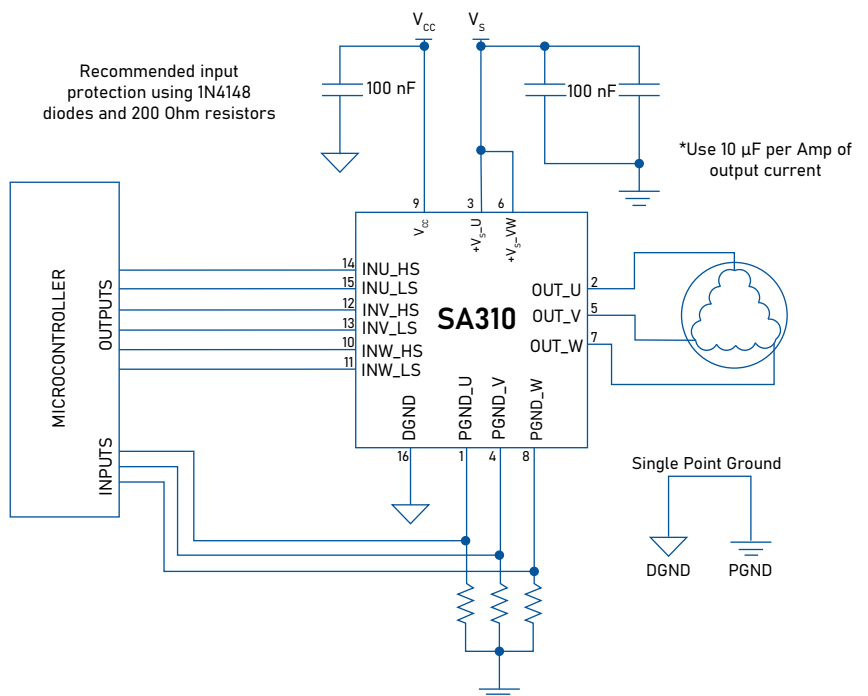
Toll Free: +1.800.546.2739
eMail: Apex.Support@apexanalog.com

SA310: 3-PHASE SILICON CARBIDE MODULE

The SA310 is a fully integrated three-phase driver designed primarily to drive Brushless DC (BLDC) and Permanent Magnet Synchronous (PMSM) motors or DC/AC converters. The module uses Silicon Carbide MOSFET technology to improve efficiency over other devices in its class. Three independent half-bridges provide up to 80A peak output current under direct microcontroller or DSC control. The SA310 is built on a thermally conductive substrate that is electrically isolated to provide the most versatility and ease in heatsinking.

The amplifier protection features include under-voltage lockout (UVLO) function and active Miller clamping to reduce switching noise and improve reliability. Also included in the module are Silicon Carbide Schottky Barrier free-wheeling diodes to protect the body diode of each MOSFET. No external output protection diodes are required. The SA310's integrated gate drivers provide transformer isolation between the inputs and high-voltage outputs.

TYPICAL APPLICATION



IEC standard 61010-1 are a little harsher. For example, the impulse voltage test in a 300Vrms OVC III environment for reinforced solid insulation is 6400V (Table K.6 in the IEC 61010-1 standard) unlike the IEC 60664-1 standard that specifies an impulse voltage test of 6000V.

The general purpose safety standard IEC/EN/UL 62368-1 about 'Safety requirements for Audio/video, information and communication technology equipment' references the IEC 60664-1 standard for the requirements for OVC III and OVC IV environments. The obsolete standard IEC 60950-1, however, required 6mm clearance for 300Vrms/OVC III areas (Table 2H of the IEC 60950-1 standard), the same as specified by the IEC standard 61010-1, but now, the replacement IEC 62368-1 standard has come into line with the IEC 60664-1 standard and raised the clearance requirement to 8mm.

Medically approved AC/DCs may enable compliance with OVC III requirements

Power supplies are available with OVC III ratings such as the RECOM board-mount RAC05-K/480 converters (Figure 3), which have an input voltage range of 85-528VAC, making them suitable for single-phase supplies and three-phase 400/480VAC line-to-line or line-to-neutral connections. This series that features 5W output power with 4kVac reinforced isolation is a class II power supply (no-earth connection) and meets industrial safety and EMC requirements without any external components. The RAC05-K/480 series offers 5, 12, or 15V DC outputs and is ideal for equipment in a harsh industrial OVC III environment such as smart meters, renewable energy, or IoT applications.



Figure 3: RECOM's RAC05-K/480 AC/DC converter rated for use in an OVC III environment

Another possibility for OVC III applications is to use its parts with medical safety ratings. The power supplies that meet the requirements for 2 x Measures of Patient Protection (MoPP) in 240Vac systems will also meet the dielectric strength and creepage/clearance requirements of OVC III, namely, 4kVrms and 8mm respectively. However, medical-grade power supplies typically only meet the OVC II level requirement of fast transient immunity by complying with the IEC 61000-4-4 standard's level 3, +/-2kV peak, even though they may withstand the 50/60Hz 4kVrms dielectric strength test. To increase the transient immunity to the OVC III level, however, requires an external surge suppressor, typically, a metal oxide varistor installed across the supply with a suitably rated upstream fuse or current limiting device to provide necessary protection should the circuit go short. Suitable AC/DC medical-rated power supplies in the RECOM range are in the RACM40-K, RACM60-K, RACM230-G, and RACM550-G series. These offer board-mount and chassis-mount options (Figure 4).



Figure 4: A selection of medically-certified AC/DC power supplies from RECOM

Medical-rated power supplies are required to incorporate double fusing on the AC power input when they could be used in 'pluggable' applications. Other standards for industrial, office, or home environments may specifically disallow this. So, while choosing a medical power supply for its compatibility with OVC III requirements but one that is also intended for being used in other applications such as industrial control, the neutral fuse may need to be replaced with a much higher value so the line fuse will always blow first. Medically-certified power supplies that are intended for permanent wiring-in may, anyway, have only a single live fusing.

Customized versions of these products intended for use in non-medical applications in a fixed-installation OVC III environment are available on request.

There are potentially easy solutions for power supplies in OVC III environments

It may have been difficult in the past to locate cost-effective AC/DC power supplies that are rated to installation in OVC III environments, but they are now increasingly available from manufacturers such as RECOM. A discussion with manufacturers' technical support teams may also show that the products with medical certification may also meet the OVC III requirements with simple modifications as they already comply with the less stringent industrial-grade safety requirements.



Steve Roberts was born in England. He obtained a B.Sc. in Physics and Electronics at Brunel University, London before working at University College Hospital. He later moved to the Science Museum as Head of Interactives, where he completed his M.Sc. at University College, London. Eighteen years ago he made his own personal Brexit and moved to Austria, becoming Technical Director for the RECOM group in Gmunden. He is the author of the RECOM DC/DC & AC/DC book of knowledge.



POWER CHOKE TESTER DPG10/20 SERIES

Inductance measurement from 0.1 A to 10 kA

KEY FEATURES

Measurement of the

- Incremental inductance $L_{inc}(i)$ and $L_{inc}(\int U dt)$
- Secant inductance $L_{sec}(i)$ and $L_{sec}(\int U dt)$
- Flux linkage $\psi(i)$
- Magnetic co-energy $W_{co}(i)$
- Flux density $B(i)$
- DC resistance

Also suitable for 3-phase inductors

WIDE RANGE OF MODELS

7 models available with maximum test current from 100A to 10000A and maximum pulse energy from 1350J to 15000J

KEY BENEFITS

- Very easy and fast measurement
- Lightweight, small and affordable price-point despite of the high measuring current up to 10000A
- High sample rate and very wide pulse width range => suitable for all core materials

APPLICATIONS

Suitable for all inductive components from small SMD inductors to very large power reactors in the MVA range

- Development, research and quality inspection
- Routine tests of small batch series and mass production

Understanding Bandwidth Requirements When Measuring Switching Characteristics in Power Electronic Applications

When using an oscilloscope for measuring signal switching characteristics in a power electronic application, one important aspect to consider is that the measurement system has sufficient bandwidth to be able to accurately measure the dynamic characteristics of the device under test. With the advent of wide bandgap semiconductors, we are facing a transition to higher operating frequencies and more importantly shorter switching times.

By Bernhard Holzinger, Michael Zimmermann, Ryo Takeda, and Mike Hawes, Keysight Technologies

This transition is asking for measurement setups with higher bandwidth. However, it also places more emphasis on the question, "Which bandwidth is good enough for doing the job?"

In a previous article, "Overcoming Challenges Characterizing High Speed Power Semiconductors" [1], Keysight had a general look into the bandwidth required for Double Pulse Test Systems. In that article, we discussed bandwidth, but with a focus on the requirement for the Double Plus Test (DPT) circuit design. We highlighted how there are different contributors to the overall system performance. In this article, we are focusing on the aspect of measuring and bandwidths that are required for specific signals.

This article proposes a method for estimating the required measurement bandwidth. Two aspects must be considered: 1) the properties of the signals to be measured, and 2) the properties of the measurement setup (i.e. oscilloscope) itself. Both aspects will be discussed to estimate the bandwidth requirements needed for measuring switching characteristics in power electronic applications accurately.

Signal Properties

A signal has many different properties which determine the measurement requirements, for instance the 'signal levels' to be measured. The discussion in this article focuses on the properties dictating the bandwidth requirements.

The bandwidth requirements are determined by two properties:

- **Transition times:** The times it takes for a signal (e.g. V_{DS}) to switch from high to low or vice versa, when a transistor is turned on or off. It is not the switching frequency of the transistors that determine the bandwidth requirements, but the transition times.
- **Ringing:** There are always parasitic capacitance and inductance present in each circuit, forming a LC-circuits. When a transistor is switching, those LC-circuits become excited and start to oscillate. The oscillations are damped by resistive elements in the circuit and therefore fade away after some time.

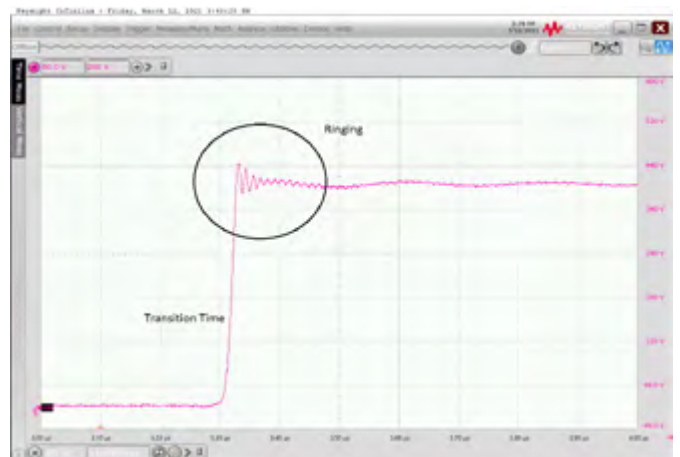


Figure 1: Switching transition and its properties.

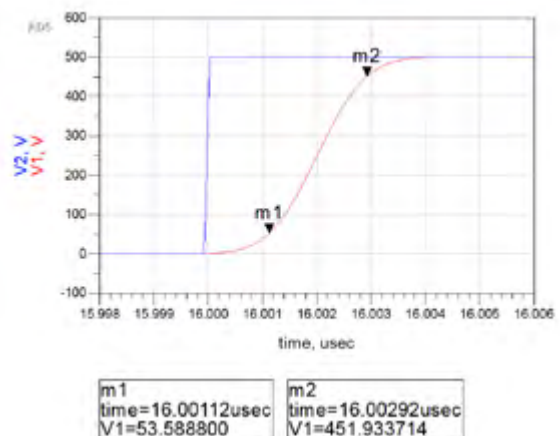


Figure 2: Simulated rising edges (limited transition time vs. ideal edge)

¹ Analog oscilloscopes use the input signal to directly deflect the electron beam in a CRT. This requires amplifying the input signal three orders of magnitude and driving the large capacitive load that the CRT deflection plates present.

Properties of Transition Times

In power electronics transistors operate as switches. They are either turned on, or off, or are transitioning between both states. Ideally, the transitions are as fast as possible to minimize switching losses. The characteristic of switching on and off is also a common theme in digital design, where one is mainly measuring and analyzing square wave signals.

In the book "High-Speed Digital Design – A Handbook to Black Magic" [2] Howard W. Jonson and Martin Graham are describing a method for estimating the maximum frequency up to which a digital signal contains significant amount of energy. Using a simulated example, we would like to introduce this approach here.

To start the discussion, we compare the signal spectrum of an ideal square wave (V2 - blue) with a waveform showing a realistic transition time (V1 - red) (see Figure 2).

V1 has a 10%-90% transition time of about 1.8ns. The markers highlight when the signal is crossing the 10% threshold (m1) and the 90% threshold (m2). V2 has an almost ideal transition time (i.e. time ~ 0 ns). Calculating the respective spectrums yields the following results (Figure 3).

The ideal spectrum of V2 (blue) shows a decline of 20dB/decade. However, the spectrum of V1 (red) starts to roll off at a certain frequency. The frequency at which the amplitude has dropped by half (6dB), compared to the ideal spectrum is labeled "knee frequency" F_{knee} [2]. In this example F_{knee} happens to be 278MHz.

We can relate F_{knee} and the 10%-90% transition time (t_r) and end up with this easy to remember formula.

$$F_{knee} = \frac{0.5}{t_r} \quad \text{Eqn.1 [2]}$$

Of course, the same formula also applies for fall times (t_f).

To summarize, using this formula, we can estimate to which frequency a square wave signal carries the significant amount of energy, given its rise or fall times. If we want to be able to accurately measure this signal, we must make sure we capture all frequency components up to this knee frequency – plus some headroom. The amount of headroom required is the topic of a following section.

2 Sampling alias errors occur when the signal has frequency content beyond half the sample rate, known as the Nyquist frequency.

Properties of Ringing

As already mentioned above, power electronic circuits contain parasitic components forming a LC-circuits, which becomes excited when there is a switching event. When it comes to estimating the required bandwidth for capturing the caused ringing, we can focus on the highest frequency oscillations of the signal only. The highest frequency oscillations are mainly created by the combination of the power loop inductance L_{loop} and the output capacitances C_{oss} of the transistor.

The schematic below (Figure 4) shows both using a typical double pulse test configuration as an example.

Knowledge of these parasitics allows us to estimate the resulting oscillation frequency, using this formula calculating the resonant frequency of an LC-circuit:

$$f_{ringing} \approx \frac{1}{2\pi\sqrt{L_{loop}C_{oss}}} \quad \text{Eqn.2}$$

Optimize the electrification properties of your EV power electronics & electric propulsion systems



Achieve near-perfect magnetic circuits with our tape wound toroidal & cut cores, specifically designed to:

- Outperform transformer laminations,
- Minimize electrical losses,
- Reduce component size & weight,
- Increase power density,
- Maximize performance characteristics

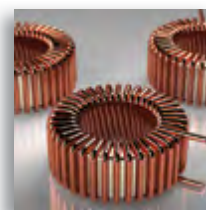
Our cores deliver the essential magnetic properties and efficiencies required for:

- Transformers that power EV Charging Stations,
- Transformers that control & monitor AC induction & DC motor performance,
- Power supplies that charge EV battery packs,

- GFCI's used in Electric Vehicles,
- Inductors, converters & inverters

We utilize the most advanced grades of soft magnetic materials, provide short turnaround times, and offer both standard and custom cores.

Contact us today to discuss which magnetic materials and core designs will give you EV components with maximum electrification properties.



Magnetic Metals

75+ YEARS
OF CUSTOMER
SERVICE



Phone: (856) 964-7842 Fax: (856) 365-8723
www.magneticmetals.com

© 2021 Magnetic Metals Corporation

C_{OSS} can be found in the data sheet of the transistor. However, strictly speaking, it is not the only contributor. Other parasitic capacitances must be considered as well. They typically are in parallel with C_{OSS} and just add onto C_{OSS} , increasing the parasitic capacitance value. If one neglects these additional capacitances, the estimate of the ringing frequency will result in a slightly higher value. It is also not straight forward to determine L_{loop} . You might use suitable circuit simulations or measurement techniques (shown later in this article), to estimate its value. If you underestimate the actual value of the loop inductance, you will estimate the bandwidth requirement a little bit too high, which provides extra margin in your measurement design

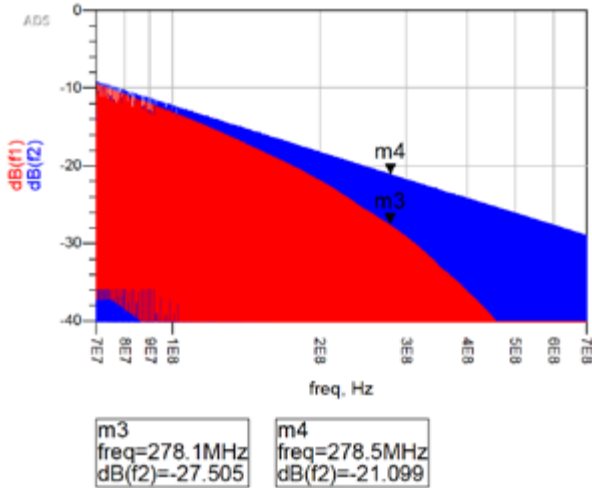


Figure 3: Extracted spectrum (limited transition time vs. ideal edge).

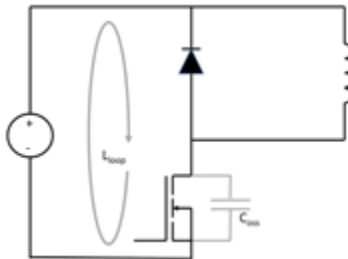


Figure 4: Main contributing parasitics to high frequency ringing in DPT system.

Oscilloscope Properties

When you combine many circuit elements with similar frequency responses, you get a Gaussian response. Traditional analog oscilloscopes chain many analog amplifiers from the input to the cathode ray tube (CRT) display and therefore exhibit a Gaussian response.

Less familiar, is probably the flat response that is now more commonly exhibited by modern, high-bandwidth digital oscilloscopes. A digital oscilloscope has a shorter chain of analog amplifiers, and it can use digital signal processing techniques to optimize the response for accuracy. More importantly, a digital oscilloscope can be subject to sampling alias errors which is not an issue with analog scopes. Compared to a Gaussian response, a flat-response reduces sample alias errors, an important requirement in the design and operation of a digital oscilloscope.

The topic of how the frequency response and the oscilloscope's system bandwidth effect the measurement results is described in more detail in the Application Note "Understanding Oscilloscope Frequency Response and Its Effect on Rise-Time Accuracy" [3] by Keysight Technologies. Here we are summarizing the key takeaways:

For an oscilloscope with gaussian frequency response, the intrinsic rise time of the step response can be calculated in the following formula:

$$t_r = \frac{0.35}{BW} \tag{Eqn.3}$$

For oscilloscopes with flat frequency response there are more variations of equations. But in general, its rise time of the step response can be estimated to be the following:

$$t_r = \frac{0.4 \dots 0.5}{BW} \tag{Eqn.4}$$

Nevertheless, you can't simply assume that an oscilloscope with gaussian frequency response yields results with higher accuracy when it comes to measurement of transition time. On the contrary, using an oscilloscope with a flat response with sufficiently high bandwidth margin yields the better results.

The bandwidth in equations 3 and 4 is referring to the system bandwidth. You might have come across the following formula for calculating the system bandwidth from the oscilloscope's bandwidth and the probe's bandwidth:

$$BW_{system} = \frac{1}{\sqrt{\frac{1}{BW_{oscilloscope}^2} + \frac{1}{BW_{probe}^2}}} \tag{Eqn.5}$$

Please be aware, this is only valid for oscilloscopes with a gaussian response. It doesn't hold true for oscilloscopes with a flat frequency response. Consequently, when you look up the bandwidth of a probe in its data sheet, normally the resulting system bandwidth is specified directly.

Determining How Much Bandwidth You Need

Bandwidth requirements being imposed by Transition Times

In a previous section, we've learned how to estimate up to which frequency (F_{knee}) a signal carries significant energy based on its transition time. We've also learned that oscilloscopes might show different types of frequency responses on their input and this must be considered when estimating when choosing the amount of required bandwidth.

The missing piece of information is how much margin should be between the knee frequency and the oscilloscope's bandwidth. For this, no formulas are available. However, the application note mentioned in the previous section [3] lists some evaluation results down to a practical limit with the accuracy of 3%.

Achievable Transition Time Measurement Error	Required Bandwidth (Gaussian Frequency Response)	Required Bandwidth (Flat Frequency Response)
20%	1.0 F_{knee}	1.0 F_{knee}
10%	1.3 F_{knee}	1.2 F_{knee}
3%	1.9 F_{knee}	1.4 F_{knee}

Table 1: Required Bandwidths

Therefore, to estimate the required bandwidth given a certain 10%-90% rise time, you should follow these steps:

1. Determine the knee frequency using $F_{knee}=0.5/tr$
2. Determine the frequency response of your oscilloscope (either gaussian response or flat response).
3. Based on the type or oscilloscope, pick the corresponding multi-

plier from the table above (e.g. for flat-response and 3% of error → 1.4).

4. Calculate the required bandwidth using this multiplier at F_{knee}

This procedure is only a tool to estimate the bandwidth you need. It is prudent to verify actual rise-time accuracy with measurements, as frequency responses vary between oscilloscope models.

Finally, you should make sure that the sampling rate is set sufficiently high. Again, we are referring to Keysight's application note [3]. The application note provides a guideline of how to derive a sufficiently high sample rate from the system bandwidth.

1. For an oscilloscope with gaussian frequency response a sample rate at least 4 times higher than the system bandwidth should be used.
2. For an oscilloscope with flat-frequency response, a factor of 2.5 between bandwidth and sample rate is sufficient.

Bandwidth requirements being imposed by Ringing

As described above for estimating the maximum frequency to expect in the ringing we should understand the expected parasitic capacitances and inductances in the circuit.

As previously discussed, for the capacitances we can use the value of C_{oss} .

One way to determine the approximate L_{loop} is to extract the value from measurement results. We can look at the transitions of V_{DS} (red) and I_S (green) of a turn on event as shown in Figure 5.

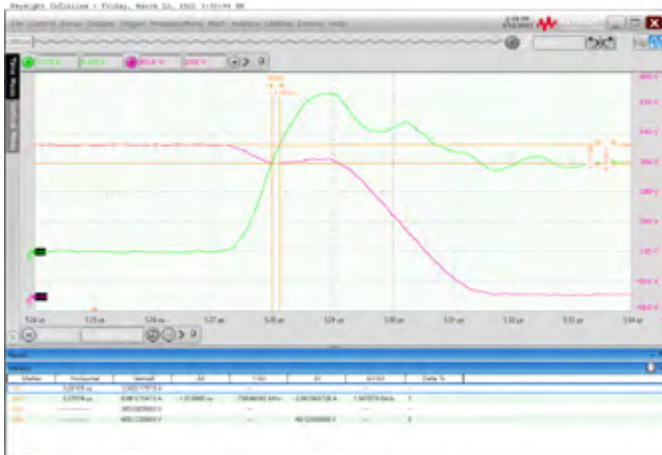


Figure 5: Extraction of power loop inductance.

We notice there is a dip in the voltage when the current is rising. This is caused by the loop inductance and is mathematically expressed as the following.

$$v = L \frac{di}{dt} \quad \text{Eqn.6}$$

The voltage (v) corresponds to the height of this voltage dip Δu , highlighted by markers M3 and M4 (i.e. 49.1V).

The derivative di/dt can be determined by measuring the change in current (Δi) over a time period (Δt), as highlighted by the markers M1 and M2 (i.e. 1.57Ga/s). Note - this is the initial slope when the dip reached its maximum height.

3 The theoretical relationship for a Gaussian system is the rise time = 0.339/bandwidth, but the industry has converged on 0.35/bandwidth as a practical formula.

4 Typical values. Varies with oscilloscope models. Refer to the oscilloscope specifications.

ice components CE RoHS

- ▶ Wide range of options available
- ▶ High creepage options in both SMT and THT
- ▶ Industry's smallest footprint available
- ▶ Models for select TI gate drivers

GATE DRIVE TRANSFORMERS

FOR WIDE SELECTION OF GATE DRIVE TRANSFORMERS VISIT US AT www.icecomponents.com/gate-drive-transformers

CUSTOM SOLUTIONS AVAILABLE Available at MOUSER ELECTRONICS

With this information, the loop inductance can be estimated as follows.

$$L_{loop} = \frac{\Delta v}{\frac{\Delta i}{\Delta t}} = \frac{49.1}{1.57 \cdot 10^9} = 31nH \quad \text{Eqn.7}$$

With this estimate of L_{loop} and C_{oss} the frequency of the ringing can be estimated, as previously described above (Equation 2).

Examples

Now it's time to test the rule of thumb being introduced in the previous section in practice.

Analysis of Transition Time

The following measurements have been taken with the PD1500A Dynamic Power Device Analyzer/Double Pulse Tester. This system is using a DSOS104A sampling oscilloscope in conjunction with the 10076C high voltage single ended probe for measuring V_{DS} . This combination provides a system bandwidth of 500MHz. The filter characteristic of the oscilloscope is a flat-frequency response.

The SCT2080KE SiC power MOSFET from Rohm Semiconductors was chosen as the DUT. Its maximum operations conditions are 1.2kV and a current up to 40A.

The measurement conditions to measure rise time and fall time are specified in the transistor data sheet. The only difference between

Parameter	Value
Supply Voltage V_{DD}	400V
Gate Drain Voltage V_{GS} on/off	18V/0V
Drain Current I_D	10A
Gate Resistor R_G	0Ω

Table 2: Test Conditions

the data sheet test conditions and the PD1500A test conditions is that the data sheets specifies a resistive load and the double pulse test system uses an inductive load.

The following screen shot from the PD1500A software shows the measurement result for V_{DS} when the transistor is turned off, captured with the maximum available bandwidth of 500MHz (Figure 6).

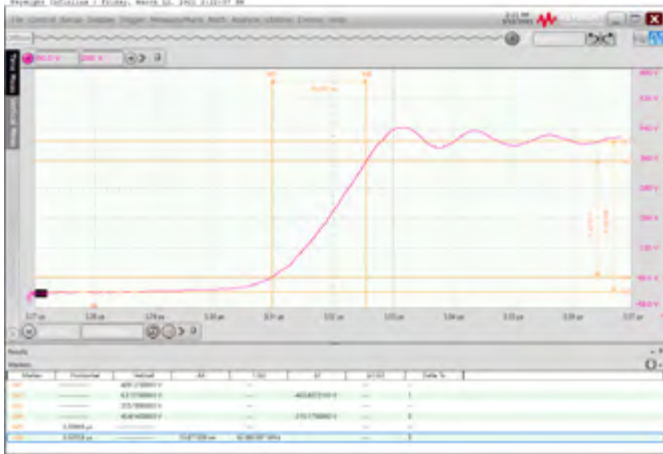


Figure 6: Rise time measurement with 500MHz bandwidth.

Note in the data sheet, in accordance with the IEC 60747-9 standard, the corresponding time is labeled “fall time” even though it is a rising edge.

Parameter	Calculation	Value
Rise time		15.9ns
Knee frequency	$F_{knee} = 0.5/t_{rise}$	31.45Mhz
Required bandwidth for 3%	$1.4 K_{knee}$	44MHz

Table 3: Calculation of Required Bandwidth

The “fall time” in the data sheet is given as 22ns. With the PD1500A we measured 15.9ns. However, since we don’t have the identical measurement conditions (i.e. inductive load instead of a resistive load), the difference may not be a concern. We have discussed correlation situation in more detail in the previous article, “Designing a Double-Pulse Test (DPT) System to Enable Correlation of Dynamic Characteristics” [4].

Nevertheless, this is a good indicator, the fall time was measured correctly, and therefore we used a sufficiently high bandwidth. With this confirmation, we can now calculate the estimate of the required bandwidth for measuring this transition with an accuracy of 3%.

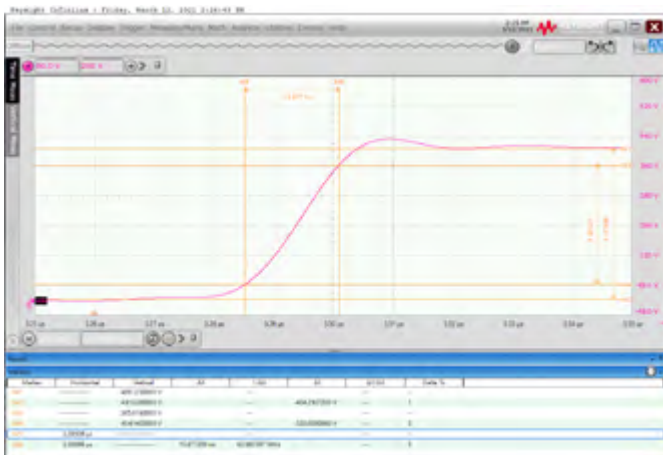


Figure 7: Rise time measurement with reduced bandwidth.

Forty-four MHz is a surprisingly low bandwidth. So, let us confirm our findings. We can use the feature of the oscilloscope to limit its system bandwidth and set it to 44MHz.

This screen shot in Figure 7 shows the measurement result.

As you can see, we’ve still measured the same rise time as before (i.e. 15.9 ns), even though we could have expected a 3% deviation from this value. You can also see that there is a significant change in the signal waveform, specifically in the amount of ringing. Please keep in mind this method is only an estimate.

Analysis of Ringing

For estimating the frequency of the ringing, we must know the output capacitance C_{oss} and have an estimate of the loop inductance L_{loop} of our measurement system.

For this example, we again use the SCT2080KE SiC power MOSFET from Rohm Semiconductors. In its data sheet, C_{oss} is specified to be 77pF. The measurement shown in Figure 8 has also been completed with the same double pulse test system used in the extraction in Figure 5, so we will use the estimate for L_{loop} to be 31nH (see equation 7). Using results and Equation 2, we end up with a required bandwidth for the ringing of 103MHz. Putting this estimate to the test, we measured the ringing on V_{DS} after the turn off event using the maximum available bandwidth of the oscilloscope (500MHz). The markers M1 and M2 were placed on the second and third maxima of the ringing. You might have noticed that the ringing doesn’t consists of a clean sine wave. There is distortion in the sine wave indicating some harmonics. Consequently, using the markers in such a way is not the most accurate way to measure the fundamental

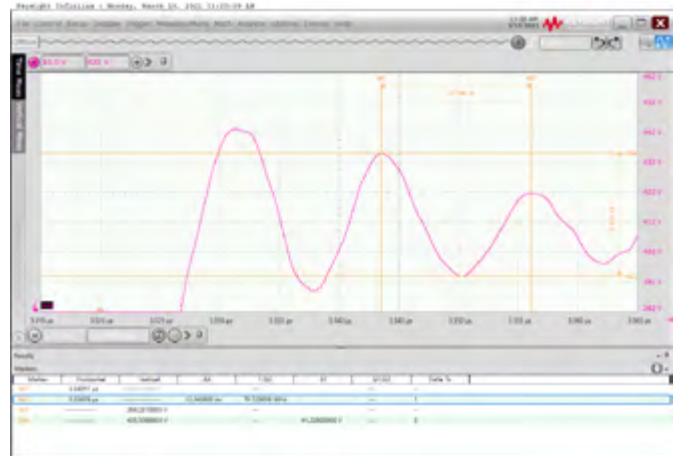


Figure 8: Measurement of ringing with 500MHz of bandwidth.

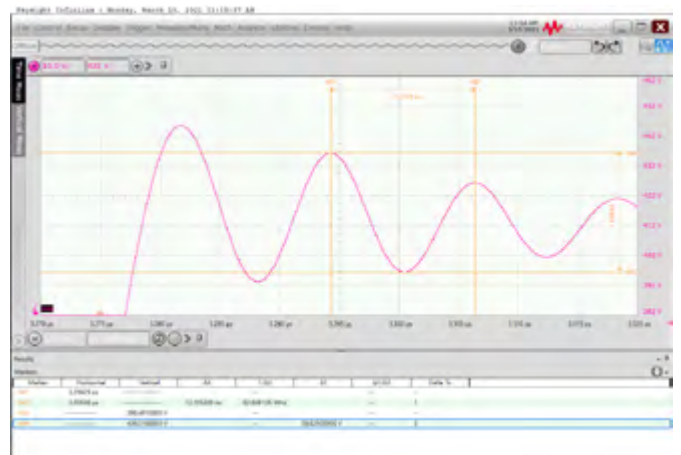


Figure 9: Measurement of rise time with reduced bandwidth.

frequency. Nevertheless, it is good enough for our purposes here and shows us a frequency of about 80MHz. As expected, this is lower than our estimate.

Markers M3 and M4 allow us to extract the initial amplitude of the ringing not taking the overshoot into account. approximately 41V.

If we followed our initial estimate, we would have done this measurement with just a bandwidth of 100MHz. So, let's limit the bandwidth of the oscilloscope and see what result we get (Figure 9).

By examining the waveforms, we notice the ringing appears much less distorted than in Figure 8. This can be explained by the fact that the harmonics causing those distortions have now been filtered. Checking on the fundamental frequency (again using markers) results in 83MHz and the amplitude reading is now 40V.

The discrepancy in the frequency between Figure 8 and Figure 9 can be explained by the simple method we used for measuring frequency. You also notice that the drop in voltage amplitude is only 0.2dB.

Conclusions

When making measurements in power electronics it is important to know the measurement bandwidth required for accurately capturing the signal waveforms. In this article, we wanted to highlight that there are two different signal parameters driving the bandwidth requirements: 1) transition times and 2) ringing frequencies. For both parameters, we have introduced a way to estimate the required bandwidth.

Transistor Type	Typical Transition Times	Required Bandwidth (Transition time)	Typical Loop Inductance	Typical C_{oss}	Required Bandwidth (Ringing)
SiC (TO247)	8-15ns	50-90MHz	30nH	60pF	120MHz
GaN (SMD)	2-5ns	150-350MHz	4nH	25pF	500MHz

Table 4: Typical Bandwidth Requirements when characterizing SiC or GaN transistors

Based on our experience with typical parameters for SiC and GaN transistors, the following table (Table 4) gives an indication regarding the bandwidth requirements you might face for different device technologies. Plus, with the methods we have introduced above, you should be able to adjust these estimates to your specific application needs.

References

1. Overcoming Challenges Characterizing High Speed Power Semiconductors, Bodo's Power Systems, April 2020.
2. Johnson, Howard and Martin Graham, High-Speed Digital Design: A Handbook of Black Magic, Prentice Hall, 1993.
3. Effect of Oscilloscope Frequency Response on Rise-Time Accuracy: Understanding Oscilloscope Frequency Response and Its Effect on Rise-Time Accuracy, Application Note, Keysight Technologies.
4. Designing a Double-Pulse Test (DPT) System to Enable Correlation of Dynamic Characteristics, Bodo's Power Systems, August 2020.

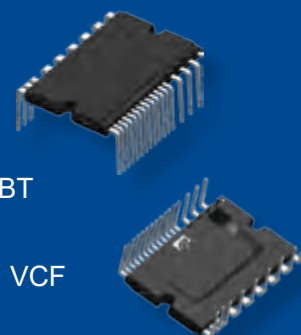
www.keysight.com

Intelligent Power Modules IPM3 Series



600V 5A - 30A

- UL Recognized
- 650V Trench Shielded Planar Gate IGBT
- PFC-Diode Integrated (option)
- Full Protection: OT, VOT, UVLO, CSC, VCF
- Isolation Ratings of 2000Vrms/min



IPM3 series Intelligent Power Module, integrated AOS latest TSPG-IGBT and super low Qrr FRD, offering the high efficiency, low EMI, and ruggedness for Inverter-driven air-conditioners, washing machines, dryers, and fan motors.

 **ALPHA & OMEGA**
SEMICONDUCTOR

Powering a Greener Future™

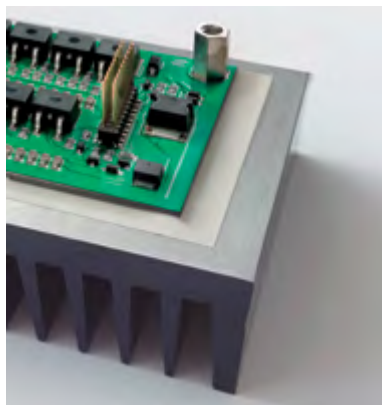
www.aosmd.com

2,2W Thermally Conductive Foil with Dielectric Strength up to 6KV used as Thermal Interface Material (TIM) in Power Electronics

The omnipresent trend in Power Electronics for higher performances at smaller space require a quick, effective and cost-efficient heat-transfer within and out of highly compact Power Modules. A well-designed Heat-Management Concept from the beginning of a new design guarantees longer lifetime of the electronic components and by that higher quality of the whole Electronic Power Module.

Uwe Lemke, Business Development Manager DACH, Aismalibar S.A., Barcelona

In numerous electronic applications, especially in the field of power electronics, it is no longer sufficient to just transfer the heat generated by the electronic components to the ambient air via the printed circuit board. Instead, additional cooling of the components is required, which is achieved using an external, active or passive cooled heat sink.



Thermal Interface: Thermal coupling of a heat source (Power Module using banks of power components) through a TIM to external heat sink is an important element in the entire cooling chain of power electronics, that needs to be considered.

The housing of the application gets more and more used as an additional cooling element for the power electronics. Hence, the protection against accidental contact through dielectric breakdown has grown to an additional safety-related significance in order to guarantee personal protection against electrical shock.

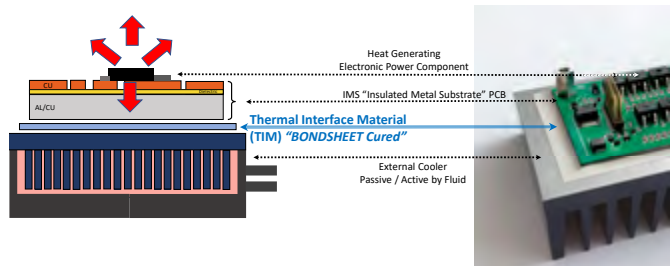


Figure 1: Schematic of a cooling chain in power electronics using the example of an IMS Power Board, coupled to an aluminum heat sink via TIM

TIM dielectric prevents or minimizes air inclusions in order to enable efficient heat transfer from the heat source to the heat sink. A technically, as well as commercially, efficient solution for the thermal and insulation challenges in power electronics, can be found in electrically insulating heat conducting dielectric layer, such as the "BONDSHEET Cured" dielectric film from Aismalibar.

Consisting of a glass fabric base, enriched with mineral fillers, this thermal interface achieves a thermal conductivity of 2.2 W/mK with dielectric strengths greater than 4 KV (70 µm dielectric) or 6 KV (100 µm dielectric thickness). Utilizing a thin film thickness (70 or 100 µm), a low thermal resistance R_{th} of 0.315 or 0.45 Kcm²/W is achieved, which efficiently dissipates the heat generated by the power components to the following cooling element for spreading and dissipation to the ambient air.

Application

Main usage area for the Aismalibar thermally conductive / electrical isolating silicon free TIM foil today are in power electronics, where best compromise of heat transfer combined with electrical isolation is essential.

Key Performances "BONDSHEET Cured" 2,2 W/mK			
Foil Thickness	70	100	µm
Thermal Resistance, R _{th}	0,315	0,45	Kcm ² /W
Dielectric Strength (AC)	≥4	≥6	KV

Maximum Operating Temperature (MOT) is 150°C

This is today successfully realized for example in electronic power modules controlling solar inverters, windmills, truck gear boxes and industrial LED Lighting. Industrial power electronics, for example in welding machines and robot drives, also use heat-conducting dielectric films for efficient heat dissipation from the control electronics. Future Projects are increasingly identified in Electric Vehicles (EV) for Power Train and On-Board-Charger applications.

Here as well, key task of the film is to efficiently dissipate heat with maximum insulation dielectric strength in order to optimally connect

YOU ARE ALREADY THE BSET SINCE YOU KNOW US.



Up to 105°C



Up to 1500V



PowerMOSFETs to the liquid-cooled micro-coolers from IQ-evolution. Extensive tests proved, that for this particular application the heat conducting dielectric film achieves the best technical-commercial combination of heat dissipation and dielectric strength compared to alternative TIM techniques.



Figure 2: Application example of a liquid-cooled, highly compact MOSFET assembly for power electronics.

Foil Manufacturing / Contouring

Starting point of the foil manufacturing at Aismalibar in Barcelona is glass fiber cloth type 106 and 1078/1080, which gets enriched with mineral fillers in an Aismalibar proprietary process to achieve thermal conductivity of the film. Apart from the pure filler material properties, particle size and distribution throughout the foil is key factor to achieve a homogeneous thermal conductivity of the TIM film. First manufacturing output in Aismalibar is a PREPREG film in B-stage, which is used by PCB-Shops worldwide for pressing Multilayers in their PCB Production.

In a following process steps at Aismalibar, the B-stage PREPREG gets cured, where it achieves it's specified key values concerning thermal conductivity and dielectric strength.

BondsHEET Cured leaves the Aismalibar manufacturing line in sheets of 1245x945mm und 1245x1040mm, which Aismalibar ships to those customers, who prefer cutting the sheets into sizes by themselves for usage in their power module assembly. Equally customers consume panel formats, which are common in the PCB industry, like 18x24" (460x610mm).



Figure 3: BONDSHEET CURED

Manufactured in formats

1245 x 945 mm / 1245 x 1040 mm

https://www.aismalibar.com/de/product_group/bond-sheet-cured-de/

At customer's request, BONDSHEET CURED film can be machined in-house Aismalibar to any rectangular or square format to be delivered in stacks of several hundred individual films for manual or automated further processing at customer's facility.

For early test samples, prototypes and small quantity pre-series, Aismalibar offers contouring of foils according to customer specification. This allows a direct foil placement to the PCB in customer's power module assembly. As the usage of the foil does not require any oil, grease, paste or silicone, an easy mounting, as well as disassembly (in case of service / upgrade) of the electronic power module is feasible.

New way for contouring the Aismalibar BONDSHEET Cured foil to customer specific PCB outline requirements is contouring by "Water Beam". This new way of shaping the foil allows a precise and flexible contouring of e.g. holes, radius, edges, just any kind of shapes than what is achievable today by drilling, milling and sawing. "Contouring by Water Beam" is a solution for quick foil sample supply down to quantity "one"

For high volume serial production, punching the foil with a customized punching tool has proved to be the most effective serial production solution.



Figure 4: Example BondsHEET Cured, Contoured

Outlook TIM / Cooling-Concept developments at Aismalibar

Aismalibar is researching future TIM foil technologies, where a combination of a Cured foil core plus B-Stage layers on top will allow the lamination of such multiple foil layer solutions at customers power module manufacturing for optimizing thermal conductivity and dielectric strength of the cooling chain.

In addition to above, Aismalibar develops thermally conductive dielectrics, that meet and increase the high technical requirements for thermal conductivity and dielectric strength. In addition, optimizing the processability is a key development target, especially for high-volume serial productions such as in the automotive sector.

One example is "Dual Thermal Coating" (DTC) process, by which two glassless dielectric layers are applied directly to a metal carrier (copper or aluminum). With this new type dielectric technology, the heat-conducting / insulation dielectric layer is a direct part of a metal carrier in very thin thicknesses.

The lower layer of the dielectric is hardened during the manufacturing process at Aismalibar to obtain the desired electrical and thermal properties as specified in the data sheet.

CU+PRIMER

Cu DUAL COATING+PRIMER 4W (50µm–75µm - 100µm)

RA Solid Copper coated with two thermal conductive polymeric resins, delivered as B-stage + polymerized layer. Used for cladding electronic components that require high dielectric strength and extremely low thermal resistance. Can be supplied with copper or aluminium substrate.

STANDARD CONSTRUCTION

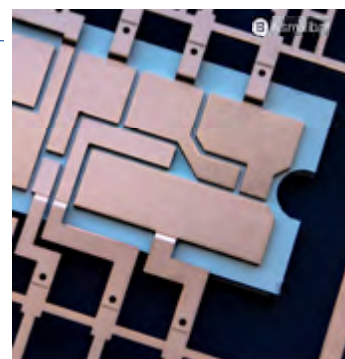


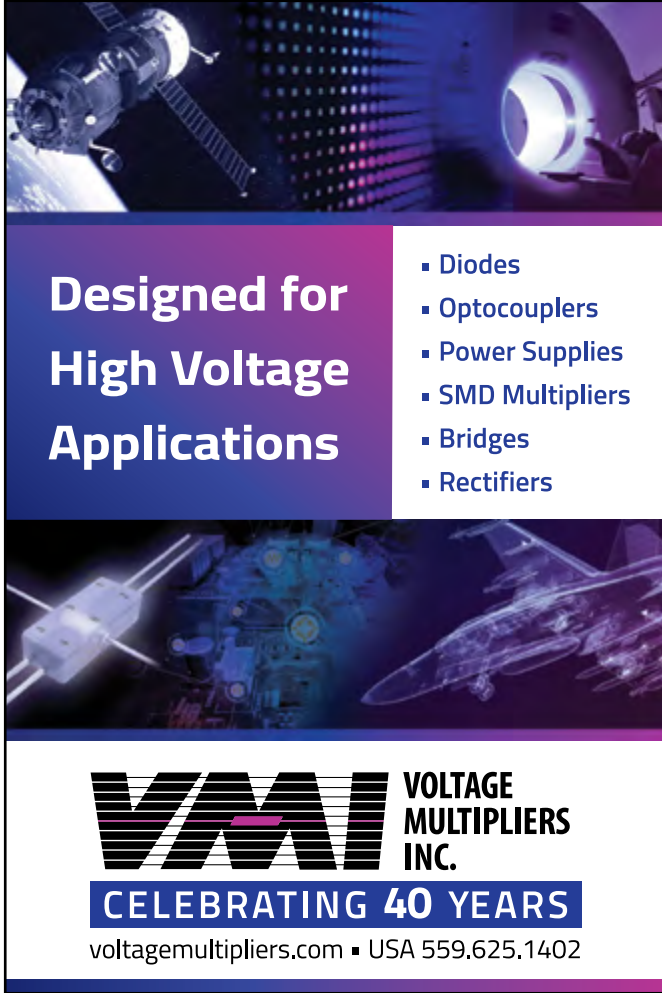
Figure 5: Copper substrate coated with two thermally conductive polymeric resins, supplied as a B-stage over a polymerized C stage layer.

An additional layer of B-stage is applied to the cured dielectric layer, which allows for further processing by the user. In its assembly, this structure (metal carrier plus two-layer dielectric) is laminated under pressure and heat to form a homogeneous overall unit. The result is a highly compact power module with optimized electrical and thermal properties, not requiring any mechanical components for pressing the different layer of the cooling chain together. DTC offers extended application lifetime throughout rough operational conditions plus long storage life, meeting the strict requirements of the electronic industry. AISMALIBAR is a longtime European Manufacturer and Innovator of substrates for the worldwide PCB Industry (FR4, CEM, IMS), since 2011 part of the Benmayor Group.

Production backbone is the development and manufacturing of IMS (Insulated Metal Substrate) technologies for thermally critical electronic applications. Manufactured in own factories in Barcelona, Spain and China, AISMALIBAR is shipping IMS materials to PCB-Shops worldwide.

In addition to the above PCB materials, AISMALIBAR is developing and producing thermally conductive foils to be used as thermal interface TIM between heat generating heat source and an external heat sink. Foil's Key Performance Indicators are high thermal conductivity (respectively low thermal resistance) in combination with highest isolation strength, as in many newly upcoming applications user protection against high voltage shock becomes mandatory. Customer's manufacturing like Bondsheet Cured film due it's silicon free status.

www.aismalibar.com



Designed for High Voltage Applications

- Diodes
- Optocouplers
- Power Supplies
- SMD Multipliers
- Bridges
- Rectifiers

VMI VOLTAGE MULTIPLIERS INC.
CELEBRATING 40 YEARS
 voltagemultipliers.com ▪ USA 559.625.1402

Removing heat from power electronics

Aismalibar thermal conductive laminates are the best solution to solve the problems with **high temperatures in PCB designs**.

- Power electronics industry;
- Welding industry by AC-DC converters (TIG,GTAW,MIG);
- Solar inverters;
- Power train systems.

By utilizing the combination of different **thermal products** in our portfolio, excess temperature can be transferred guaranteeing the **electrical insulation**.

aismalibar.com




Aismalibar®
 COOLING ELECTRONICS

Stay cool



Eliminating Voltage Overshoots for High-performance Modules in the Mega-watt Range

High-performance IGBT modules switch currents in the kA range, whereby unwanted and in some cases harmful voltage overshoots can occur due to DC link leakage inductances. To counteract this, TDK offers extremely low-inductance snubber and DC link capacitors.

*By Dipl. Ing. Wolfgang Rambow,
Senior Director Sales Technical Support,
TDK Electronics AG, Munich, and
Dipl. Ing. Marco Honsberg, MBA,
Senior Manager Product Management
Intelligent Power Modules and Electronics,
SEMIKRON GmbH+Co., Nuremberg*

With its latest development, the SkiiP®4 IGBT module manufacturer Semikron has optimized both design and performance. The new model has a DBC concept (Direct Bond Copper) with no base plate and on a newly developed high performance -cooler. As a result, the power module SKiiP2414GB17E4-4DUHP, which in this example is made up of four half, can now switch up to 25% higher currents of significantly more than 2400 A at a voltage of up to 1700 V at the IGBT.

Most conventional DC link designs quickly reach their limits with these high currents due to their leakage inductances. One feature of the SkiiP®4 module is the integrated intelligent adaptation of the power-off speed at very high DC link voltages, which protects the semiconductors against excessive transient overvoltage at the moment of turn-off. However, this protection function can generate additional losses and during continual operation is actually an indication of excessive DC link inductance. Therefore, it to reduce the DC link inductance to decrease the voltage stress when turn off the IGBT and simultaneously reduce the IGBT's turn-off losses.

Low-inductance DC link capacitors are essential

TDK has developed the B256* series of particularly low-inductance EPCOS DC link capacitors especially for new generations of IGBT modules. Table 1 and Figure 1 provide an overview of these models.

Series	DC voltage [V]	Capacitance [μ F]	ESL [nH]	ESR up to 100 kHz [m Ω]	Terminals
B25632* ULSI series	700 - 2000	20 - 270	<13	<1.5	2
B25690* Resin top	700 - 3000	110 - 5500	<20	<2	2
B25689* 4T Metal top	700 - 3000	50 - 3000	<10	<2	4

Table 1: Overview of the low-inductance EPCOS DC link capacitors



Figure 1: EPCOS DC link capacitors in different versions for the latest IGBT generations

These DC-Link capacitors provide an outstanding performance with particularly low losses due to their very low ESL (self inductance) and ESR (series resistance). DC link capacitors are connected to the SkiiP®4 modules either individually or as a capacitor bank. They are usually positioned directly next to the power modules in order to allow low inductances thanks to short lead lengths. However, in many cases this type of installation is not possible due to the existing construction space.

Tailor-made snubber capacitors dramatically reduces overvoltages

TDK is now launching its EPCOS special-snubber capacitors with mechanical and electrical parameters that are tailored to all SkiiP®4 modules to achieve a low-inductance design without any extreme voltage overshoots. One particular feature is the height offset of the connection lugs, which has been precisely adapted to the corresponding geometry of the SkiiP®4 modules (Figure 2 and lead image).

Advert

An additional benefit of the new development of the special snubber capacitors lies in the fact that it allowed for the optimization of their special inner structure as well. The maximum inductance values are therefore extremely low at less than 6 nH. There are currently two capacity values that have proved optimal for the SkiiP®4 modules: 330 nF and 470 nF with a rated voltage of 1600 V. These two special capacitors complete the EPCOS B32656S/58S series with the circuit diagram T12 for which TDK has a range of film capacitors. This makes it possible to use these capacitors in connection with other busbar configurations. The capacitors are easy to install and use in combination with the SkiiP®4 module. This constitutes an optimized and cost-reducing solution compared to more complex DC link designs.



Figure 2: the EPCOS snubber capacitors have been mechanically and electrically tailored to the Semikron SkiiP®4 modules.

As shown in Figure 3, the geometry's adaptation made it possible to screw the capacitors directly onto the module's busbar connectors, leading to lower leakage inductance of the DC link. The significantly lower overvoltages that were achieved during double-pulse tests as a result (measurements: Mankel-engineering.de) speak for themselves, and make it possible to operate the SkiiP®4 module with a much higher output current even with less improvable DC link constructions.

The optimized housing shape as well as the snubber capacitor connections and their different heights allow for the lowest possible insertion inductance and therefore the very effective performance of the

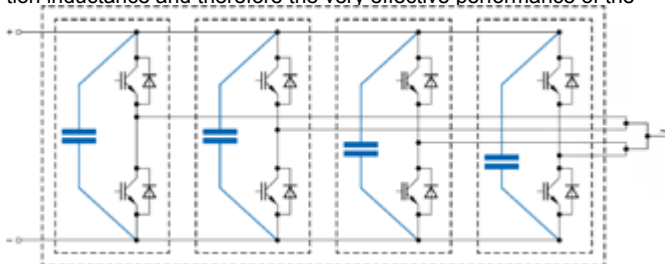


Figure 3: Simplified wiring diagram for the SkiiP®4 module as a half bridge with the EPCOS DC link snubber capacitors

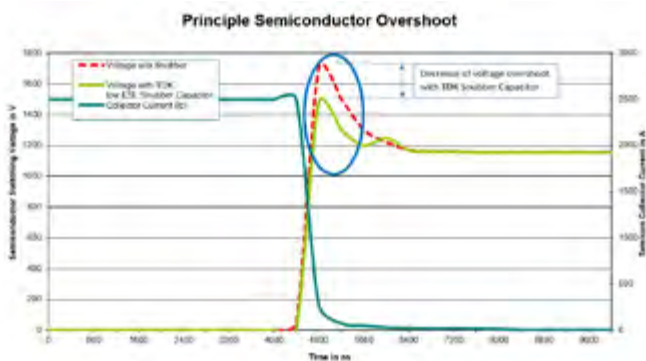


Figure 4: Thanks to the EPCOS snubber capacitors, the voltage overshoot that occurs when quickly turn off the current of 2500 A is reduced by more than 200V.



TRANSFORMERS
Innovation • Design • Performance
www.PaytonGroup.com











PAYTON AMERICA / CHINA / JAPAN / EUROPE

- Planar, Conventional or Hybrid solutions for high Efficiency & low Cost
- 10 Watts to 90,000 Watts in a single unit for all SMPS
- Fast Designs and Samples
- TS16949, AS9100, ISO9001, SQ-1000 & ITAR register

PAYTON PLANAR MAGNETICS
1805 S. POWERLINE ROAD, SUITE 109
DEERFIELD BEACH, FL 33442 USA
Tel: (954) 428-3326 x203 | Fax: (954) 428-3308
jim@paytongroup.com

snubber capacitor. This optimization does not lead to the reduction of creepage and clearance paths. At the same time, it allows the optimal usage of the existing construction space. Less optimized snubber capacitors would end up losing capacitance. In critical situations, maintaining the snubber capacity and ensuring its stability is crucial to prevent damage to the IGBT modules. Figure 4 clearly shows the effect of the EPCOS special-snubber capacitors connected to the SkiiP®4 modules when powering off a current of 2500 A.

The new EPCOS special-snubber capacitors can be used for new designs, but they also offer an attractive base for the simple retrofit-upgrade of existing converters. Even with DC link designs that are not fully optimizable, retrofitting with the snubber capacitors can help achieve significant performance improvements when using the new SkiiP®4 modules on high-performance coolers. Table 2 shows the characteristic data for the specified snubber capacitors.

	B32656S1474K412	B32656S1334K412
Width [mm]	19.0	19.0
Height [mm]	37.5	37.5
Length [mm]	42.0	42.0
Capacity [nF]	470	330
Voltage [V DC]	1600	1600
ESL [nH]	6	6
ESR [mΩ]	4	4

Table 2: Characteristic data for the EPCOS snubber capacitors optimized for SkiiP®4 modules

The described special-snubber capacitors are specific products.

www.tdk-electronics.tdk.com

Evaluate Junction Temperature from Inside

Measuring the conduction voltage of semiconductors in operation allows real time temperature evaluation

Junction temperature is directly related to system reliability. With TO packaged transistors it was possible to add a thermocouple to the case and get a good idea of the junction temperature this doesn't work for most SMD parts.

By Nigel Springett, Ing Büro Springett

Directly measuring the junction of SMD components is almost impossible, for the following reasons. There is no space for placing a thermocouple which can also influence the measurement. Top cooled cases allow us to measure the heatsink temperature, but poorly defined thermal resistance between transistor and heatsink, makes impossible to reliably calculate the junction temperature. In product development, worst case junction temperature is often estimated based on data sheet values of R_{th} . Production end tests measure many electrical parameters, but I have never seen the junction temperature being checked. Although this is critical for reliability. I remember 2 cases of early device failure, due to bad mounting of TO-247, transistors. The leads were stiffer than the heatsink clips, so the cooling tab did not lie flat on the heatsink.

Often the weak link in the cooling system is the thermal interface material (TIM) between the transistor and the heatsink. The power density is highest and the thermal resistance poorly defined. To keep thermal resistance low, a thin thermal interface material with high conductivity and low elasticity is used. The package dimensions of modern WBG transistors can have tolerances of over 300 μ m, and the TIM used is often thinner than the tolerances, to keep thermal resistance low. Figure 1 shows an exaggerated worst case, with the middle transistor higher than the outer devices.

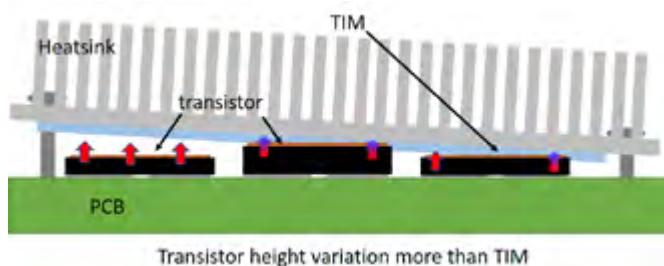


Figure 1: Poorly cooled transistors influence reliability.

The outer devices Q1 and Q3 will be badly cooled and run hotter than designed. Other factors such as solder thickness, foreign particles, pcb copper planarity etc only add to the tolerances.

In design qualification, thermocouples or thermal imaging are often used. A thermal camera looks through the package at the junction; the hot spot could be detected (figure 2); from here on we need a "magic factor" to arrive at an estimated junction temperature.



Figure 2: MASTERGAN1 hotspot measured, unknown junction temperature

This gives a number with an unknown accuracy, but even this cannot be used when a top cooled package is used. Here the heatsink is mounted over the transistor, there is usually no thermal connection to the backside of the pcb and the transistor is so small there is no possibility of reliably attaching the thermocouple to the device pad.

Real time junction temperature evaluation

Modern HEMTs and FETs, have a clear dependency between $R_{ds(on)}$ and temperature. The conduction voltage of Schottky and SiC diodes can also be temperature dependent. Despite its dependence on current and gate voltage, the conduction voltage still gives very good indication of the junction temperature. The various component technologies have different characteristics and for SiC and GaN the device design, saturation currents and dynamic $R_{ds(on)}$ also play a role, so the exact operating conditions are needed for a reliable estimation of the junction temperature. This is particularly important during design qualification, where a reliable measurement is the basis for the approval and field reliability prediction. In production testing and quality assurance, where the build quality is being tested, a comparison of the semiconductor conduction voltage under the same test conditions between production units under the same operating conditions gives a good indication if the thermal management is working as designed. Hot parts generally have a higher conduction voltage.

Current Sensor CFS1000

Smaller. Faster. Tougher.

Highest flexibility for your **e-mobility application.**

It's wide bandgap-ready!

- ✓ Bandwidth of 500 kHz
- ✓ Response time < 1 μ s
- ✓ High stray field immunity
- ✓ Based on MR-effect

Sensitec GmbH · www.sensitec.com



EV/HEV APPLICATIONS

DC/DC CONVERTERS

INVERTERS

CHARGING STATIONS

ON-BOARD CHARGER

Heraeus

Electronics

Unlock Your Potential

with Materials Solutions from Heraeus Electronics

Visit us @ PCIM Europe digital days
on 3-7 May 2021

Look for our new product,
Microbond PE830 solder paste

www.heraeus-electronics.com

Reliability

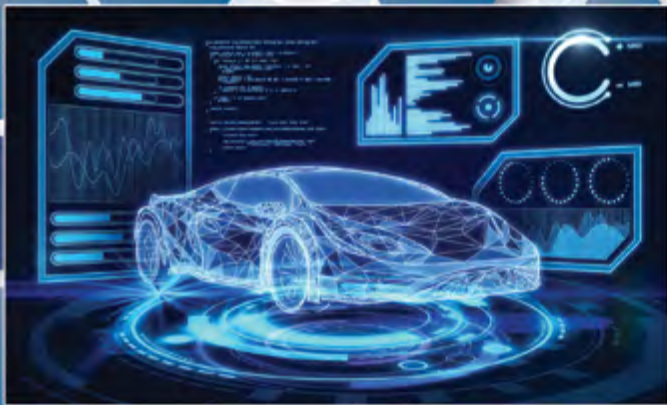
Performance

Solutions

Heraeus
Electronics

Materials

R3500 4-Channel High Accuracy Voltage Detector



Datasheet



The Ricoh R3500, a 4-channel high-accuracy window voltage detector operates up to 42V and is intended for use in automotive, industrial and consumer applications. Each channel has an independent sense pin and two detectors for monitoring overvoltage and undervoltage. A built-in hysteresis makes the detector less sensitive to noise on the measured voltage and ensures stable operation. The internal voltage regulator is used to power the IC directly from the car battery and stabilizes supply voltage fluctuations, even during a cranking condition. An additional test pin provides a diagnostic function to verify the proper operation of the voltage detectors periodically.

Features (automotive version):

- ▶ Operating/Abs/Peak Voltage 3.0 to 42 / 50 / 60 V
- ▶ Operating Temperature Range -40° to 125°C
- ▶ Supply Current Typ. 10 μ A
- ▶ Overvoltage Detection 1.0 to 5.9 V (10 mV step)
- ▶ Undervoltage Detection 0.9 to 5.0 V (10 mV step)
- ▶ Detection Release Hysteresis Max. 0.75%
- ▶ Over / Undervoltage Accuracy -1.25 to +0.75%
- ▶ Detection Delay Time Typ. 20 μ s
- ▶ Release Time Delay Typ. 4 ms (Cd = 0.01 μ F)
- ▶ Output Type N-channel Open Drain
- ▶ Package (5.2 x 6.2 x 1.45 mm) HSOP-18



www.n-redc.co.jp/en/

Compared to the older TO-220 transistors, the modern transistor packages have a small thin contact area with little copper and a very low thermal mass. With little to heat up the temperatures rise fast. When the heat is not being properly carried away by the cooling system, 2W losses heat up an SMD transistor junction at about 36°C/s. This is fast enough and large enough to be easily seen in a production end test during the normal full load power testing.

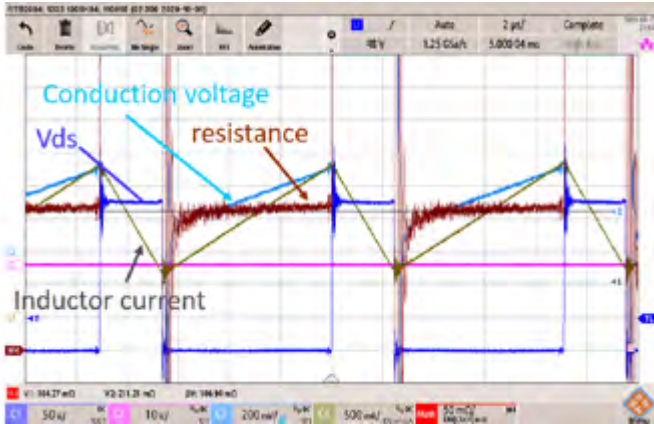


Figure 3: MasterGan hot Rds(on) measurement in 500ns

Testing in practice is very simple; a Springburo clipper or similar can be used and simply connected over the transistor. An optional quality 10:1 differential probe can reduce potential issues with circulating currents. The clipper cuts out the high switching voltage over the DUT, so the conduction voltage can be seen in detail. We use a scale about 200mV/div. To calculate resistance a current signal also needed. Most modern DSO can then perform a math function as shown in Figure 3. The math channel shows the $R_{ds(on)}$ at about 211mΩ, this is 150% of the measured cold value of 140mΩ. For the data sheets this means the junction is about 77°C, significantly hotter than 49°C shown in the thermal image in Figure 2.

In Figure 3, the displayed $R_{ds(on)}$ takes about 500ns to stabilise, this is because a lazy setup was used with long wires to the clipper; as would be the case in a production environment. If faster measurements are needed then the clipper must be connected directly at the component body, to minimise the effects of lead and wiring inductance. Figure 4. shows achievable performance. The settling time is reduced from 500ns to 100ns. The time base is 80ns/div; the MOS-

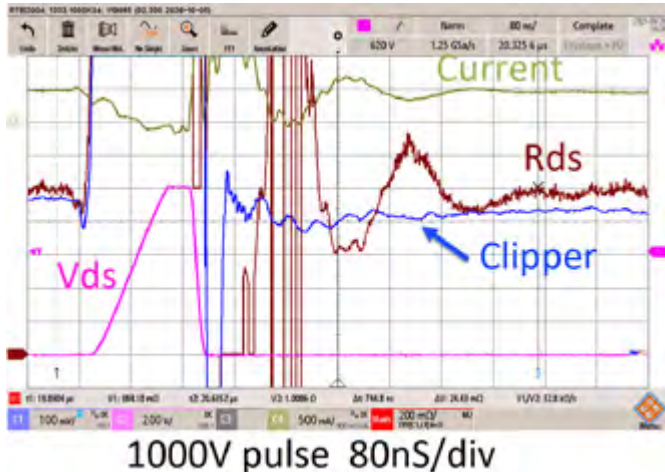


Figure 4: Conduction voltage measurement in 100ns after switching 1000V

FET drain on Ch2@200V; the MOSFET is turned off for about 200ns and then turned on switching 1000V in about 15ns.

The clipper output is shown on Ch1@ 100mV, Ch4 is the switch current, with ringing. The clipper output has recovered and is showing the MOSFET has a conduction voltage of about 400mV, slightly lower than before it turned off, 100ns after the switching event. This is because the inductor current has fallen during the off-time. The R_{ds} calculated from the current and clipper voltage; is the same before and after the switching event. This confirms that a fast and accurate measurement within a few 100ns of the conduction voltage is possible, even with an off state of 1000V and a conduction voltage of 400mV. This is useful for evaluating components and ensuring they are being turned on and off properly.

Accurate measurements need care

Measuring the conduction voltage in the application is looking at a few hundred millivolts in hundreds of volts, and then needing an accuracy of a few percent. In the example shown in Figure 4, a 20mV error would give a 5% error in the calculated resistance. 20mV in 1000V is .002% error. This is way outside the possibilities of scope probes. Typical probes specify a DC accuracy of about 2%, (AC accuracy is not specified), well outside the accuracy needed for reliable conduction measurements. (We tried lots of different solutions but needed something easy to use, that we could trust without careful calibration etc).

For junction temperature evaluation, when dynamic resistance or switching characteristics is not the focus, the conduction voltage can be measured in the middle of the switching cycle. This means that very short connections are not necessary. As timing is not important for comparative measurements, common mode filters can be added to reduce ground ringing. The CLP1500V15 is a passive probe with no offset and with a voltage transfer under the clipping voltage close to 100%. It is not isolated and has a common ground connection with a scope. This works well if the DUT is supplied from an isolated power supply, but even then there is a risk of common ground currents affecting the measurement accuracy. A 100MHz differential probe can be used to block these currents as shown in Figure 5. If large common mode voltages are present, the differential probe can add significant errors. Alternatively, an optically isolated probe or analogue isolator can be used on the clipper output. A floating isolated scope is another possibility, note we have seen that some scopes don't like the common mode switching and behave "strangely".

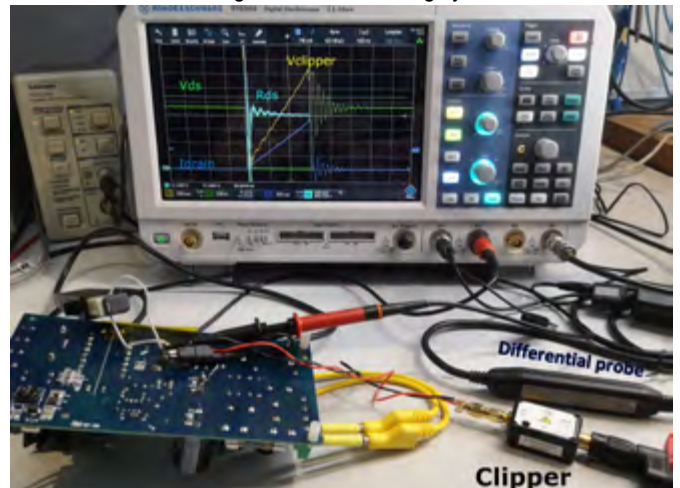


Figure 5: Lazy measurement setup with long leads, Rds measurement valid after 1µS

Figure 5 shows a lazy test setup, on a flyback power supply. The clipper is connected to the transistor with about 20cm leads. The MOSFET is switching about 900V. When the MOSFET is turned on, the clipper output falls to zero and rises to 3V. The R_{ds} , calculated from the current and voltage is 1.7Ω; close to the typical data sheet value of 1.8 Ω; confirming that even with long leads to the clipper, (such as a production test probe or test point,) good measurement accuracy can be achieved. The settling times are just longer. In the above example 1μs is needed before settling, this is a typical value.

New possibilities

Being able to “look at the junction” conduction voltage, with the clipper gives new test possibilities for design and production screening. Monitoring transient effects, such as overload or start-up. Recording mains frequency temperature variation in PFC and inverters. Observing junction temperature stress under power boost in new generation SiC and GaN EV inverters, is now a real possibility. The need for Xray control for solder voids under SMD power components could be reduced by confirming conduction voltage and junction temperature in production end tests; or during extra QA testing. Looking for a needle in a haystack can be difficult, but with the correct tools, X-ray or magnetic sensors etc it is easy. Checking semiconductor conduction voltage in operation was once difficult and can now be done fast and efficiently with the clipper.

www.springburo.org

CPS TECHNOLOGIES www.alsic.com
 Norton MA
 508 222-0614

AISiC Thermal Management
62 mm Baseplate
Industry Standard Design

190 W/mK
 7.4 ppm/°C
 3.01 g/cm³

High Reliability for
 Traction, Avionics, EV
 Inverters/Converters, EV
 Charging Stations,
 Industrial Automation,
 Welding, Solar, Wind

IN STOCK - FAST
 DELIVERY - WITH OR
 WITHOUT PLATING

105.6 x 61.6 x 3.4 mm
 220 μm Cooler Surface Curvature
 Designed for WBG Applications

ELYTONE

Precision Meets Robust
Current Sense
Transformer

- Current up to 1000A
- Accuracy 0.2%~5%
- Frequency 10Hz to 1MHz
- Ratio up to 1:10000
- Wide operating temperature

Customize focused
 IATF 16949 ISO 13485

Our Product Lines

Clamp type up to 500A SMD type up to 35A DIP type up to 40A

sales_magnetics@elytone.com.tw www.elytone.com.tw

Superior Performance
superior price.

Standard and Fast Recovery
High Voltage Diodes up to 45kV

Most diodes in stock.
 Custom solutions at standard product prices.

Contact DTI today to discuss
your high voltage design.

DEAN TECHNOLOGY

+1.972.248.7691 | www.deantechnology.com

Ride Through the MLCC Shortage by Reducing Capacitance Requirements in Your Power Supplies

The worldwide supply of multilayer ceramic capacitors (MLCCs) is not keeping up with demand. This is due in no small part to increased electronic complexity of cell phones, increased sales of electric cars, and a worldwide expansion of electronic content across industries.

By Atsuhiko Furukawa, Field Applications Engineer, Analog Devices

Some smartphones have doubled MLCC usage over a few years; an electric vehicle can quadruple usage over a typical modern internal combustion engine (Figure 1). The supply shortage of MLCCs, appearing near the end of 2016, has made it especially difficult to obtain large-capacity products (several tens of μF or more) necessary for the operation of prolific power supplies used in the latest electronics. Manufacturers looking to reduce their MLCC requirements inevitably look to the capacitor requirements of power supplies—in particular, switching regulators. This places power supply designers on the front lines of mitigating the cap shortage.



Figure 1: Increases in worldwide MLCC use in electric automobiles (a) and cell phones (b), without commensurate increases in production, have led to shortages. 1

Power Circuits Use Capacitors, A Lot of Capacitors

A typical dc-to-dc buck converter uses the following capacitors (see Figure 2):

- Output capacitor: Smooths out both output voltage ripple and supply load current during load transients. Generally, a large capacitor measuring several tens of μF to 100 μF is used.
- Input capacitor: In addition to stabilizing the input voltage, it plays the role of instantaneously supplying the input current. In general, several μF to several tens of μF are used.
- Bypass capacitor: Absorbs noise generated by switching operation and noise from other circuits. 0.01 μF to 0.1 μF are generally used.
- Compensation capacitor: It secures the phase margin in the feedback loop and prevents oscillation. Several hundreds of pF or

several tens of nF are often used. Some switching regulator ICs incorporate the compensation capacitor.

The best way to reduce capacitance is to focus on minimizing the output capacitors. A strategy for reducing output capacitance is explored next, followed by solutions to reducing bypass capacitor requirements and, to some extent, input capacitors.

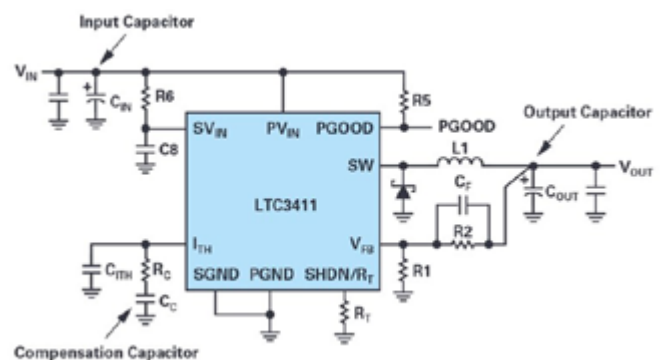


Figure 2: Capacitors used in a typical buck regulator.

Increase Switching Frequency to Reduce Output Capacitance

Figure 3a shows a typical current-mode buck converter block diagram, with the shaded area denoting the feedback loop and the compensation circuit.

The characteristic of the feedback loop is shown in Figure 3b. The frequency at which the loop gain is 0 dB (gain = 1) is called the crossover frequency (f_c). The higher the crossover frequency, the better the load step response of the regulator. For example, Figure 4 shows the load step response for a regulator supporting a rapid load current increase from 1 A to 5 A. The results are shown for crossover frequencies of 20 kHz and 50 kHz, resulting in 60 mV and 32 mV dropouts, respectively.

On the surface, increasing the crossover frequency looks like an easy choice: load step response is improved by minimizing the output voltage drop, so the output capacitor can be reduced. Raising the crossover frequency, though, brings up two issues. First, it is necessary

to secure a sufficient phase margin of the feedback loop to prevent oscillation. Generally, a phase margin of 45° or more (preferably 60° or more) is required at the crossover frequency.

The other issue is the relationship between switching frequency (f_{SW}) and f_c . If they are similar in magnitude, negative feedback can respond to the output voltage ripple, threatening stable operation. As a guideline, set the crossover frequency to one-fifth (or less) of the switching frequency, as shown in Figure 5.

To increase the crossover frequency, you must also raise the switching frequency, which in turn results in higher switching losses via the top and bottom FETs, reducing conversion efficiency and generating additional heat. Any savings in capacitance is offset by the complexity of additional heat mitigation components: fins, fans, or additional board space.

Is it possible to maintain high efficiency at high frequency operation? The answer is yes. A number of Power by Linear™ regulator ICs from Analog Devices do just that by incorporating a unique FET control that keeps efficiency high even at higher switching frequencies (Figure 6).

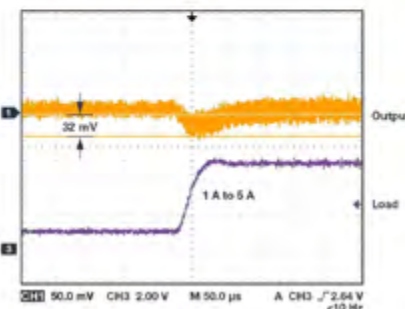
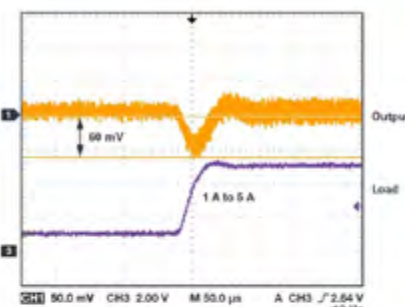
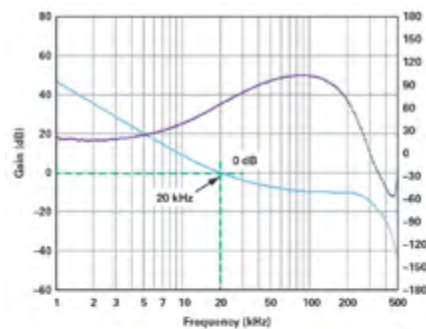
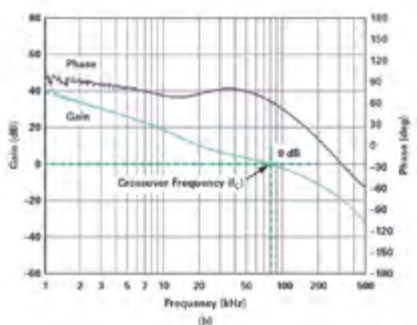
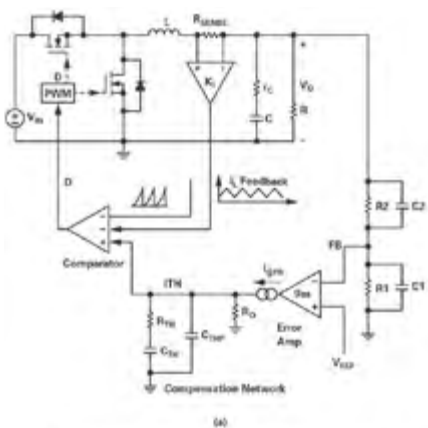


Figure 3: Block diagram of a typical buck regulator (a) and typical feedback characteristic (b).

Figure 4: Comparing the load step responses of a buck regulator at two crossover frequencies.

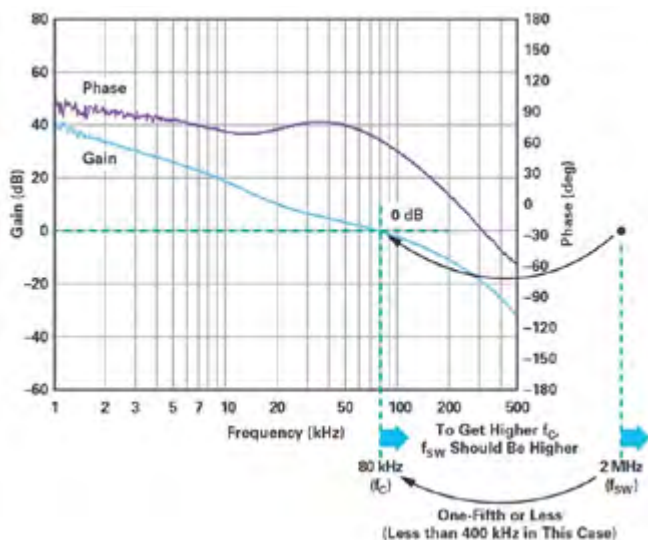


Figure 5: If the switching frequency and control loop crossover frequency are too close, the negative feedback may respond to output voltage ripple. It is best to keep the crossover frequency below one-fifth of the switching frequency.

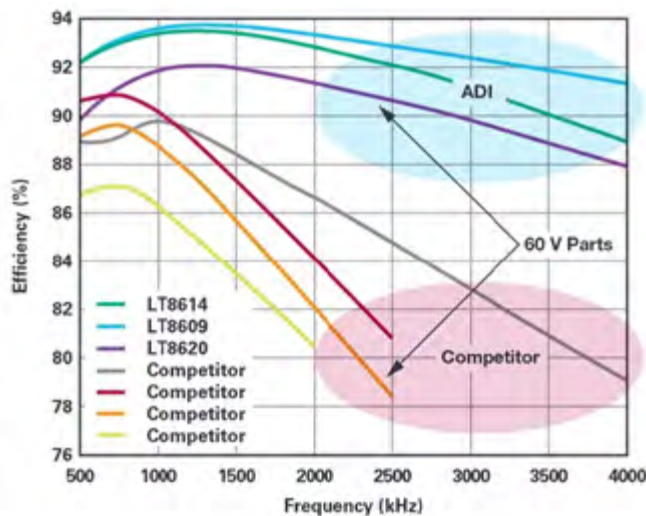


Figure 6: Power by Linear regulators vs. competition. In a typical regulator, when the switching frequency goes up, efficiency goes down. ADI Power by Linear regulators can maintain high efficiency at very high operating frequencies, enabling the use of smaller value output capacitors.

For example, the LT8640S 6 A output buck regulator maintains greater than 90% efficiency over its full load range (0.5 A to 6 A) while operating at a frequency of 2 MHz (12 V input and 5 V output).

This regulator also lowers the capacitance requirements by reducing inductor current ripple (ΔI_L), which in turn reduces the output ripple voltage (ΔV_{OUT}) as shown in Figure 7. Likewise, a much smaller inductor can be used. With a higher switching frequency, the crossover frequency can be increased, improving load step response and load regulation, as shown in Figure 8.

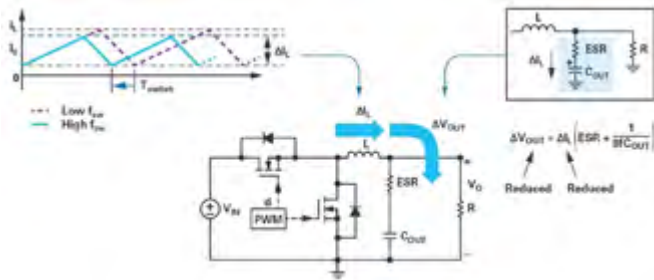


Figure 7: Increase switching frequencies to reduce capacitor and inductor size.

Silent Switcher Regulators Significantly Reduce Bypass Capacitance

How about reducing bypass capacitance? The main role of the bypass capacitor is to absorb the noise generated by switching operation itself. If switching noise is reduced in other ways, the number of bypass capacitors can be reduced. A particularly easy way to achieve this is through the use of a Silent Switcher® regulator.

How does a Silent Switcher regulator reduce switching noise? A switching regulator has two current loops: when the top FET is on and the bottom FET is off (red loop) and when the top FET is off and the bottom FET is on (blue loop) as shown in Figure 9. The hot loop carries a fully switched ac current—that is, switched from zero to I_{PEAK} and back to zero. It has the highest ac and EMI energy, as it produces the strongest changing magnetic field.

Slew-rate control can be used to suppress switching noise by slowing the rate of change of the gate signals (lowering di/dt). While effective in suppressing the noise, this increases switching losses, producing additional heat, especially at high switching frequencies as previously described. Slew-rate control is effective under certain conditions and Analog Devices also offers solutions with this feature.

Silent Switcher regulators suppress electromagnetic noise generated from the hot loop without slew-rate control. Rather it splits the VIN pin in two, allowing the hot loop to be split into two symmetrical hot loops. The resulting magnetic field is confined to the area near the IC, and significantly reduced elsewhere, thus minimizing radiated switching noise (Figure 10).

The LT8640S, the second generation of this technology—Silent Switcher 2 (Figure 11)—incorporates the input capacitors in the IC. This ensures maximum noise suppression, eliminating the need to carefully position the input caps in the layout. This feature, of course, also reduces the MLCC requirements. Another feature, spread

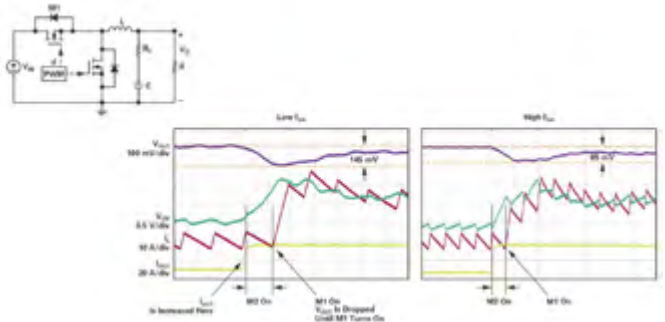


Figure 8: Increased switching frequency results in improved load step response.

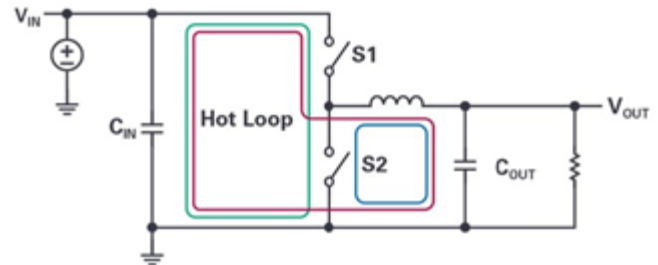


Figure 9: The hot loop in a switching regulator produces the bulk of the radiated noise because of the alternating magnetic field it generates.

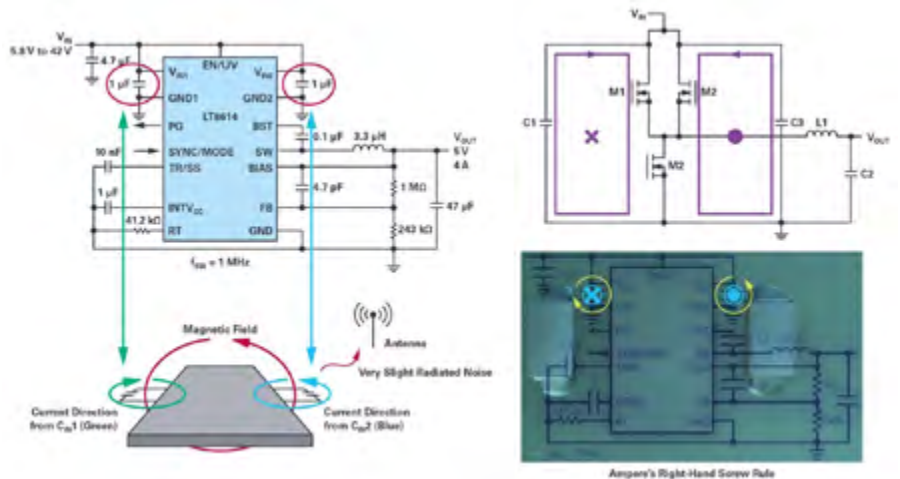


Figure 10: Patented Silent Switcher technology.

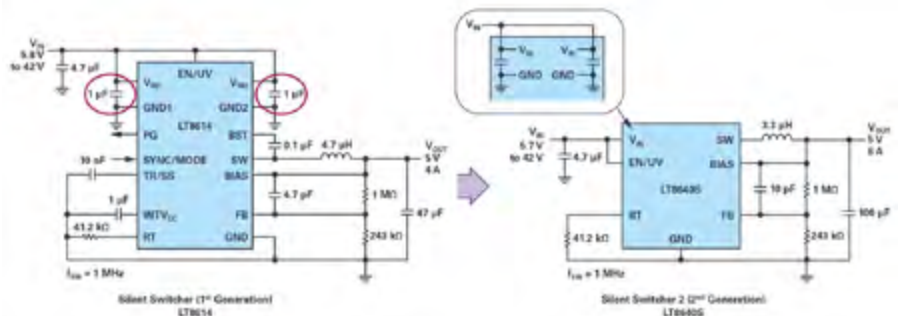


Figure 11: Silent Switcher 2 technology from ADI brings the input caps within the IC, simplifying layout and improving noise suppression.

spectrum frequency modulation, lowers noise peaks by dynamically changing the switching frequency. The combination of these features enables the LT8640S to clear CISPR 25 Class 5 EMC standards for automobiles with ease (Figure 12).

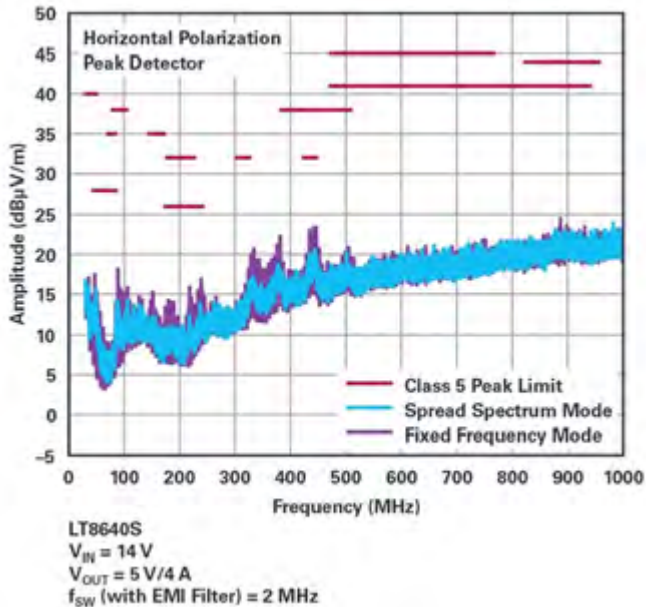


Figure 12: The combination of noise suppression features in a Silent Switcher 2 device, such as the LT8640S, enables easy clearance of CISPR 25 Class 5 peak limits even while reducing input and bypass capacitance.

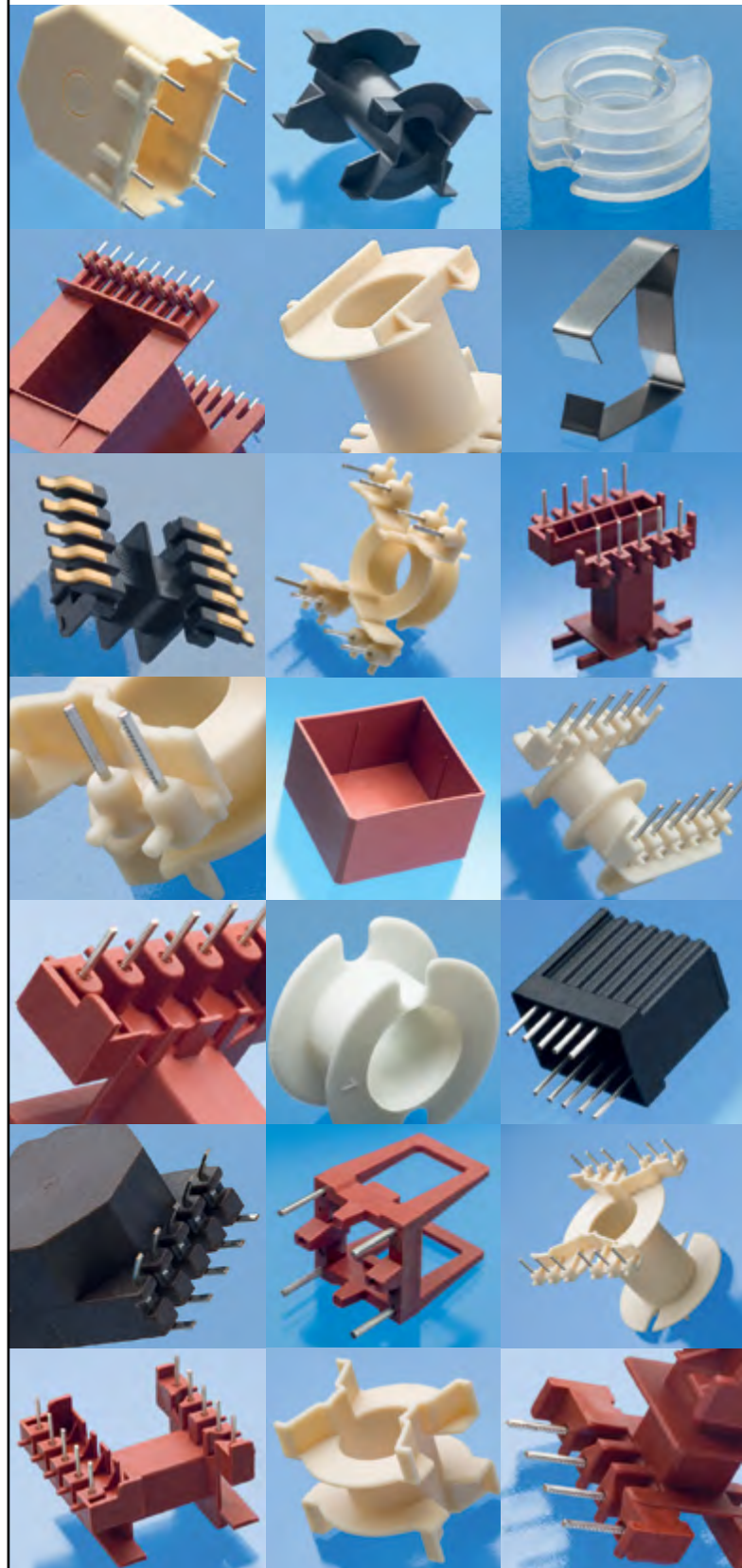
Conclusion

Power by Linear devices from ADI can help reduce MLCC requirements, helping designers ride through the MLCC shortage. Output capacitance requirements are reduced by using high frequency operation while maintaining uncommonly high efficiency. Devices that feature Silent Switcher architecture significantly suppress EMI noise, reducing bypass capacitor requirements. Silent Switcher 2 devices further reduce MLCC needs.

References

- 1 Robin Blackwell. "Investor Presentation February 2018." KEMET, February 2018.
- LT8640S Data Sheet. Analog Devices, Inc., June 2017.
- Seago, John. "OPTI-LOOP Architecture Reduces Output Capacitance and Improves Transient Response." Analog Devices, Inc., August 2007.
- Zhang, Henry J. "Modeling and Loop Compensation Design of Switching Mode Power Supplies." Analog Devices, Inc., February 2016.

www.analog.com



Upscaling Small Real-Time Simulators for Large Power Electronic Systems

The vast variety of power electronic conversion systems, characterized by differences in voltage and power ratings, operating and switching frequencies, as well as application specific requirements, offers a high number of possibilities from the R&D viewpoint. Mainly due to increasing affordability and availability of computational resources, various software toolchains have become an integral part in the design of power converters over the years.

*By Stefan Milovanovic and Drazen Dujic,
Power Electronics Laboratory, EPFL, Switzerland*

Nowadays, apart from the indispensable engineering skill, power electronics designers rely on the use of accurate simulation tools. These allow for simulation of almost any part of the converter circuit ranging from semiconductors and magnetics all the way to control algorithms governing multiple processes in any relevant domain (e.g. electric, magnetic, dielectric, etc.). Moreover, simulations in different domains can be executed independently, however, mixed-mode simulations and co-simulations do not represent a rarity either.

When it comes to control software development, Real-Time Hardware-in-the-Loop (RT-HIL) systems have become an essential and irreplaceable design tool, allowing for control algorithms, typically developed and supported by offline simulations, to be deployed and validated on the real embedded controller used inside the final product. For the low power converters and switching frequencies exceeding tens or hundreds of kHz, RT-HIL systems are not yet capable of providing an adequate support for the reasons falling out of this article's scope. However, in the domain of high-power converters, which rely on the use of digital controllers, while switching at frequencies not exceeding several kHz, RT-HIL systems have become widely adopted for commissioning and testing of control software.

Even though an RT-HIL system can be used in various ways, Figure 1 illustrates its typical role implying the support to the control software development and commissioning. Thanks to their computational power, stemming from the use of FPGAs and/or CPUs, RT-HIL systems provide the means for high-fidelity real-time simulations of the converter hardware parts. Typically, this includes converter topology with all the parts defining its internal dynamics, along with the relevant elements connected to its terminals (e.g. networks, power supplies, loads). Connecting the dedicated embedded controller to an RT-HIL system through a suitable interface, which often requires custom development as there are many RT-HIL systems on the market, gives control engineers the possibility to explore performances of various control algorithms, without the controller ever realizing that it drives the converter model, running on the employed RT-HIL system, instead of the real power hardware. Consequently, a risk-free environment for development and testing of control schemes is ensured, which is crucial especially if large and expensive systems, such as MW-level

power electronics converters, are considered. What is more, development of control algorithms and converter hardware parts can take place in parallel, as depicted in Figure 1, which reduces the development time of the converter as a whole.

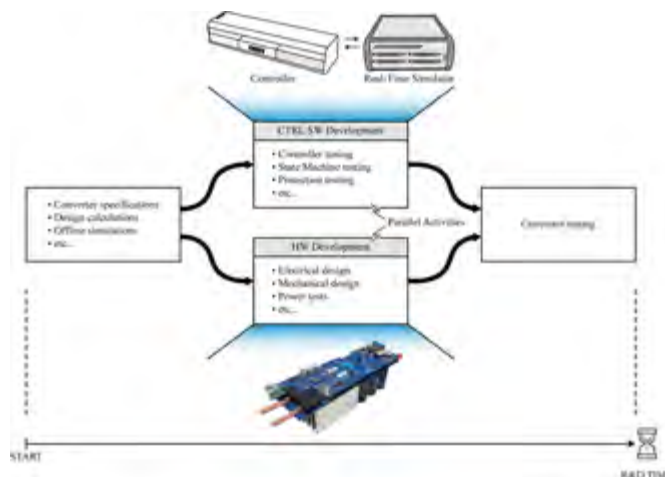


Figure 1: The RT-HIL systems decouple hardware and software development during the R&D process.

Going for the RT-HIL System

Today, numerous RT-HIL vendors are present on the market, which makes the question of the real-time simulator choice rather non-trivial. The decision-making process is quite often affected by different factors and offered performance figures, which are too complex for a short description. Nevertheless, a few important aspects influencing the adoption of a certain RT-HIL system can be listed as:

- Performance in terms of computational capabilities, e.g. how large is the system (the number of state variables and switching devices) that can be simulated in a given time (in power electronics, cycle times ranging from one to a few microseconds are used as reference).
- Performance in terms of connectivity, e.g. how many digital/analogue inputs/outputs are available at the user interface, what are the sampling rates, voltage levels, etc.

- Costs of the ownership and type of RT-HIL toolchain, e.g. are there any license fees, is the software environment standalone or it depends on the 3rd party products (e.g. MATLAB), can the RT-HIL be reused after the project is over, etc.

between the hardware elements and the employed controller. For our design, with eight full-bridge submodules [4] per one MMC branch (48 submodules in total, considering there are six branches), and with a relatively modest number of electrical analog/digital inputs/outputs offered by a single RT-Box unit [5], it became quickly clear that multiple

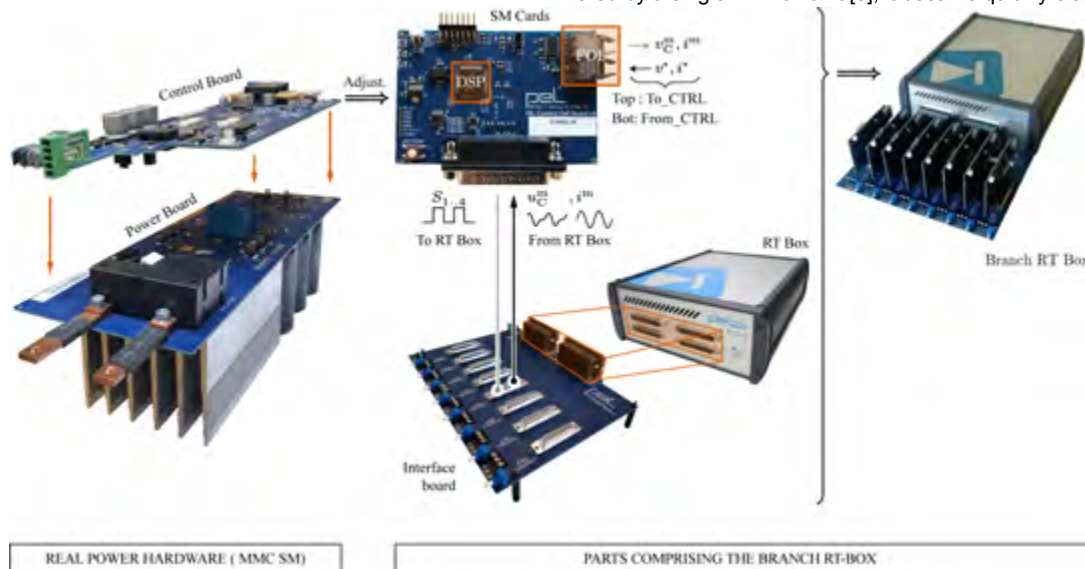


Figure 2: The development steps, from the existing MMC submodule to the MMC RT-HIL system (Digital Twin).

Having been PLECS user for many years and after gaining initial practical experience with single RT-Box units, such a platform is selected for development of a large-scale RT-HIL system to support control software development for the high-power medium voltage Modular Multilevel Converter (MMC) [1].

MMC RT-HIL System

Owing to the outstanding scalability [2] and the ability to perform various types of conversion [3], the MMC is nowadays considered a suitable candidate for numerous applications. While its modular nature simplifies the hardware design, it requires a complex control structure, where substantial amount of information needs to be exchanged

units are needed to host model of the converter hardware and application served by the it. Figure 2. illustrates some of the design steps, starting from the available MMC submodule [4] having its Power Board, which has been modeled on the RT-Box, and the Control Board, which was cost-optimized for the purpose of RT-HIL while preserving all relevant interfaces and communication capabilities. Finally, one RT-Box unit hosts the model of eight MMC submodules, forming the so-called Branch RT Box, which is replicated six times.

Application RT-Box, visible in Figure 3., hosts the model of an arbitrary application the MMC is serving (e.g. grid-connected converter, drive, etc.). To connect the RT Boxes described above with the con-

TAMURA

WELCOME TO TAMURA

Your One and Only Company



The Tamura Group supplies an original range of products and services, highly regarded in the global electronics market, to satisfy the evolving needs of customers, employees and shareholders supporting the Group's growth.

Please visit our website!
<https://www.tamuracorp.com/>

WEB



LinkedIn



Tamura Corporation, Tokyo, Japan

troller used for verification of various control schemes, suitable interfaces are developed, as presented in Figures. 3 and 4. Thus, seven RT-Boxes are interfaced and synchronized, for the first time, using available SFP links to host and run the complete model of an MMC.

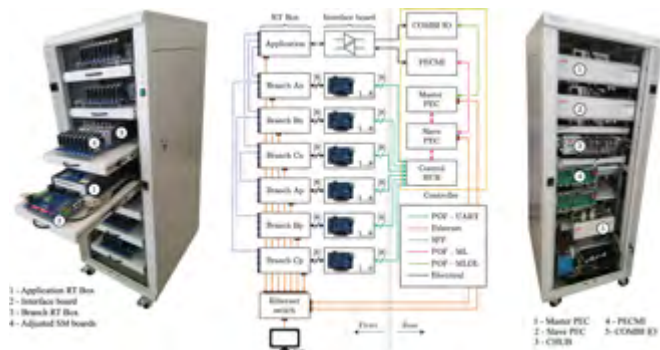


Figure 3: Assembled HIL system: Left - Front view; Middle - Wiring diagram; Right - Rear view

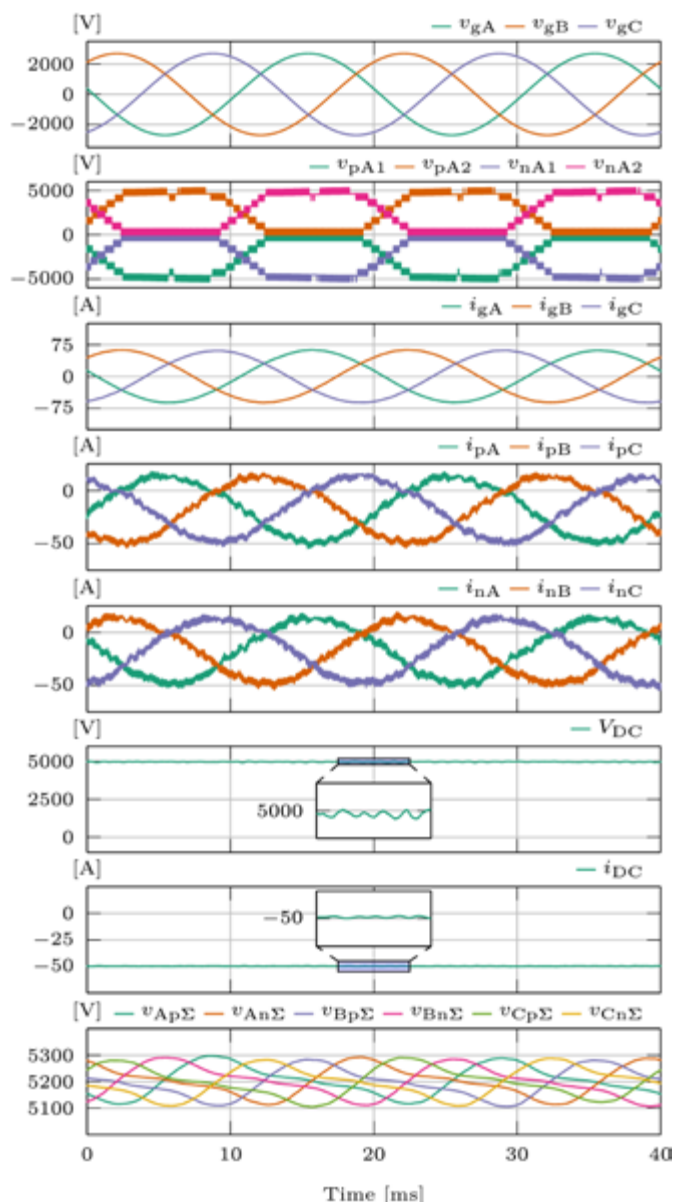


Figure 4: Typical RT-HIL waveform during MMC operation

The complete MMC RT-HIL system is shown in Figure 3, and four identical units were assembled in Power Electronics Laboratory at EPFL. Actual controller hardware is based on the industrial controller from ABB (AC800 PEC) where the complete control application software is deployed. Coordination between multiple MMC is managed by Master PEC, while the Slave PEC actually executes the control algorithms such as grid synchronization, grid current control, energy balancing or any other application specific control. A few other control boards are used to gather relevant signals and to communicate with local MMC submodule DSP-based controller through a Plastic Optical Fiber (POF) links, as in the real medium voltage MMC prototype. Figure 3 also illustrates wiring diagram of the system. As can be seen, there are multiple communication channels used, such as electrical connections, POF links with specific protocols, SFP links, or Ethernet based communication, and so on.

RT-HIL Results

Developed RT-HIL system as whole, supported by the models deployed on RT-Box units, allows for exploration of all operating modes of the MMC in any desired given configuration. For the sake of illustration, Figure 4 presents the MMC operating waveforms, obtained from the RT-HIL, in case the energy is transferred from AC to DC side (rectifier mode) at the power level equal to 250kW. Typical MMC operating waveforms are produced thanks to high fidelity of RT simulation models and system level integration with the real controller. Testing of state machine transitions (e.g. from charging to operating), various protection functions, control algorithms of the external and internal variables, or application specific scenarios, can easily be investigated in a time-efficient manner.

Conclusions

This article provided a short description of the MMC RT-HIL realized by means of the small-scale HIL units (i.e. RT Boxes). For the first time, the MMC model, suitable for real-time simulations, was sectioned and distributed over seven RT Boxes, demonstrating flexibility and scalability of this real-time simulation platform. Validation of the assembled system was performed by means of an industrial controller, while further upscaling is being currently investigated.

References

- [1] A. Lesnicar and R. Marquardt, "An innovative modular multilevel converter topology suitable for a wide power range - Power Tech Conference Proceedings, 2003 IEEE Bologna," 2003 IEEE Bol. PowerTech - Conf. Proc., vol. 3, pp. 1–6, 2003,
- [2] S. Milovanović and D. Dujic, "On Facilitating the Modular Multilevel Converter Power Scalability Through Branch Paralleling," 2019 IEEE Energy Convers. Congr. Expo., pp. 6875–6882, 2019.
- [3] M. Utvic, S. Milovanovic, and D. Dujic, "Flexible medium voltage DC source utilizing series connected modular multilevel converters," 2019 21st Eur. Conf. Power Electron. Appl. EPE 2019 ECCE Eur., pp. 1–9, 2019,
- [4] M. Utvic, I. P. Lobos, and D. Dujic, "Low Voltage Modular Multilevel Converter Submodule for Medium Voltage Applications," PCIM Eur. 2019; Int. Exhib. Conf. Power Electron. Intell. Motion, Renew. Energy Energy Manag., no. May, pp. 1–8, 2019.
- [5] Plexim GmbH, "RT Box Manual." <https://www.plexim.com/sites/default/files/rtboxmanual.pdf>.

The Premier Global Event
in Power Electronics™

APEC®

2021

Virtual Conference + Exposition

JUNE 14-17TH, 2021



AC-DC Converter ICs for Appliances, Sensors and Metering Applications

Power Integrations announced a member of its acclaimed LinkSwitch™-TN2 AC-DC converter family. The LNK3207 ICs facilitate higher-power offline buck converter designs for appliances and industrial applications by increasing the available output current from 360 mA to 575 mA, while also reducing BOM count. Power Integrations' LinkSwitch-TN2 ICs increase output current from 360 mA to 575 mA & target mass-market appliances such as washers, dryers, coffee makers and more. Design engineers can easily upgrade existing designs while reducing BOM count. Silvestro Fimiani, product marketing manager at Power Integrations said: "These LinkSwitch-TN2 ICs are pin-to-pin compatible with previous generations, making it simple for customers to upgrade to higher-power designs. A high-current buck converter can be created using a minimal number of easily available components while saving at least one diode over previous solutions." The LNK3207 AC-DC converter ICs increase the available current by 60% while also delivering greater than 80% efficiency and no-load consumption of less than 30 mW. Each monolithic LinkSwitch-TN2 IC incorporates a 725 V power MOSFET, oscillator, on/off control for high efficiency at light load, a high-voltage switched current source for self-biasing, frequency jittering, fast (cycle-by-cycle) current limit, hysteretic thermal shutdown, and output and input overvoltage protection circuitry. The LinkSwitch-TN2 ICs target mass-market appliances such as washers, dryers and coffee makers, which benefit from their design simplicity. They are also suitable for



sensor-based devices that require low power such as home security cameras and smart thermostats, as well as metering and IoT installations. Devices are available in three packages, PDIP-8C, SMD-8C and SO-8C, for design flexibility. The SMD-8C package is ideal for high-temperature ambient 85/105 °C applications.

www.power.com

Isolated Gate Driver Safely Controls Silicon-Carbide MOSFETs

Joining STMicroelectronics' STGAP family of isolated gate drivers, the STGAP2SiCS is optimized for safe control of silicon carbide (SiC) MOSFETs and operates from a high-voltage rail up to 1200V. Capable of producing a gate-driving voltage up to 26V, the STGAP-2SiCS has a raised Under-Voltage Lockout (UVLO) threshold of 15.5V to meet the turn-on requirements of SiC MOSFETs. If the driving voltage is too low, which can be caused by low supply voltage, the UVLO ensures the MOSFET is turned off to prevent excessive dissipation. The driver features dual input pins that let designers determine the gate-drive signal polarity. With 6kV of galvanic isolation between the input section and the gate-driving output, the STGAP-2SiCS helps ensure safety in consumer and industrial applications. Its 4A output-sink/source capability is suited to mid- and high-power convertors, power supplies, and inverters in equipment such as high-end home appliances, industrial drives, fans, induction heaters, welders, and UPSes. Two different output configurations are available. One has separate output pins that allow independent optimization of turn-on and turn-off times using a dedicated gate resistor. The second



is featured for high-frequency hard switching, with a single output pin and active Miller clamp that limits oscillation of the SiC MOSFET gate-source voltage to prevent unwanted turn-on and enhance reliability. The input circuitry is compatible with CMOS/TTL logic down to 3.3V, which allows easy interfacing with a wide variety of control ICs.

www.st.com

Power Inductors Reduce DC Resistance

Coilcraft's XGL4030 Series of high-performance, molded power inductors offer up to 40% lower DCR than the previous best-in-class inductors as well as extremely low AC losses, resulting in the best overall efficiency over a wide range of AC ripple current. They are ideal for DC-DC converters with switching frequencies ranging from hundreds of kHz to 5 MHz and above. The XGL4030 features an expanded inductance range, including 18 values from 0.13 to 12.0 μ H, with current ratings up to 26.5 Amps and soft saturation characteristics. It also offers a

30% increase in Irms self-heating current, allowing the XGL4030 to operate much cooler than previous-generation components. XGL4030 Series inductors are qualified to AEC-Q200 Grade 1 standards (-40° to +125°C ambient) with a maximum part operating temperature of +165°C and exhibit no thermal aging issues, making them suitable for automotive and other harsh-environment applications. They feature RoHS-compliant, tin-silver-over-copper terminations and are halogen free. Their composite construction also minimizes audible buzzing.



www.coilcraft.com



85/85 THB-rated AC Filter Capacitors for Harsh Environments

Designed for harsh environments, Cornell Dubilier's ALH series of AC-rated filter capacitors offer 50% greater life than competitive 85/85 THB-rated film capacitors.

The Temperature, Humidity at Bias (THB) test exposes parts to the harsh conditions of 85 °C at 85% relative humidity with rated voltage applied. CDE's testing has been validated for 1,500 hours, while competitors validate their series for 1,000 hours under the same conditions. This demanding test



Cornell Dubilier Electronics ALH Series
85/85 THB-Rated AC Harmonic Filter Capacitors
cde.com/new-product/alh

www.cde.com

Leakage Current Sensor for Electric Vehicle Charging Stations

LEM launches the CDSR, a leakage current sensor based on its open-loop Flux-gate Technology. The CDSR is innovative, extremely compact and safe, allowing manufacturers to optimize the electronic design of their charger products. Since 2016, IEC standards and more specifically IEC 62955 / IEC 62752, require the detection of a Direct Leakage current at 6 mA DC to avoid the home Residual Current Device (RCD) Type A being ineffective. This effect, called "the blinding effect", appears when an EV develops an insulation fault. EV architecture integrates a battery pack, powered by Direct Current (DC), which can generate a leakage current that can deactivate a home RCD. To protect the RCD and avoid the need to install an RCD type B in the electrical panel of home EV owners, EV chargers include a device to detect the DC leakage current. This detection is the role of the CDSR.

The CDSR has been developed to meet market demand for a residential and commercial charging station, offering a version for single-phase architecture and another for three-phase topology. With a maximum current per phase of 32A rms, the CDSR can

simulate the extremely harsh operating conditions encountered in many commercial and industrial inverter applications that can cause conventional film capacitors to fail early due to heat and moisture penetration. The ALH Series is optimized for AC harmonic filtering on the input and output sides of inverter circuits. Capacitance ranges from 0.22 to 50 µF at 160-450 Vac, 50/60Hz with high rms current ratings for handling higher ordered harmonics. The series offers self-healing, metalized polypropylene-film construction in a robust board-mount package that also meets the rigors of automotive AEC Q200 testing. The solvent-resistant, box-style plastic case and resin-seal are both UL/cUL 94V-0 recognized for construction designs, with tin-plated copper RoHS compliant terminations. Their superior construction makes these capacitors ideally suited for solar, wind, UPS, EV, and other inverter applications that may be subjected to wide-ranging environmental conditions.



be integrated into AC chargers from 3.7 kW to 22kW. Following the trend towards digital electronics, the CDSR provides not only an analog communication output but also a Serial Peripheral Interface (SPI), enabling simple interfacing of hardware. The CDSR operates from a +3.3VDC supply and has a typical current consumption of just 50 mA when measuring 150 mA as a maximum primary residual current.

www.lem.com



WIMA DC-Link Capacitors

WIMA DC-LINK capacitors are designed for the high power converter technology. At high frequencies they show a higher current carrying capability compared to electrolytic capacitors. Further outstanding features are e.g.:

- Very high capacitance/volume ratio
- High voltage rating per component
- Very low dissipation factor (ESR)
- Very high insulation resistance
- Excellent self-healing properties
- Long life expectancy
- Dry construction without electrolyte or oil
- Particularly reliable contact configurations
- Customer-specific contacts, capacitances or voltages

WIMA DC-LINK capacitors are available with capacitances from 1 µF through 8250 µF and with rated voltages from 400 VDC through 1500 VDC. The components are environmentally compatible with the RoHS 2011/65/EU regulations.

www.wima.com

Wide-bandgap Ready: Current Sensors for Power Electronics with High Power Density

The programmable current sensor CFS1000 has been developed for the highly dynamic electronic measurement of DC, AC or pulsed currents with integrated galvanic isolation. It consists of an anisotropic magnetoresistive (AMR) sensor element combined with a specific



ASIC as system in package (SIP) in a JEDEC compliant SOIC housing. The current sensor gives the end user the flexibility to create "his own" bus bar according to the required current range and the geometric general conditions. The high bandwidth combined with high precision enable users to achieve higher power density in their power electronics, particularly when the sensor is used in combination with new wide band gap power transistors, e.g. SiC or GaN. Due to its compact design the CFS1000 can be integrated even deeper into the power modules to achieve a further reduction of size of inverters or converters. The current sensor exhibits no hysteresis as observed in iron core based Hall-sensor solutions. Since AMR sensors are very sensitive, a flux concentrator is not necessary. The sensor system works in closed loop operation, providing high linearity and a low temperature dependency. Typical applications are in the automotive sector, electrical speed drives (industry, e-mobility), in frequency converters, for battery management and renewable energy. Evaluation boards are available.

www.sensitec.com

AC-DC Active Bridge Rectifier Solutions

Alpha and Omega Semiconductor announced a family of active AC-DC bridge rectifiers. Aply trademarked AlphaZBL™ for "zero bridge loss," this family of products virtually eliminates the bridge rectifier



losses in AC-DC power supplies and adaptors. Typical end applications include high power 100W and above adaptors used for high-end laptops and televisions as well as power supplies for Desktops, Game consoles, Servers, and Telecom. The first two members of the family include a controller, AOZ7200, in a SOT-23 package and an integrated product AOZ7270, which integrates a 600V, 190mOhm MOSFET in a DFN 5x7 package. The AOZ7200 offers maximum flexibility to trade off performance and cost by pairing it with AOS's benchmark super junction family of MOSFETs. The AOZ7270 takes advantage of AOS's capabilities in novel IC design, benchmark MOSFET technology, and innovative packaging to reduce component count and design time. Both products are self-powered from the AC line and do not require external circuitry. The proprietary self-biasing scheme sips minimal power from the AC line making it very efficient in light load or standby mode of operation. In a typical 100W application, the AOZ7270DI delivers efficiency improvements of 0.89% at 115VAC and 0.44% at 230VAC over a diode bridge. Both products exceed lightning surge requirements that are a critical requirement in AC-DC applications.

www.aosmd.com

Bridge Rectifier Features 1000V Rating in Standard GBU Package

Taiwan Semiconductor announces the availability of the GBU150x family of standard bridge rectifiers. These GBU-packaged, 15A-rated rectifiers are available with peak repetitive reverse voltage ratings (VRRM) from 600V to 1000V and 1.0ms peak forward surge current (IFSM) of 600A. The highest rated (1KV) device, offered at the same price in production quantities as the others in the family, provides added design margin that can facilitate meeting regulatory standards, such as IEC61000-4-x and IEEE C62.XX ringing waveform requirements, in a wide

range of mains-connected power conversion products. "Since higher-voltage bridge rectifiers typically are more expensive, engineers trained to optimize price and performance will select 600V or 800V PIV devices to achieve cost targets," said Vice President, TSC Products, Sam Wang. "The GBU1507, with an industry-leading 1000-volt PIV rating, is offered at the same price as the lower-voltage-rated parts in the series. This gives engineers a cost-effective opportunity to adding safety margin for new designs as well as upgrading existing GBU sockets.



www.taiwansemi.com



electrical energy storage

Europe's Largest and Most International Exhibition
for Batteries and Energy Storage Systems
MESSE MÜNCHEN, GERMANY

JULY
21-23
2021

www.ees-europe.com



- Production and automation solutions for the storage industry
- Access to the world's leading battery manufacturers
- Technological innovations and industry trends
- For equipment suppliers, factory planners, manufacturers and distributors
- Meet 50,000+ energy experts and 1,480 exhibitors at four parallel exhibitions

Part of

THEsmarter
EUROPE



AEC-Q200 Compliant High Current Shielded Power Inductor Series

Bourns introduced three AEC-Q200 compliant high current shielded power inductor series. Helping to meet the high current density, high



temperature and reliability requirements for power management and EMI filtering in a variety of consumer, industrial and telecom electronics applications, Bourns Model SRP1580CA, SRP1510CA and SRP1513CA inductors offer high current capacity, compact size, high operating frequency and a high operating temperature range. The three AEC-Q200 compliant inductor series are manufactured with flat wire and Bourns' uniquely formulated metal alloy powder core using a molded construction manufacturing process. This process enables a superior magnetically shielded construction that offers low DC resistance, high heating / saturation current, low buzz noise and excellent temperature stability for low magnetic field radiation. In addition, all of the models are built with flat enameled coated wire with self-lead terminal for ultra-low DC resistance. Plus, the high current shielded inductors have an operating temperature range of -55 to +155 °C, and are designed with the same 16.5 x 15.5 mm interchangeable footprint. The Bourns Model SRP1580CA, SRP1510CA and SRP1513CA series are available now and are RoHS compliant* and halogen free.

www.bourns.com

Laser Driver IC Family for Augmented Reality

EPC announces the introduction of a laser driver that integrates a 40 V, 10 A FET with a gate driver and low-voltage differential signaling (LVDS) logic level input in a single chip for time-of-flight lidar systems used in robotics, drones, augmented reality, and gaming applications. The EPC21603 is a laser driver that is controlled using LVDS logic and is capable of very high frequencies exceeding 100 MHz and super short pulses (< 2 ns) to modulate laser driving currents up to 10 A. The EPC21603 is a single-chip driver plus eGaN® FET using EPC's proprietary GaN IC technology in a chip-scale BGA form factor that measures only 1.5 mm x 1.0 mm. The LVDS logic control allows the eToF™ laser driver IC to be controlled from an FPGA for applications where noise immunity is critical, such as augmented reality. "The EPC21603 joins the recently announced EPC21601 as the initial products in our new family of GaN ICs that dramatically improve the performance while reducing size and cost for time-of-flight lidar systems," said Alex Lidow, CEO, and co-founder of EPC. "This new family of GaN integrated circuits will continue to expand to higher currents, higher voltages, as well as furthering integration of additional control and logic features on a single chip."



www.epc-co.com

Advertising Index

Aismalibar	61	Heraeus	65	Plexim	21
Alpha & Omega	57	HIOKI	23	Ricoh	65
APEC	75	Hitachi	9	Ridley Engineering	19
APEX Microtechnology	49	Hitachi ABB Power Grids	47	ROHM	7
Coilcraft	6	ICE Components	55	Sensitac	65
CPS Technologies	67	Infineon	15+39	STMicroelectronics	35
Danfoss	45	J&D Smart Sensing	59	Tamura	73
Dean Technology	67	Kendeil	37	TIGRIS Elektronik	33
DOWA	43	LEM	5	UnitedSiC	27
ed-k	51	Magnetic Metals	53	Vincotech	13
ees	79	Magnetics	29	VMI	61
Electronic Concepts	1+25	Mitsubishi Electric	17	WIMA	77
Elytone	67	MUECAP	31	Würth Elektronik eiSos	3
EPC	C4	NORWE	71	ZEZ SILKO	38
Fuji Electric Europe	11	Payton Planar	63		
GvA	C2	PCIM Asia	C3		

pcim
ASIA

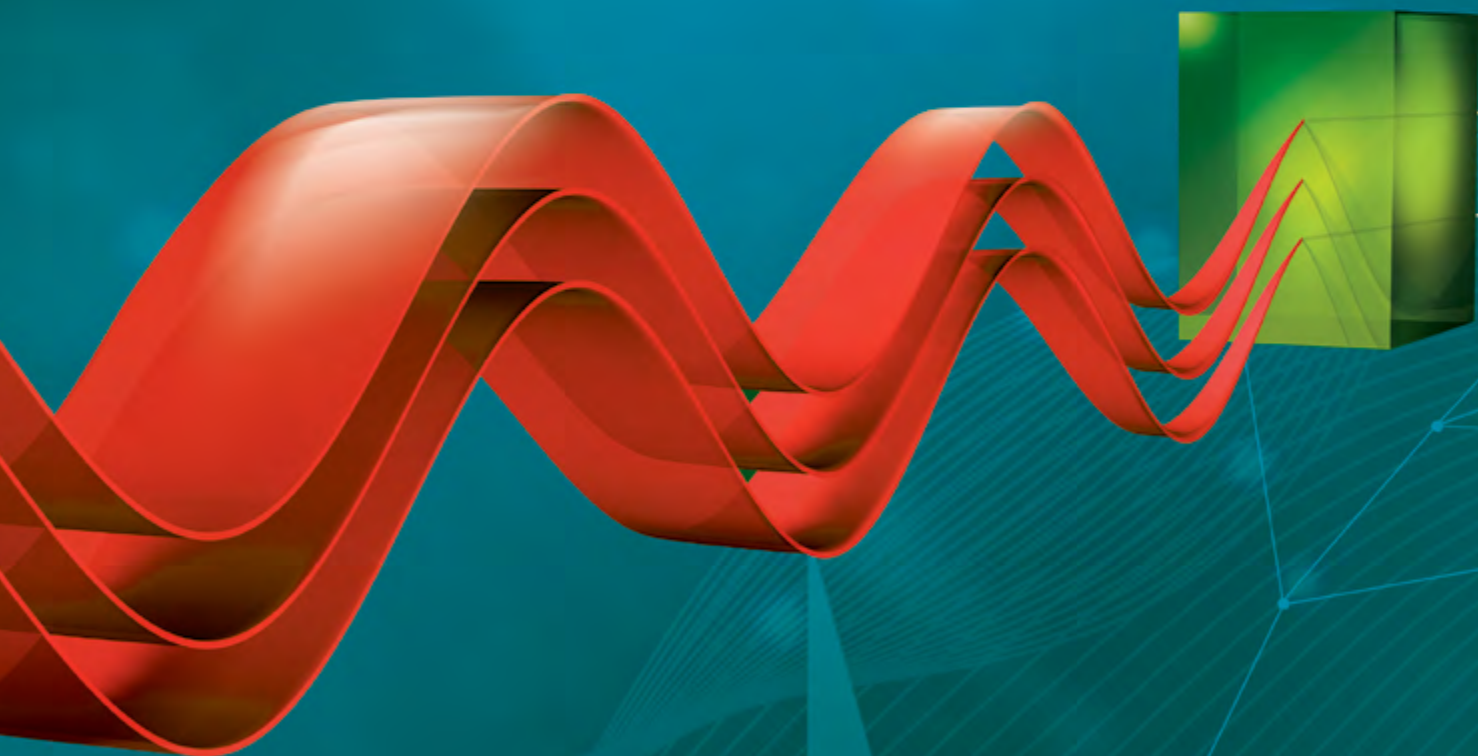
电力电子、智能运动、可再生能源
深圳国际电力元件、可再生能源管理展览会
International Exhibition and Conference
for Power Electronics, Intelligent Motion,
Renewable Energy and Energy Management

Power electronics towards a sustainable new era

9 – 11. 9. 2021

Shenzhen World Exhibition & Convention Center, China
Shenzhen, China

www.pcimasia-expo.com



mesago
Messe Frankfurt Group

 **messe frankfurt**

EPC21603

eToF™ Laser Driver IC



Integrated Laser Driver

1 mm x 1.5 mm

Capable of 200 MHz & <2 ns pulses



AUTOMOTIVE



MOBILE



ROBOTICS



SERVER



SOLAR



SPACE



TELECOM

eGaN® ICs Augment Your Reality

pcim
EUROPE *...digital days*

Time-of-flight sensors for robotics, drones, 3D sensing, gaming, vacuum cleaners, and autonomous vehicles need the speed and high current capability of eGaN® FETs and ICs for higher resolution and faster readings.

Integrating an eGaN FET plus driver on one chip generates an extremely powerful, blazingly-fast IC and reduces the size and cost for advanced autonomy and augmented reality.



Note:

Scan QR code to download the ebook and learn more.

<http://bit.ly/eToFIC>



epc-co.com